

Review

Aerosol Nanoparticle Control by Electrostatic Precipitation and Filtration Processes—A Review

Felipe de Aquino Lima , Gabriela Brunosi Medeiros , Paulo Augusto Marques Chagas, Mônica Lopes Aguiar and Vádila Giovana Guerra * 

Department of Chemical Engineering, Federal University of São Carlos, Rodovia Washington Luís, km 235, C.P. 676, Sao Carlos 13560-970, SP, Brazil

* Correspondence: vadila@ufscar.br

Abstract: The growing increase in emissions of ultrafine particles or nanoparticles by industries and urban centers has become worrisome due to the potential adverse health effects when inhaled. Particles in this size range have greater ease of pulmonary penetration, being able to access the bloodstream and deposit in other regions of the body. Thus, the development and optimization of equipment and processes aimed at the removal of aerosols of nanoparticles have been gaining importance in this current scenario. Among the equipment commonly used, electrostatic precipitators and filters stand out as being versatile and consolidated processes in the literature. This review explores and analyzes the theoretical bases of these two processes in the collection of such small particles in addition to providing a general overview of the development of technologies and studies on these topics.

Keywords: nanoparticle; ultrafine particle; electrostatic precipitation; air filtration; air pollution



Citation: Lima, F.d.A.; Medeiros, G.B.; Chagas, P.A.M.; Aguiar, M.L.; Guerra, V.G. Aerosol Nanoparticle Control by Electrostatic Precipitation and Filtration Processes—A Review. *Powders* **2023**, *2*, 259–298. <https://doi.org/10.3390/powders2020017>

Academic Editor: Paul F. Luckham

Received: 9 February 2023

Revised: 21 March 2023

Accepted: 29 March 2023

Published: 10 April 2023



Copyright: © 2023 by the authors. Licensee MDPI, Basel, Switzerland. This article is an open access article distributed under the terms and conditions of the Creative Commons Attribution (CC BY) license (<https://creativecommons.org/licenses/by/4.0/>).

1. Introduction

Sustainability has become a major concern for many companies, organizations, and governments. With the growing appreciation for this concept, the search for technologies to reduce the effect of anthropogenic actions on the environment and society has also increased. In this context, nanotechnology has allowed for the creation of materials that provide significant advances in areas such as energy, electronics, and medicine [1–4]. These advances are partly associated with the different optical, magnetic, and electrical properties that nanoparticles exhibit when compared with the same material at larger scales, such as micrometric [5–8]. Based on this, there is concern regarding the potential negative effects that these changes can have on the environment and health and, therefore, there seems to be a paradox between the development and application of nanotechnology [9].

Toxicological studies and environmental effects have shown evidence of the bioaccumulation of nanoparticles and transfer through the food chain in aquatic organisms, as well as changes in the dynamics of soil bacterial communities [10–12]. Negative effects are also felt by humans due to the fact of health damage caused by the inhalation of nanoparticles [13–16]. These nanoparticles, even at a smaller mass, are more numerous, have high surface, neurotoxicity, ease of pulmonary penetration, and ability to be transported through the bloodstream and access other organs, cells, and subcellular structures [17–20]. Because of this ability, research involving exposure to metal nanoparticles in rats has shown that they can reach the brain, cause stress and decreased cell viability, and increase the incidence of neurodegenerative diseases such as Alzheimer’s, Parkinson’s, mental illness, and reduced intelligence [21–25].

Therefore, with the increase in ultrafine particle emissions (<100 nm) by industries and urban centers, it is necessary to implement efficient means for its removal from the air [14,26–29]. Another important point is the improvement of processes, not only to mitigate the damage caused by this particle size but also for the recovery of materials

that can present added value. Depending on the concentration of emissions, the recovery of ultrafine particles of iron oxides, silver oxides, titanium oxides, and aluminum oxides at an industrial scale could lead to long-term cost reductions in the implementation of emission control equipment [4]. Other processes that would benefit would be the recovery of nanoparticles of gold, silver, zirconia, and palladium at the laboratory and industrial scales [30–34], drugs in the pharmaceutical industry [35–37], or nanoparticles in biomedical applications [38–40].

Studies aimed at the removal of nanoparticles have proposed the use of equipment such as bubble columns, membrane filters, electrocyclones, diffusion batteries, and electrostatic precipitators, as well as the development of filter media for bag filters [8,41–49]. Among these types of equipment, electrostatic precipitators and filters stand out because they are consolidated processes and are widely investigated in the literature [6,50]. The concomitant use of these two types of equipment, so-called hybrid filters, is also interesting in the removal of materials in this size range [51]. This review aims to assist in understanding the behavior and emissions of aerosols at the nanoscale, as well as the applications and health impacts of nanoparticles. Based on this, the theory and studies of the main processes of the removal of nanoparticle material is explored, including electrostatic precipitation and air filtration.

2. Air Pollution and Ambient Particulate Matter (PM)

Air pollution is a global problem that has increased with industrialization and urbanization. The introduction of substances to the atmosphere affects air quality and causes major problems to the environment and public health. Among contaminants, such as nitrogen oxides, sulfur oxides, carbon monoxide, and carbon dioxide, particulate matter (PM) stands out for presenting varied compositions and characteristics, many of which contribute to its dangerousness. Its effects, which are dependent on the toxicity, exposure time, and concentration, are the targets of several studies. Many of these have demonstrated evidence that air pollution is associated with the development of diseases in the lower respiratory and cardiovascular systems, such as allergies, asthma, pneumonia, and cancer [52–54].

The environmental and health effects and the time that particles remain suspended vary according to their size. In practical terms, PM₁₀ (less than 10 µm) can penetrate the lower respiratory system, while PM_{2.5} (less than 2.5 µm) can penetrate the gas exchange region of the lung. Special attention should be paid to ultrathin particles such as PM_{0.1} (less than 100 nm) which, even with a lower mass, are more numerous, with high surface area, ease of pulmonary penetration, and ability to access organs, cells, and subcellular structures [17,18]. Based on this, there is a consensus that particles with smaller diameters have a greater potential to cause adverse effects on human health [14], and nanometric particles have begun to be the target of numerous studies reporting various epidemiological and clinical evidence of the damage caused by their inhalation [13–16,55–57].

3. Ultrafine Particles and Nanoparticles

Ultrafine particles and nanoparticles are particles on the nanometric scale (10^{-9} m) that present themselves in various forms in the environment. Particles of this size have unique characteristics in relation to macroscopic particles and surfaces [3]. It is important to highlight that the terms nanoparticles (NPs), ultrafine particles (UFPs), and PM_{0.1} are interchangeably used in the atmospheric field [58], but there are small differences among these definitions. Ultrafine particles refer to particles that are generated incidentally in the environment, generally with a heterogeneous composition and size, often as by-products of fossil fuel combustion, condensation of semivolatile substances, wood burning, and industrial emissions [59,60]. Nanoparticles are manufactured by controlled engineering processes, with a homogeneous composition and size [59,61,62]. More broadly, the term nanoaerosols is used to refer to environmental ultrafine particles and engineering nanoparticles, while PM_{0.1} is exclusively particles of an aerosol that are less than 100 nm,

regardless of the particle type [20,58,63]. The ISO/TS 12025:2012 [5] defines these particles as those that comprise the nanoscale, i.e., between 1 and 100 nm. However, there is no consensus in the literature concerning which aerodynamic diameter can be used to consider a particle as a nanoparticle. Most authors consider nanoparticles to be those smaller than 100 nm [19,26,46,61], while others define them as less than 50 nm [6,64,65], less than 250 nm [47,66,67], or less than 300 nm [68,69].

The intrinsic characteristics of ultrafine particles and nanoparticles guarantee new and unique properties. Such properties are associated with their size at the nanometric scale, greater reactivity and surface groups, solubility, state of aggregation, morphological structure, and characteristics related to their chemical composition, such as purity, crystallinity, and electronic properties [61,62]. Nanotechnology currently appears as one of the technologies with great potential to solve problems involving sustainability and the use of energy resources [9]. The applications of nanomaterials and nanoparticles have allowed for the development of a range of products, such as medicines and drug release techniques, cosmetics, adsorbents, water and soil treatments, and supercapacitors and batteries [2,4,14].

The Nanodatabase portal [70], developed by DTU Environment, the Danish Ecological Council, and the Danish Consumer Council, is a database for information collection and the categorization of nanomaterials used in consumer products. In the inventory, accessed on 13 December 2022, 5286 products containing nanoparticles have been cataloged. The Project on Emerging Nanotechnologies [71], carried out in partnership with the Woodrow Wilson International Center for Scholars and the Pew Charitable Trusts, maintains an online database of consumer nanoproducts (Project on Inventory of Consumer Products for Emerging Nanotechnologies 2009). This platform catalogs consumer products that openly advertise the use of nanocomponents. As of its most recent update, accessed on 13 December 2022, there were 1833 products cataloged. Based on the Woodrow Wilson International Center project, Vance et al. [4] evaluated the inventory launched in October 2013, which included 1814 consumer products from 622 companies in 32 countries. Among the total number of registered products, 42% refer to the category health and good form. In addition, 37% of the products warn of the use of metals and metal oxides, with silver being the most widely used nanomaterial (24%). Other materials include titanium oxides, zinc oxides, silicon oxides, and gold. Among carbonaceous nanomaterials (89 products), carbon nanoparticles are the most used (39 products). However, 49% of the products included in this platform do not provide the composition of the nanomaterial used.

The recent advances in nanotechnology, while opening up new opportunities for advances in technology and medicine, can also cause adverse health effects upon exposure to humans. Further research is needed to clarify the safety of nanoscale particles, as well as to elucidate the possible beneficial use of these particles in the treatment of diseases [61]. The increase in nanotechnological processes has also increased emissions of nanoparticles [14,26–29] and has raised concerns regarding how particles so small can interact with the human body and their potential effects on health and the environment [28,29].

The same properties that make nanoparticles so unique can also negatively affect the environment. However, research involving its impacts cannot keep pace with the rapid proliferation of research for the development and application of nanomaterials. This concern for its negative effects comes from problems arising from other materials that have also shown promise in the past. As in the case of asbestos, with its decades of long latency and health effects, there are many legitimate concerns regarding the unknown consequences for the human health of nanomaterials [14,55].

3.1. Emissions of Nanoparticles and Effects on Human Health

Even though the development of nanotechnology is recent, the presence of ultrafine particles in the air is neither recent nor unusual. However, they became a problem with the increase in emissions and the difficulty in characterizing them geographically or over time, since the concentration is influenced by parameters such as humidity and ambient temperature, wind direction, and distance from the emission source [61,72]. In addition, there is

also the fact that they have long been difficult to measure, and better results are coming from improvements in measuring equipment. On average, the number of ultrafine particles in urban areas is in the order of 10^4 particles/cm³, while in rural areas they are in the order of 10^3 particles/cm³ [73,74]. However, populous or industrial regions have concentrations in numbers with larger orders of magnitude, such as 10^6 or 10^7 particles/cm³ [75].

It is important to note that the emission of nanoparticles directly into the atmosphere by anthropogenic processes [14,26–29] is not the only way they can be present in the environment. Primary emissions of nanoparticles are those emitted directly into the atmosphere and include, for example, brakes and wheels, mineral dust, industrial emissions, black carbon, organics emitted by traffic, organics emitted by cooking, and marine spray aerosol [76–79]. However, these ultrafine particles are also abundantly formed in the atmosphere (i.e., secondary emissions) by photochemical sources or reactions with various atmospheric oxidants [77,80,81]. For example, so-called secondary organic aerosol is formed from organic gaseous precursors as part of photochemical smog [78,82], secondary inorganic aerosols formed from reactions in the atmosphere [79], in addition to the homogeneous nucleation of new particles [79,80,83].

Many studies involving ultrafine particles focus on urban areas and highways, mainly caused by vehicle emissions [27,84–89]. Cheng et al. [85] conducted a study on a toll booth on a Taiwanese highway with the traffic of 227,000 vehicles per day and showed that people working in this region are exposed to concentrations of ultrafine particles in the range of 9.3×10^3 – 1.6×10^5 particles/cm³. Rönkkö et al. [86] performed measurements of heavy-duty diesel truck and light-duty vehicle emissions during engine braking conditions and demonstrated that there is a contribution of 20–30% of nanoparticles emitted during engine braking (10^5 – 10^8 particles/cm³). Holmén and Ayala [87] identified emissions in the orders of 10^4 particles/cm³ and 10^6 particles/cm³ for buses using compressed natural gas and diesel, respectively. Calderón-Garcidueñas and Ayala [27] reported much higher levels for diesel vehicle emissions, in addition to verifying that professional drivers are exposed to ultrafine particles in cabins at concentrations ranging from 17.9×10^3 to 37.9×10^3 particles/cm³. Mayer et al. [88] also observed these orders of magnitude (10^3 particles/cm³) in the cabs of vehicles that used other fuels.

In industrial processes, the increase in particles in this size range is also expressive. Cheng et al. [90] showed that the concentrations of ultrafine particles in an iron foundry were between 2.07×10^4 and 2.82×10^5 particles/cm³. In a study by Heitbrink et al. [69], in a machining and engine assembly facility, the concentrations of ultrafine particles were 7.5×10^5 particles/cm³ when natural gas heaters were used and 3×10^5 particles/cm³ when steam heaters were used. Wheatley and Sadhra [91] reported, through parallel measurements of diesel smoke levels in the air in tanks using diesel-powered forklifts, an exposure of ultrafine particles in the range of 5.8×10^4 – 2.3×10^5 particles/cm³. Jiayuan Wu et al. [92] collected samples from representative coal-fired power plants in China and verified emissions in the order of 10^7 particles/mg, mainly from Fe, Ti, and toxic metals. They also noted that nanoparticles have a remarkable contribution when evaluated by number and not by mass/volume.

Elihn and Berg [93] studied the characteristics of ultrafine particles in seven industrial plants and measured the concentrations in ten work activities, such as welding, laser cutting, casting, core manufacturing, molding, concreting, grinding, sieving, and washing. Concentrations of 1.5×10^4 to 8.8×10^4 particles/cm³ were obtained in activities with steel welding, grinding, and washing of cast steel, from 2.5×10^4 to 3.9×10^4 particles/cm³ for iron casting, from 5.0×10^4 to 1.3×10^5 particles/cm³ for steel casting, from 1.2×10^4 to 2.2×10^4 particles/cm³ for concrete constructions, and from 1.2×10^4 to 9.6×10^4 particles/cm³ for molding and sieving steel powders.

Nanoparticle emissions are a real problem and are present in various places and sectors of society. Although only the amount of these emissions were evaluated here, the compounds involved can further increase the dangerousness and its effects on human health. Several studies have demonstrated worrisome and known health-damaging compounds,

such as metals and toxic metals [92,94,95], arsenic [96], mercury [95], and magnetite [97]. In general, inhalation is one of the most dangerous access routes for nanoparticles. The presence of nanoparticles in atmospheric air is worrisome due to the fact of their high lung deposition efficiency, long service life in the atmosphere, and ability to be transported for thousands of kilometers and remain in the air for several days. Studies show that after being inhaled, nanoparticles can reach the gas exchange region, cross the air–blood barrier, access the bloodstream, and redistribute in other parts of the body, such as different organs (e.g., kidneys, heart, liver, and brain [15,16,18,20,22,97,98]) and secondary tissues, causing systemic health effects [13–15,20]. This occurs because the particles are extremely small, which allows them to translocate by diffusion through the lipid bilayer of the cell walls of alveolar epithelial cells [59,99]. In any case, a large part is retained in the lungs, where it can cause inflammatory responses [16,57,100]. For example, in the brain, nanoparticles can cause neuroinflammation and neurodegeneration [24,25], increasing the likelihood of developing diseases such as Parkinson’s disease, Huntington’s disease, primary brain tumors [23], and Alzheimer’s disease [22].

Thus, it is important to consider that research is still needed to conclusively affirm the effects that nanoparticles and ultrafine particles can have on human health. However, with the available data, it can be inferred that nanoparticles are a problem that deserves attention and forms of mitigation to ensure robustly and validated nanosecurity for processes and people. As a result, research involving the development of nanoscale particle removal equipment is important to ensure sustainable development and reduce the negative impact on people’s health. Therefore, it is important to know the behavior and characteristics of these small particles in order to understand the impact of their collection by atmospheric emission control equipment.

3.2. Characteristics of Nanoparticles

Particle aerosols at the nanoscale are more dynamic and have unique characteristics in relation to micrometric particles due to the fact of their greater sensitivity to physical effects, such as Brownian diffusion [5–8]. To explain these effects, two concepts should be understood: gas mean free path and Brownian motion. The mean free path (λ) is defined as the average distance that the gas molecule travels between successive collisions (Equation (1)), and Brownian motion is the random and irregular movement of particles caused by collisions of gas molecules against the particles [6,101,102].

$$\lambda = \frac{\mu}{0.499P(8M/\pi RT)^{0.5}} \quad (1)$$

In this equation, μ is the gas viscosity (Kg/ms), P is the pressure (Pa), M is the molecular weight, and T is the absolute temperature (K).

Particles with a micrometric magnitude, on average, will have traveled a distance equal to the mean free path (0.066 μm under standard conditions) since the last collision with another gas molecule. Its diameter is much larger than this mean free path, and the particle behaves as if in a continuous medium [6,8]. Figure 1 shows a comparison between the particle size and the mean free path. As particles decrease in size, for the same air mean free path, they begin to escape contact with the gas molecules. Thus, the way the particle interacts with the gas molecules is different, presenting interactions with other chemical entities and random diffusion in all directions. When this occurs, extremely small particles behave differently and see the medium as something discontinuous [6,86]. This effect is demonstrated when observing the diffusion coefficient for particles of different sizes. At 20 °C, for a particle of 0.01 μm , the diffusion coefficient is $5.4 \times 10^{-8} \text{ m}^2 \cdot \text{s}^{-1}$, and for a particle of 10 μm , it is $2.4 \times 10^{-12} \text{ m}^2 \cdot \text{s}^{-1}$. That is, the diffusion transport is 20,000 times faster for particles of 0.01 μm . As the diffusion coefficient characterizes the intensity of Brownian motion, it has been observed that this phenomenon is well pronounced in smaller particles [6].

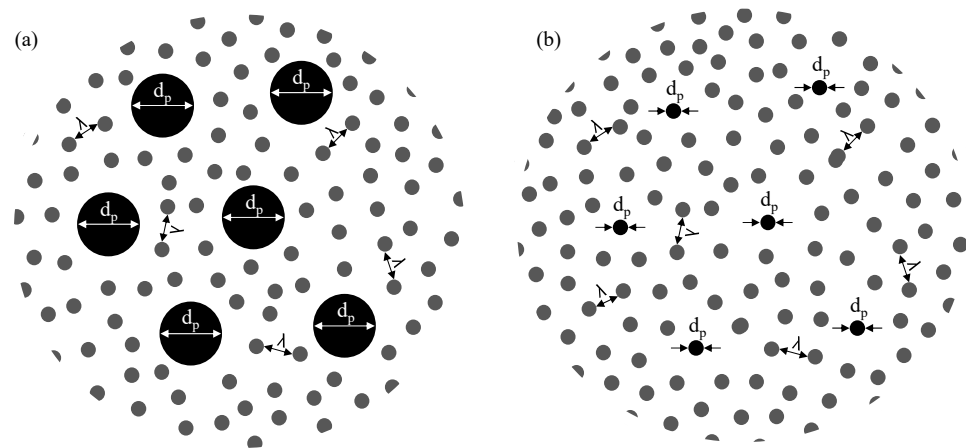


Figure 1. Representation of the particle size in relation to the mean free path of the gas where the (a) particle diameter (d_p) is much larger than the mean free path of the gas molecules and (b) the particle has a diameter (d_p) approximately equal to the mean free path of the gas molecules. Black color refers to particles and gray color refers to air molecules.

The behavior of a particle can also be evaluated by the Knudsen number, which relates the average free path of the gas molecules and the particle diameter (d_p), provided by Equation (2). If $Kn < 0.1$ and $d_p > 1.3 \mu\text{m}$, the particle is larger than the mean free path and behaves as if it were in a continuous medium. For $Kn \leq 0.3$ and $d_p \geq 0.04 \mu\text{m}$, it is called slipstream. For $Kn > 10$ and $d_p < 0.01 \mu\text{m}$, the particle has the same order of magnitude as the gas molecules and interacts as if it were a molecule before the gas molecules. With a Kn between 0.3 and 10 and $0.01 < d_p < 0.4 \mu\text{m}$, it is called the transition region, and when $Kn \approx 1$, there is difficulty in determining the behavior, and the data are unreliable [6,101].

$$Kn = \frac{2\lambda}{d_p} \quad (2)$$

With these different properties, along with their small size and surface area, particles at the nanoscale have begun to be investigated to optimize their collection by emission control equipment. However, several difficulties have been observed in collecting particles at the nanometric scale. In this size range, the Brownian motion is intense, and it is the main mechanism for collecting used by most separation equipment [6]. As particles increase in size, the diffusion collection mechanisms have a much smaller contribution, which makes the process simpler and avoids the effect of this complex mechanism. Among the most used equipment in the collection of ultrafine particles are electrostatic precipitators and filters. The next sections explore the technologies used with this equipment and how the diffusion mechanisms affect this collection.

4. Use of Electrostatic Precipitators in the Collection of Nanoparticles

4.1. Electrostatic Precipitation Process

Electrostatic precipitation is a separation process widely used in the removal of particulate matter from gas flows, even for very small particle sizes [50,103,104]. Based on electrical forces, gases can be cleaned using high volumetric rates simultaneously with low-pressure drops. Electrostatic precipitators (ESPs) have been used industrially for almost a century for the collection of particulate matter and have a good service life of approximately 20 years [105,106]. Electrostatic precipitators stand out for their versatility, high efficiencies, possibility of being operated at high temperatures, low maintenance requirements, and, if operated dry, allowing for the direct recovery of materials [8,105,106]. Figure 2a shows a scheme of the electrostatic precipitation process.

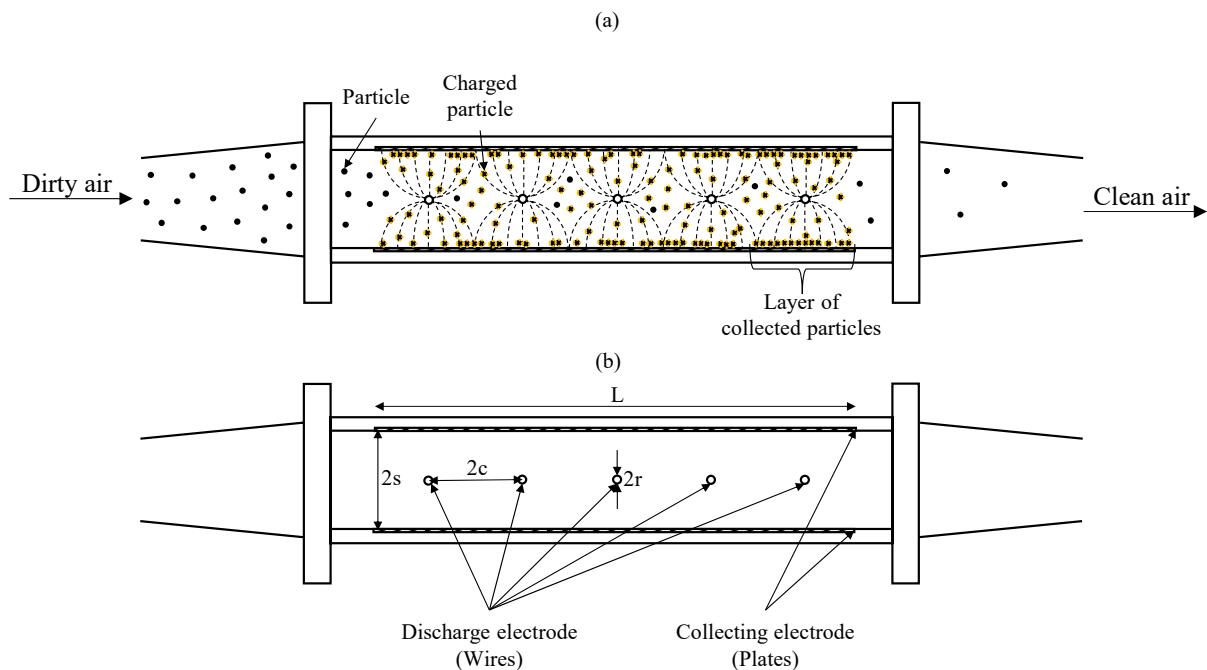


Figure 2. (a) Representation of the electrostatic precipitation process and (b) the main dimensions and elements of a wire-plate electrostatic precipitator, where $2s$ is the plate spacing, $2r$ is the diameter of the wires, and $2c$ is the wire spacing.

The basic principle of operation for an ESP is the removal of particles by passing the aerosol through a previously ionized region. The ions will transfer charge to the particles, which migrate to the collecting plates and are deposited and removed from the gas [8,50]. Although there are several methods of gas ionization, such as triboelectric, ultraviolet, and radiation effects, for applications in industrial precipitators, corona discharge is universally used as the most efficient and economical approach [107–111]. To produce a large number of ions, it is necessary to apply a high voltage to the discharge electrodes to exceed the value of the critical electric field. When this value is exceeded, an electric current can be measured between the discharge and collection electrodes, indicating the beginning of the corona (corona onset voltage), as evidenced by the current–voltage curve provided in Figure 3. An additional increase in the applied voltage will lead to a progressive increase in the detectable electrical current to a limit when there is the formation of an electric arc, indicating the dielectric rupture of the gas (i.e., breakdown point) [106,107].

Usually, the gas contains a large number of neutral molecules per volume. Natural ionization of the gas is very low due to the fact of electron and ion recombination immediately after ionization. If an electric field is present during ionization, the electron will be accelerated and rapidly separated from the remaining positive ion. This ionization is produced by free electrons due to the fact of their great electrical mobility. If the kinetic energy of the electrons is sufficient, it will be able to form positive ions and additional electrons when it collides with another neutral gas molecule, producing an avalanche of electrons. The region where ionization processes occur is called an active zone, as shown in Figure 4a. It is usually present near the discharge electrodes and produces a luminescence effect, with a faint blue glow in addition to a crackling noise [106,107]. Electrons move to the maximum electric field region, away from the wire. When they enter the lower intensity region of the electric field, called the passive zone, they are not able to ionize other molecules but bind to a molecule of electronegative gas, thus forming negative gaseous ions. In this zone, the particles are charged by the gas ions and migrate toward the collecting plates under the influence of the electrical force [107].

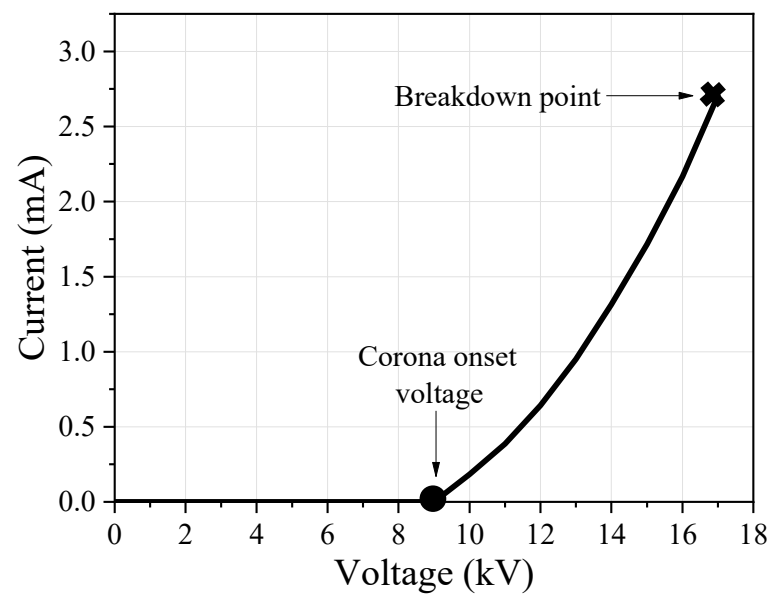


Figure 3. Representation of a current–voltage curve under typical conditions of a velocity of 4 cm/s and a small scale.

Positive or negative polarization can be used to generate corona discharge [112]. In a negative corona, the electrons migrate toward the collection electrode and the positive ions toward the discharge electrode [113,114]. In a positive corona, the electrons are attracted to the discharge electrodes, while the positive ions migrate to the collecting electrode [115,116]. A negative corona requires larger electric fields to cause dielectric air disruption to occur and ends up requiring a higher energy expenditure [117]. However, this type of polarization is used more industrially because it is more stable and allows for working with higher voltages and currents [112]. In addition, a negative discharge requires gases with electronegative components, being quite common in industrial activity. However, this type of polarization produces a large amount of ozone, making positive polarization used more in indoor air ventilation systems [112,118,119].

When negative corona polarization is used, particle charging occurs in the area between the active zone and the passive surface of the electrode. In this area, a large number of neutral ions and negative ions and some free electrons move toward the passive electrode as a result of the electric field. The removal of particles depends on Coulomb's law, being proportional to the intensity of the applied electric field and the magnitude of charge acquired by the particles [64,107,113,114]. Two charging mechanisms can occur, and they depend on the particle size range: field charging (for particles larger or approximately $1\ \mu\text{m}$) and diffusion charging (for particles smaller than $0.01\ \mu\text{m}$) [50,105,112].

In field charging, the ions formed in the corona discharge move in an orderly manner along the electric field lines formed between the discharge electrodes and collection electrodes. The discharged particles that enter the region that the electric field is present in distort it and cause a concentration of these field lines around them (Figure 4b). The degree of distortion depends on the dielectric constant of the material and the particle charge. The negative ions moving on these field lines collide with the particulate matter, transferring charge to them (Figure 4c). This charging occurs until eventually the particle reaches its saturation charge, where its charge is sufficient to generate a repulsion field, preventing the collision of other ions, as shown in Figure 4d [6,112,120,121].

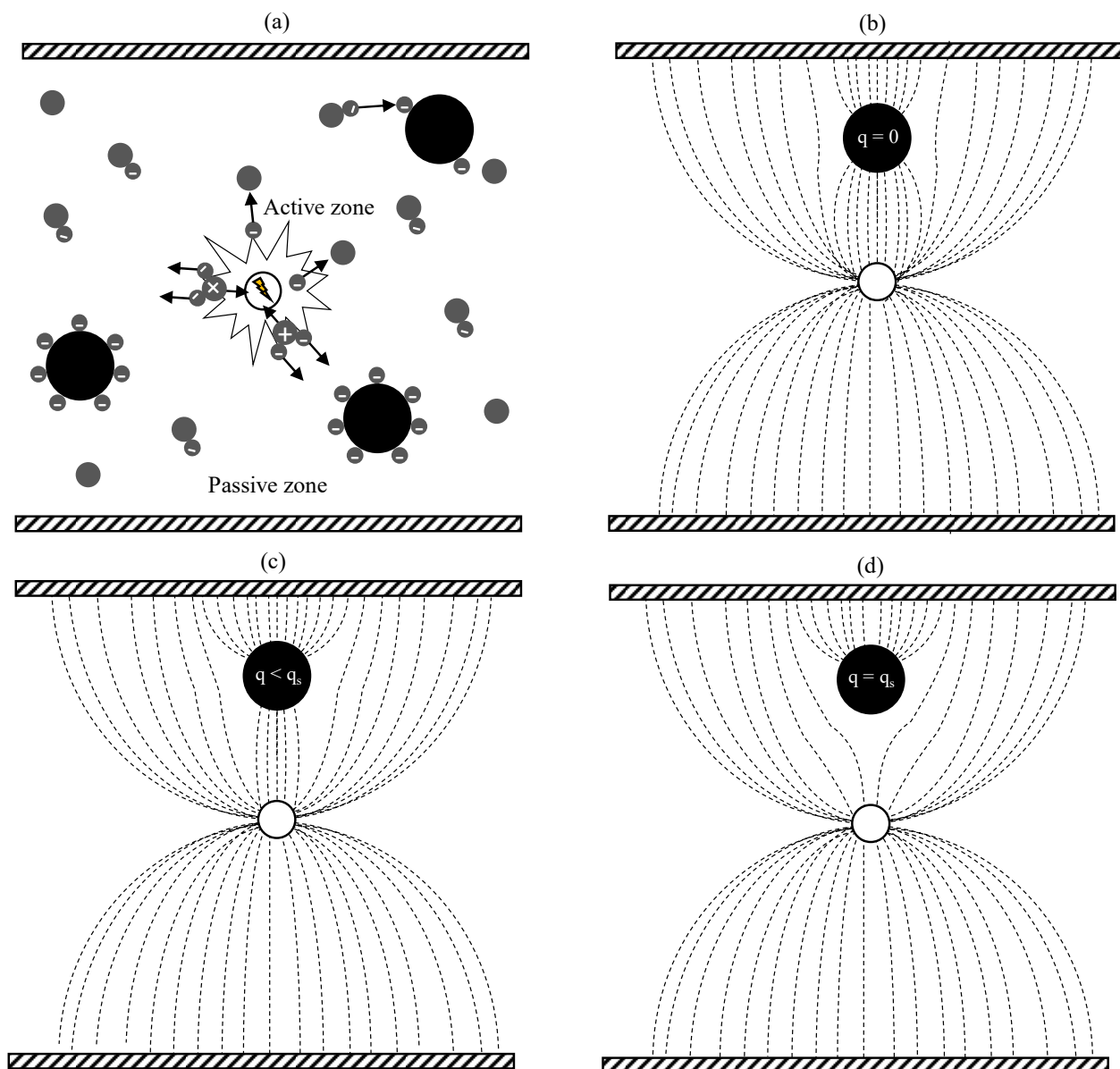


Figure 4. (a) Principle of the corona effect and development of the electron avalanche. Representation of the electric field lines to a conductive particle in a uniform electric field considering a wire discharge electrode and the plate collector electrodes: (b) uncharged particle; (c) partially charged particle; (d) particle with saturation charge. Black color refers to particles and gray color refers to air molecules.

Diffusion charging is based on the random movement of gas ions that arise by a temperature effect, following the kinetic theory of gases (that is, from Brownian motion), which intensifies with the decrease in particle size [7,106]. This diffuser transport depends on the density gradient on the particle surface and is independent of the external electric field. This predominant process in submicrometric particles (Figure 5b) also presents collisions of negative ions with particles in the aerosol, but, unlike field charging, these collisions occur by the thermal movement of the ions. With this, there is also the formation of an electric field of repulsion around the particle as it acquires charge, reducing the charging rate [6,107,122–124]. This complex mechanism depends on factors such as the distance between the particle and the electrode, possible additional interactions between particles, and other disturbances that also cause random collisions between these elements [123,125,126]. After charging, particles tend to follow the field lines and migrate to the collecting elec-

trode [127,128]. The collection efficiency of an electrostatic precipitator can be calculated experimentally by relating the inlet and output concentrations.

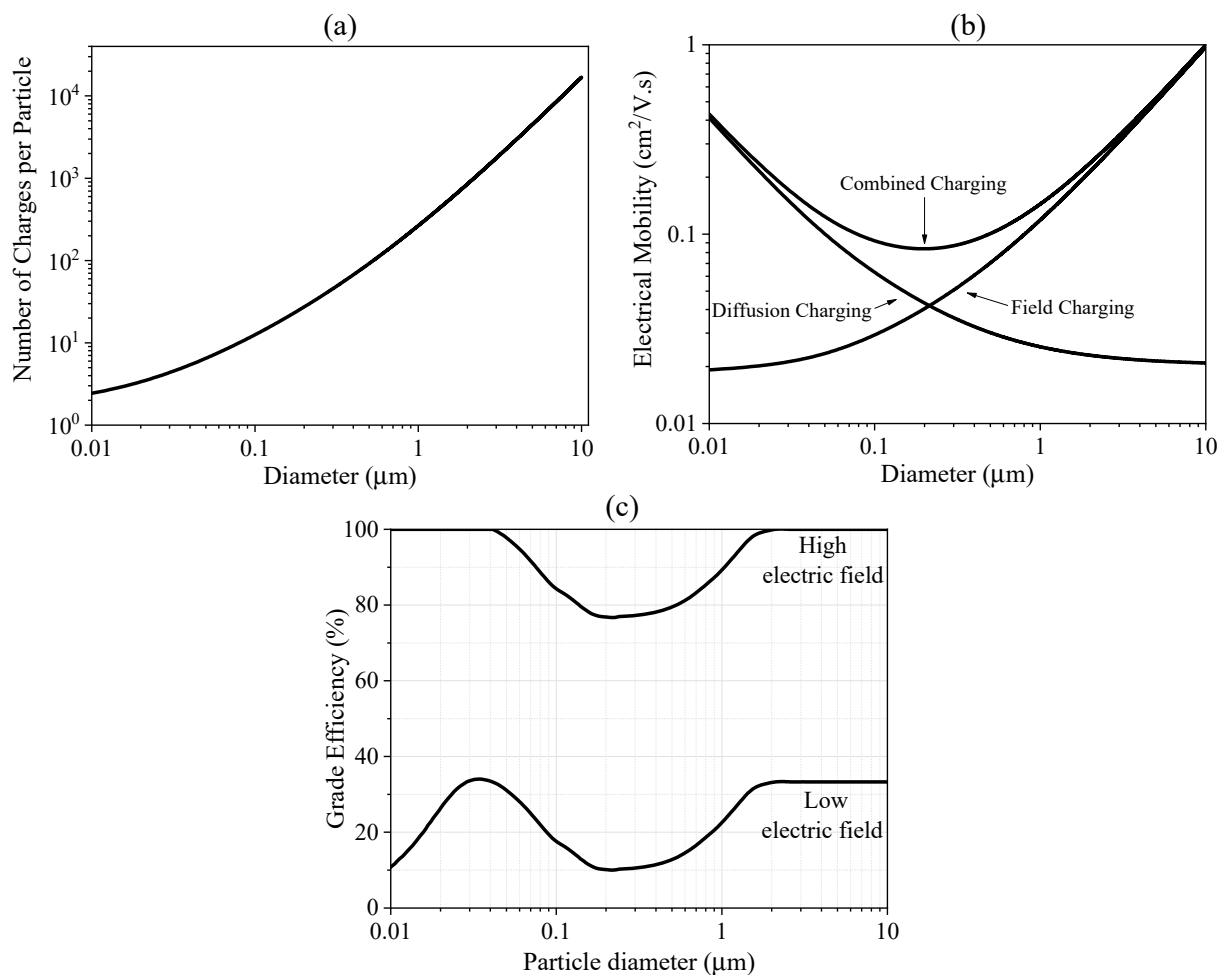


Figure 5. (a) Number of charges per particle, (b) electrical mobility, and (c) grade efficiency for different charging mechanisms by electrostatic precipitation. Typical behavior of electrostatic precipitation at low velocities (<5 cm/s), as given in Lima and Guerra [46] and Parker [50]. The values were 4 cm/s for the velocity and 4 kV/cm for the electric field in addition to particles of NaCl were used in (a,b). Values above 4 kV/cm were considered for high electric fields and values below 3 kV/cm for low electric fields at low velocities.

The parameters of ESPs (such as velocity, voltage, particle resistivity, plate and wire spacing, and other geometries) affect the collection of nanoparticles by altering the electric field or fluid dynamics inside the equipment. It is important to note that there is difficulty in collecting small particles due to the small number of charges that these particles acquire (Figure 5a) [8,46,66]. Decreasing the airflow increases the residence time, which allows for a longer time for the particles to be charged and, thus, an increase in the collection efficiency. As for the shape of the particles to be collected, these must be known and previously evaluated in the project dimensioning. Generally, the irregularity of the particle shape does not affect the electric field strength [129]. The wire shapes they affect can affect the performance of the precipitators, as the wires can come together and cause a short circuit [50,106]. The parameters that increase air ionization and increase energy inside the equipment favor the collection of nanoparticles. For example, the decrease in electrostatic shielding increases the current inside the equipment, favoring ionization and increasing the likelihood of particles acquiring diffusion charges [7,46,47]. The presence of ionic

wind favors diffusion charging due to the increased turbulence and consequent increase in randomness and particle energy [130,131].

Another highlight is the behavior of the grade efficiency in the collection of nanoparticles when using electrostatic precipitation, as shown in Figure 5c. Similar behavior has been seen in most of the articles mentioned in the next topic discussed, and it is directly linked to the effect of diffusion charging. These behaviors are caused by the influence of field and diffusion charging. Where a charging mechanism is predominant, the efficiency remains high, falling in the transition region between diffusion and field charging up to a minimum value [127,132–135]. This is due to the competition between the two types of charging that reduces the collection efficiency [50]. Analyzing only the nanometric range shown in Figure 5c, when the applied electric field is strong enough to ensure air ionization and allow particles to reach their saturation charge, the collection efficiency in the nanometric range presents high values [46,47,66]. However, low electric field values do not have enough force to ensure air ionization and particle charging and do not favor the balance between the maximum number of electrical charges that could be acquired by a particle and its electrical mobility (Figure 5) [46,66,67,136]. In these low electric fields, the influence of diffusion charging can be better verified. As seen from Figure 5c, it was found that most articles present a maximum efficiency point explained by the higher charge density required to collect particles smaller than 20 nm due to the fact of their high surface areas [133,135,137] in addition to the limitations imposed by their electrical mobility and charging inefficiency [67,136,138,139].

The fall in efficiency for particles smaller than 20 nm is due to the short lifetime they can remain charged due to the fact of their extremely small size. This is because electrons and ions can remain connected for only a few seconds, and this limits the ability of ESPs to intercept ultrafine particles [6,50,112]. In addition, by joining this charging limitation with its high electrical mobility, it makes collisions less likely and decreases the likelihood of them becoming charged [67,139]. The collection of particles at a nanometric scale is a problem that has been discussed for decades but which still presents itself as a challenge in several aspects. It is necessary to better understand the phenomena involved in the collection of particles so small and the influence of each operational and geometric parameter, as well as methods to favor diffusion charging.

4.2. Studies Involving the Use of Electrostatic Precipitators in Particle Collection

The presence of particles in the air can cause several health problems, mainly ultrafine particles or nanoparticles, as mentioned earlier. The use of electrostatic precipitators is well elucidated regarding the removal of micrometric particles. However, their application at the nanoscale range still requires research to optimize the collection efficiency. Several experimental studies on the use of ESPs are found in the literature. They are divided into three major strands: evaluation of operating conditions, use of wet precipitators and particle agglomeration, and evaluation of geometric conditions.

4.2.1. Evaluation of Operating Conditions

Most of the studies evaluate some operational conditions, be it velocity or residence time, voltage or electric field, concentration, humidity, or type of particulate matter. This is addressed in the works that focus mainly on the evaluation of such parameters. This was one of the first ways to investigate this process and determine the impact on the collection of nanoparticles. The main parameters and conditions used in the studies are shown in Table 1. It is important to mention that most of these studies used the particle size to calculate the efficiencies.

Table 1. Summary of studies with an evaluation of the operating conditions, agglomerants, and precharging/ionization.

Study	Type	Equipment Changes	Type of Agglomeration	Particle Material	Particle Size (nm)	Dimensions	Velocity or Flow	Voltage	Efficiency
Mertens et al. [140]	Dry, Wire-Tube	No	No	Diesel engine	5–200	L: 80 mm D: 58 mm	2.4 m/s	−10 kV	96%
Oliveira and Guerra [141]	Dry, Wire-Plate	No	No	NiO	<200	L: 300 mm H: 100 mm W: 40 mm	9.7 cm/s	−9 kV	99.9%
Oliveira and Guerra [142]	Dry, Wire-Plate	No	No	NiO	<200	L: 300 mm H: 100 mm W: 40 mm	3.3–9.9 cm/s	−8 to −10 kV	99.9%
Miller et al. [143]	Dry, Wire-Triangular Tube	Yes; - Portable; triangular cross-section	No	NaCl	30–400	W: 3 mm	55 cm ³ /min	−6.4 kV	86%
Roux et al. [144]	Dry, Wire-Tube	Yes; - Portable	No	Ambient	10–3000	L: 170 mm D: 10 mm	5 L/min	−8.5 to −9.9 kV	98%
Oliveira and Guerra [67]	Dry, Wire-Plate	No	No	NaCl	<200	L: 300 mm H: 100 mm W: 40 mm	3.3 cm/s	−8.0 kV	99%
Oliveira and Guerra [66]	Dry, Wire-Plate	No	No	NaCl	<200	L: 300 mm H: 100 mm W: 40 mm	6.6 cm/s	−7.9 to −8.2 kV	88.82%
Vaddi, Guan, and Novoselov [145]	Dry, Wire-Tube	Yes; Two stages: charging and collection - Corona needle - Rounded, rounded edge electrode	No	Ambient	10–150	L: 25 + 3 mm D: 3 + 3.5 mm	0.2–5 m/s	−3 to −5 kV	<85%
Yoo et al. [136]	Dry, Wire-Plate	Yes; - Two stages: charging and collection	No	NaCl	30–300	L: 60 + 197 mm W: 45 + 5.9 mm	1.9–4.1 m/s	−6 kV	93–98%
Nouri et al. [146]	Dry, Wire-Plate	No	No	Exhaust	200–1000	L: 200 mm H: 100 mm W: 100 mm	0.5 m/s	+32 kV	<90%
Liu et al. [147]	Wet, Wire-Plate	No	Yes; Chemical agglomeration	Flue gas	2.3–9314	W: 0.15–0.45 m	350 Nm ³ /h	−30 kV	<85% Up to 45% fewer ultrafine particles when using agglomerants
Bin et al. [148]	Wet, Wire-Plate	No	Yes; Chemical	Flue gas and anthracite ash	2.3–9314	W: 300 mm	350 Nm ³ /h	−40 kV	<85% Increase of up to 20% with ultrafine agglomeration particles
Bin et al. [149]	Wet, Wire-Plate	No	Yes; Chemical and turbulent	Flue gas and ash	7–760	L: 1300 mm W: 100 mm	15 L/h	−40 kV	<85% Increase of up to 15% with ultrafine agglomeration particles
Zongkang Sun et al. [150]	Wet, Wire-Plate	No	Yes; Chemical and turbulent	Coal ash	3–10,000	L: 3000 mm W: 100 mm	300 Nm ³ /h	−40 kV	<90% Increase of up to 11.5% with ultrafine agglomeration particles
Zongkang Sun et al. [151]	Wet, Wire-Plate	No	Yes; Turbulent	Coal ash	3–10,000	L: 3000 mm W: 100 mm	300 Nm ³ /h	−40 kV	<90% Increase of up to 11% with ultrafine agglomeration particles
Kim et al. [152]	Dry, Wire-Plate	Yes; - Addition of an electrospray	No	SiO ₂	Mean diameter of 180 nm	L: 150 mm H: 100 mm W: 25 mm	0.8 m/s	−9.5 kV	<80%
Kim et al. [153]	Wet, Wire-Plate	- Two stages: ionization and collection - Added wet pore electrodes in the collection stage	No	KCl	Mean diameter of 72 nm	- Ionization part: W: 40 mm - Collecting part: W: 120 mm D: 10 mm H: 120 mm - Carbon brush bundles: D: 7 mm, L: 3 mm	6.8 cm/s	- Ionization part: −3 kV - Collection part: −6.66 kV/cm	99.2%
Son et al. [154]	Wet, Wire-Plate	Yes; - Two stages: ionization and collection - Added wet pore electrodes in the collection stage	No	KCl	Mean diameter of 84.3 nm	- Ionization part: W: 40 mm - Collecting part: W: 120 mm D: 10 mm H: 120 mm - Carbon brush bundles: D: 7 mm, L: 3 mm	>0.4	13.3 kV/cm	99.5%
Sung et al. [155]	Wet, Wire-Plate	Yes; - Addition of an ion spray	Yes; Electrostatic	Ambient	250–230	- Ion spray: H: 85 mm L: 120 mm W: 180 mm	2 m ³ /min	−5 kV	<40%
Tepper and Kessick [108]	Wet, Wire-Plate	Yes; - Used electrospray to assist in aerosol ionization	No		300, 500, and 5000	- Ionization part: W: 26 mm - Collection part: L: 300 mm W: 20 mm	6 cm/s	+ 6.8 kV	90–99.9%

Table 1. Cont.

Study	Type	Equipment Changes	Type of Agglomeration	Particle Material	Particle Size (nm)	Dimensions	Velocity or Flow	Voltage	Efficiency
Teng, Fan, and Li [156]	Wet, Wire-Plate	Yes; - Atomization of charged water drop	No	Talc	<3000 nm More than 90% were nanoparticles	L: 400 mm W: 200 mm H: 200 mm	0.1–0.19 m/s	–2 to –5 kV/cm	<99%
Anderlohr and Schaber [157]	Wet, Wire-Plate	Yes; - Direct transfer of particles into liquid suspensions	No	SiO ₂	Mean diameter of 75 nm	L: 370 mm D: 54 mm	3.7 Nm ³ /h	–30 kV	99.99%
Chen et al. [158]	Wet, Tube-Plate	No	No	SiO ₂	30–10,000	W: 192 mm A: 0.034 m ²	0.062 m/s	–15 kV	99.2–99.7%
Dey and Venkataraman [159]	Wet, Tube-Plate	Yes; - Three sections: ion generation section, charging, and collection	No	Polystyrene latex	91 and 150 nm	- Ion generation section: D: 12.7 - Charging section: D: 32 mm - Collection section: D: 42 mm	50 cm ³ /s	- Ion generation section: 0–10 kV - Charging section: D: +4.2 kV - Collection section: D: –3.5 kV	<90%
Saiyasitpanich et al. [160]	Wet, Tube-Plate	No	No	DPM	10–10,000	L: 914 mm D: 178 mm	1.38–5.61 m/s	75 kV	<97.5%

L: length; W: width; H: height; D: diameter; A: area.

Some authors have proposed and evaluated electrostatic precipitation for particle removal of various types of real emissions, such as particles of gas treatment systems of a wide variety of medium- and large-scale industrial installations [140], in vitro collection of hygroscopic aerosols emitted from e-cigarette and heated tobacco products [161–163], ultrafine diesel particulate matter (DPM) generated from a nonroad diesel generator [160], nanoparticles emitted in semiconductor manufacturing [158], and nanoparticles emitted from a diesel engine [164]. Studies with electrostatic precipitation indicate that increased voltage causes an increase in the efficiency of nanoparticle collection. This is due to the fact of a larger electric field inside the equipment, which allows for greater ionization of the air, greater chances of collisions of nanoparticles with the ions, and, consequently, greater charging by diffusion. This was observed in studies by Miller et al. [143], Roux et al. [144] using a handheld ESP, and Oliveira and Guerra [141] using a lab-scale ESP. An interesting phenomenon called partial charging occurred in several studies with particles smaller than 30 nm [136,165–170], which caused a significant drop in efficiency.

However, studies in the literature with velocities below the typical rate (3 cm/s to 10 cm/s) indicate that low velocities increase the time of residence of particles in an ESP, allowing for a longer time for particle collision and favoring diffusion charging [7,66,67,106,107,171]. Vaddi, Guan, and Novosselov [145] verified that smaller particles have a lower transmission due to the increased particle charge resulting from their exposure to the electric field and ionic wind. In the rated velocity range, the increase in residence time increased the particle charge. In addition, there is favoritism of diffusion charging due to the fact of electrohydrodynamic flow. Of the few works that have managed to perform good removals at high velocities, Pirhadi, Mousavi, and Siotas [172] achieved a high PM_{2.5} removal efficiency using an ESP with a high flow rate (i.e., 50–100 lpm), where the optimized condition was a flow rate of 75 lpm and applied voltage of +12 kV.

However, such situations can also cause the sputtering of the electrodes, as indicated by Oliveira and Guerra [94], causing particle release and increasing the concentration of particles in certain diameter ranges in the ESP's output. Another point raised by Oliveira and Guerra [67] was that, usually, the evaluations of the residence time of several studies of the literature present a cross-influence of the particle concentration. A proportional variation in the particle feed flow rate with the gas flow rate, maintaining a constant concentration even in the evaluation of different velocities, is a better method to study the electrostatic precipitation phenomenon. In addition to the concentration and residence time, the relative humidity of the gas also affects the performance of electrostatic precipitators. Nouri et al. [146] verified that the collection efficiency increases with the increase in moisture, probably due to the increase in the conductivity of particles in the presence of

water on its surface and, especially, due to the increase in the cohesiveness of particles in the collecting electrodes and the particle charge in the space between the electrodes.

The evaluation of the operational conditions in the collection of nanoparticles has already been widely investigated and consolidated in the literature. Thereby, it is encouraging to seek new ways to optimize the process of electrostatic precipitation for the removal of nanoparticles. Such optimization involves, in addition to operational parameters, changes in the characteristics and configurations of the equipment, evaluation of the influences of geometric parameters, and agglomeration of particles to facilitate collection by the electrostatic precipitator.

4.2.2. Use of Wet Precipitators and Particle Agglomeration

As demonstrated before, there is difficulty in collecting particles so small due to the complexity of the diffusion mechanism and the difficulty of charging. In an attempt to increase the collection efficiency with wet ESP, several authors have made modifications to the equipment, such as adding wet pore electrodes in the collection stage in addition to always maintaining the environment with high humidity [153,154], transferring the particles from the gas phase to the liquid [157], or using a continuous flow of liquid over the collection plate [159].

One way to increase the filtration efficiency is by particle agglomeration, that is, by increasing the diameter of the particles. In this way, field charging becomes preponderant and makes the process simpler. Several techniques can be used to perform this agglomeration, and Figure 6 demonstrates the main ones (chemical, turbulent, and electrostatic). Wet precipitators are generally used when agglomeration techniques are used, as in addition to favoring agglomeration, it also favors the removal of particles in the collecting plates. In the case of chemical agglomeration, the choice of the substances used is a key point, as they can affect the resistivity of the material and its chemical characteristics [8,147]. Techniques such as turbulent agglomeration and electrostatic agglomeration are still new technologies and have disadvantages in relation to the conventional process, such as the need to use substances, increasing the cost of operation, and the need for major changes in projects, which increase installation costs [8].

Several studies in the literature make use of a size range that varies from the nanometric to the micrometric scale when evaluating the agglomeration. However, the focus of agglomeration is on ultrafine particles due to the benefits mentioned earlier. A study developed by Liu et al. [147] used agglomerants solutions (xanthan gum 0.05% and pectin 0.05%) together with a humidifying agent and a pH controller. Using xanthan gum as an agglomerant agent, it was observed that there was an increase in the size of the particles of up to four times, while for pectin there was a reduction of 47.4% in the mass concentration of the fine output. Bin et al. [148] found that a sodium alginate solution increased the average particle diameter from 0.1 μm to 1 μm . In another study, Bin et al. [149] used a similar experimental device but with a pretreatment using chemical and turbulent agglomeration, with good performance, increasing the particle diameter from 0.07 to 0.76 μm . Along the same line, Zongkang Sun et al. [150] also suggested the combination of chemical and turbulent agglomeration. In another work, Zongkang Sun et al. [151] evaluated only the types of turbulent agglomerants for the removal of fine particles emitted in coal combustion. More information on increased efficiency can be seen in Table 1.

Another method was employed by Kim et al. [152], Sung et al. [155], and Tepper and Kessick [108], who used an electrospray system to charge or agglomerate the particles (similar to Figure 6c) by spraying water droplets charged into the system or via a precharger [173,174]. In addition to observing an increase in efficiency, the authors also noted the possibility of reducing ozone emissions, a common problem in electrostatic precipitation. Instead of using traditional water film and mechanically atomized spray, Teng, Fan, and Li [156] investigated particle removal with the atomization of a charged water drop. The efficiency of collection increased by up to 4%. The authors found that the

atomization of the charged water drop resulted in significantly reduced water consumption while also maintaining removal efficiencies at a level comparable to traditional processes.

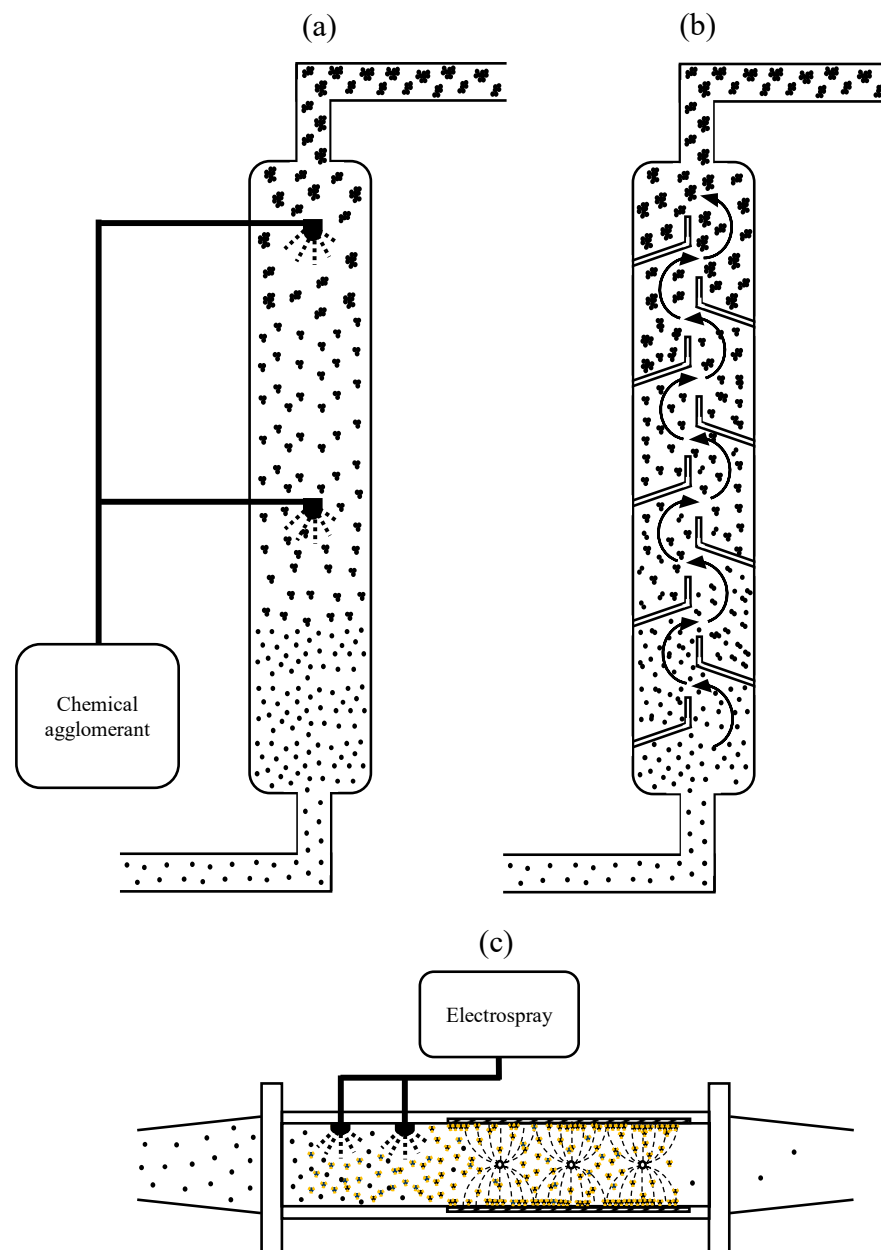


Figure 6. Schematic representation of (a) chemical agglomeration; (b) turbulent agglomeration; (c) electrostatic agglomeration.

Table 1 presents a comparison of all studies evaluated so far, informing on the main conditions employed and the best collection efficiency. It can be verified that most articles with agglomeration obtained an increase between 10 and 40% in the collection efficiency. However, the efficiency continued to remain close to other works that only evaluated the operational conditions (as can also be seen in Table 1). In addition, chemical agglomeration may cause increased operating costs by the addition of polymers and other substances, as well as the generation of wastewater with polymers, stabilizing agents, and acids, which will require treatment processes for disposal. However, this process can be advantageous in the case of an already active plant that cannot make major changes.

Another approach is the evaluation of the best geometric conditions in the design of nanoparticle collection equipment. Studies in this area, in addition to helping to under-

stand the real impact of such parameters on a nanometric process, also contribute to the development of new configurations for this equipment.

4.2.3. Evaluation of Geometric Conditions

Most studies focus on verifying the influence of operating conditions on the removal of nanoparticles. Thus, it is encouraging to look for new ways to optimize the process of electrostatic precipitation for the removal of nanoparticles. This optimization involves, in addition to operational parameters, the evaluation of the influences of geometric parameters on the collection of nanoparticles. The main strategies adopted by the authors were to change the layout of the elements of the equipment, such as in the work carried out by Li et al. [175] in which a new type of wet electrostatic precipitator was designed, where the discharge wires were connected directly to the surface of a dielectric plate to facilitate the installation of the wires, minimize the particle deposition, and reduce the emission of ozone while maintaining a high efficiency of particle collection (80–100%). In the evaluation of a double-stage ESP, one working as an ionizer/charger and one as a collector, Chen et al. [176], Dobrowolski et al. [37], and Huang and Chen [177] verified high removals in addition to concluding that it is economically feasible to use single-stage precipitators for particles smaller than 16 nm and double-stage for particles larger than 16 nm. Another aspect is to change the shape of the discharge electrode to increase the current emission and the electric field. In this respect, a study by Yang et al. [174] showed that the corona current and the maximum collection efficiency were classified in the order of pins, sawtooth, and rod type. It is important to note that these electrodes can be found in different shapes, from a simple round wire, square or barbed wire to so-called controlled emission electrodes for specific tasks [178,179]. The presence of pointed elements, called emitters, assists in the formation of corona discharge [106]. When evaluating the geometry of the plates, they can be found with different configurations, such as a flat plate, plate with chicanes [106,179], or barbed plate [180]. The location of these electrodes can also influence the process. In general, they are usually placed in the space between the collecting electrodes or above the collectors from an isolated structure [50].

Several authors have also evaluated the geometric conditions that inhibit some phenomena that can affect the collection efficiency of nanoparticles, such as electrostatic shielding and electro-hydrodynamic flow. Authors such as Ning et al. [131], El Dein and Usama [181], and Andrade and Guerra [47,182] showed that a greater number of wires favors particle collection due to the greater number of current emitters. When evaluating the diameter of the wires, they verified that the smallest diameter led to a lower voltage for the beginning of the corona and higher current values for all applied voltages. It is important to note that for the same applied voltage, the current in smaller diameter wires is more intense than the current emitted by larger diameter wires [47,183]. When increasing the wire spacing, there was an increase in the current and breakdown point, explaining this fact, again, by the effect of electrostatic shielding [46,47,131,181]. Lima and Guerra [46] evaluated the wire spacing and plate spacing in the collection of nanoparticles under the perspective of diffusion charging and electrostatic shielding. The authors determined that there was an increase in the current with the increase in the wire spacing and was associated with the decrease in electrostatic shielding. The larger plate spacings also had a greater influence on this phenomenon. It was also observed that the impact of this phenomenon on the collection of nanoparticles is greater before the particles reach their saturation charge by the diffusional mechanism.

It also has gaps concerning the understanding of electrostatic shielding and how other geometries can influence this process. In addition, it is necessary to conduct a mathematical evaluation and simulation of its effect and model its process exclusively with nanoparticles. However, developing a complete model presents great difficulties due to the complexity of the diffusive process. It is also important to keep in mind that these geometric changes are ways of allowing for an increase in the velocity used, since efficient collections of nanoparticles are usually obtained at low velocities. There are also limitations as to the

diameter range collected, even in the nanometric range. As previously demonstrated, particles smaller than 20 nm tend to have a low collection efficiency due to the fact of their greater electrical mobility. When verifying the research, there is a scarcity of studies evaluating these topics.

Electrostatic precipitation was not initially suggested for submicrometric particles due to the fact of its low efficiency [50,105]. Although the above studies showed high efficiency (up to 99%), most focused on the laboratory scale. Scale ups should be very well studied to ensure that these efficiencies will occur in an industrial plant. Until then, the largest focus was on indoor rooms, such as cleaning small environments and cleanrooms [8,46]. Other equipment, such as filters, usually has a greater prominence when it comes to this scale. As can be seen below, there are several studies at the laboratory and industrial scales, with reasonable efficiency, as well as optimizations involving the development of more efficient filter media with differentiated techniques that allow for a better collection of nanoparticles.

5. Use of Filters in the Collection of Nanoparticles

5.1. Filtration Process

Filtration is one of the most common methods for removing particulate matter from the air, capturing particles from the synergistic effect between physical barriers of the fiber and the forces of adhering to particles [6,184]. Fibrous filters are simple and economical materials capable of efficiently removing aerosol particles with high efficiency in different media, from industrial equipment to indoor environments and automotive cabins [43,185]. Although the process of filtering aerosol particles in fibrous filters is very complicated, its theory is quite consolidated and based on the assumption of basic single-fiber filtration efficiency [43,184–188].

Usually, three stages of filtration can be observed in the collection of particulate matter. In stage 1, there is internal filtration with effects on the structure of fibers and particles. The fiber is clean and there have been no changes due to the particles being captured in the filter. In stage 2, there is also internal filtration but with great retention capacity. Particles are effectively captured by adhesion forces and the properties of the filter media, such as the efficiency and pressure drop, change over time. In stage 3, surface filtration occurs with the particles filtering themselves. The formation of the cake causes particles to be collected almost perfectly by cohesive forces, and there is a linear increase in the pressure drop [184,189,190]. Several filtration mechanisms govern the interactions between the fibers of the filter media and the particles. These mechanisms are generally affected by the fluid flow, fiber diameter, and particle size. Taking into account these characteristics, the main mechanisms of particle collection involved in filtration are Brownian diffusion, interception, impaction, and gravitational or electrostatic attraction [184,186], as shown in Figure 7.

The diffusional mechanism is the result of Brownian motion, since the particles move from their initial trajectory randomly, which allows for the shock with the fiber and, thus, its capture. This type of mechanism primarily captures particles with sizes below 0.1 μm under low gas velocities. The interception mechanism is given when the particle is captured by simply approaching the fiber, attracted by the forces of Van der Waals. This mechanism occurs when the particle radius is equal to or greater than the particle/fiber distance. The interception mechanism occurs with particles from 0.1 to 1 μm , and the interception capture efficiency increases with an increased particle size [186,191]. When a sudden change in air velocity occurs, particles larger than 1 μm cannot maintain the same direction as the airflow current lines. Thus, these particles are part of the current line and deposit in the fibers along their original trajectory. Passing through the filter becomes more difficult for particles at high velocities [186,191]. When the filters are electrostatically charged or when there is an external electric field, it is possible to attract the particles by the particle/fiber electrostatic attraction mechanism [188,192]. This mechanism can retain submicrometric particles without increasing the pressure drop. However, filtration conditions change to nanoscale filters, which would change the aerodynamic behavior of airflow. The efficiency

of the filter media can increase in this case without changing the air resistance of the filters [186,191], also called permeability. In high-efficiency air filters, the action of gravity becomes negligible, since when it comes to ultrafine particles (less than $0.5\ \mu\text{m}$) gravity has no contribution to their removal [191].

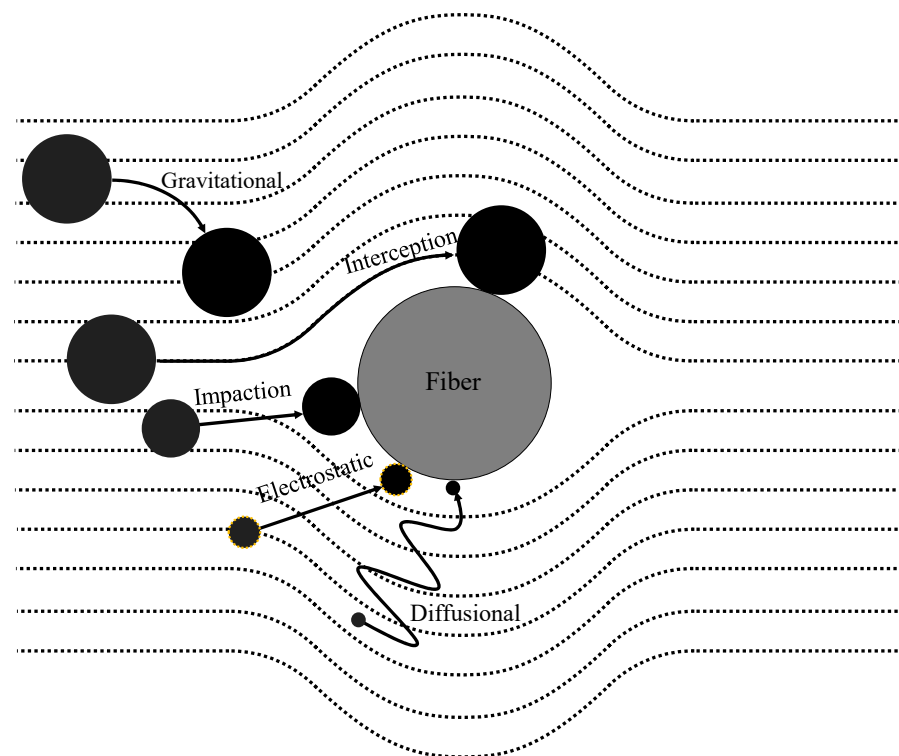


Figure 7. Particle collection by Brownian diffusion, interception, impaction, gravitational, and electrostatic mechanisms.

The combined effect of these capture mechanisms results in mechanical filtering efficiency. The filter collection efficiency for various particle sizes under different face velocities (correlated to particle velocities) combined with the collection mechanisms can be seen in Figure 8. The equations and conditions used in the figure can be found in the book by Hinds [6]. In Figure 8a, it is noted that the increase in the collection of particles by Brownian motion occurs with a decreasing particle size. An increased interception filtration, inertial impaction, and gravitational sedimentation occur with an increasing particle size. The effect of face velocities on the filter efficiency as a function of the particle size is shown in the graph in Figure 8b. The maximum efficiencies are observed at lower face velocities [6,193].

For decades, it was considered that the mechanism of collecting nanoparticles on the filter surface was due to the fact of its Brownian motion [187]. However, due to the extremely small size and the possibility of nanoparticles behaving like a gas molecule, a phenomenon called thermal rebound can occur [43,187,194]. This occurs when the nanoparticle has a kinetic energy greater than the fiber adhesion energy or when energy loss occurs during impact [43]. This causes the particle to ricochet and not be captured, so it is believed that the filtration efficiency decreases for these small particles [187]. If you consider that particles follow a Maxwell–Boltzmann distribution, this phenomenon depends on the thermal velocity of the particles, their diameter, fiber characteristics, and other molecular-level interactions [43,187,194].

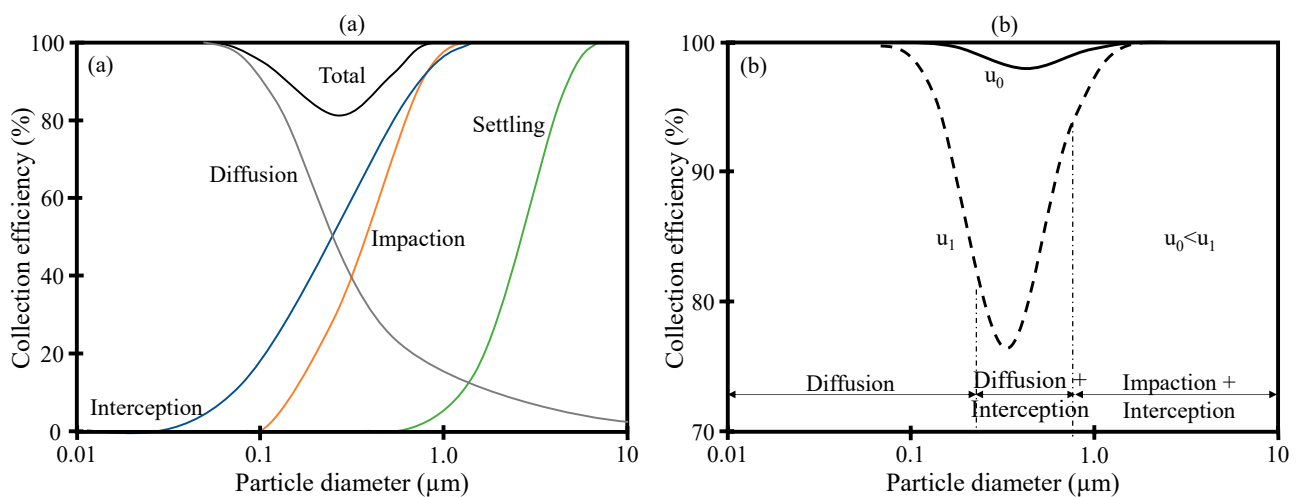


Figure 8. (a) Collection efficiency curves from the combined effects of particle capture mechanisms and total efficiency; (b) total efficiency for two different face velocities. Values of $u_0 = 1 \text{ cm/s}$, $u_1 = 10 \text{ cm/s}$, and mean fiber diameter of $2 \mu\text{m}$ were used. Adapted from Hinds [6].

After the collection of particles by filters and the formation of the cake, air pulses are usually used to clean the filter media [189,190]. However, this procedure causes large emissions of particles in the clean area [189]. But it is important to note that the operation with submicrometric aerosols or nanoparticles is usually performed at low velocities, mainly to favor the diffusion mechanism that is predominant in this range. Thus, it is expected that the time of variation for the pressure drop is long enough and takes time to occur in the formation of the cake [184].

To obtain the best specification for a given application, it is essential to know the physical, chemical, and thermal properties of the filter media, which must be compatible with the gas and powder to be collected. Among the properties that should be analyzed are air permeability, tensile strength, abrasion resistance, chemical resistance, operating temperatures, textures, and physical finishes [195,196]. In addition to these, fiber diameter and porosity also exert a direct influence on the filtration [197]. To characterize the performance of a fibrous media, two parameters are used: filtration efficiency and pressure drop. These two parameters are related to the geometric characteristics of the medium, particle characteristics, and operating conditions [188]. Another parameter usually analyzed is the most penetrating particle size, which is defined as the particle size for which the filters have the lowest collection efficiency [6,43]. An ideal filter should have a high collection efficiency with a low-pressure drop.

The particle shape can also affect the collection efficiency. Particles with spherical shapes tend to penetrate the filter media more than particles with irregular shapes. Thus, the filtration efficiency for spherical particles is higher than for irregular particles with the same equivalent diameter [198]. The reason for this fact is associated with the movement of particles on the surface of the fibers. Spherical particles slide or roll, and irregular shapes slide or fall when they collide with the fiber. In this way, the probability of the retention of irregular particles is lower, as the contact surface between the fiber and the particle is smaller [43]. Another parameter that influences the particle collection efficiency is the airflow. Increased airflow causes a decrease in the collection efficiency, since the residence time for high airflow values is lower, making collection difficult with the predominance of the interception mechanism. For lower airflow values, that is, a longer residence time, diffusion and electrostatic mechanisms predominate [198].

The probability of collision between particles and fibers in a streamline is increased due to the abnormal motion of the particles. The diffusion rate becomes more perceptible as the particle size or face velocity decreases. Thus, the diffusion mechanism is more effective in ultrafine particles and nanoparticle filtration than interception [198]. However,

the efficiency of collecting particles with diameters of approximately 0.3 μm is generally minimal, and this particle size limits many filtration test methods. Face velocity and fiber size influence the most penetrating particle size range [193]. Therefore, the development of filters and technologies capable of capturing particles with diameters smaller than 0.3 μm is the objective of some studies.

5.2. Studies Involving the Use of Filters and Membranes in the Collection of Particles

The growing demand for air filters with a high filtration efficiency and low-pressure drops has led several authors to look for ways to achieve this goal in an economically viable way. In addition, the evaluation of nanoparticles has several different characteristics because of the collection mechanisms, and it is important to evaluate the behavior of efficiency and permeability in different filter media. Within this scenario, microfibers and nanofibers are also interesting in the diameters compatible with the size of the nanoparticles. In addition, the introduction of substances and/or nanoparticles can functionalize the fibers and provide different properties, such as microbial, virucide, catalytic, and electrical activity. Several studies on the use of filters and filter media are found in the literature. They are divided into four major topics: evaluation of different filter media and operating conditions; development of filter media with nanofibers; coating, precoating, and other surface treatments; and hybrid filters and electrostatic filtration.

5.2.1. Evaluations of Different Filter Media and Operating Conditions

Several filter media with microfibers can be used to collect nanoparticles with reasonable efficiencies, such as fiberglass filters, fibrous filters, quartz, and high-efficiency particulate air (HEPA) [199–203]. The most diverse types of membranes can be applied in the collection of nanoparticles, such as recycled polyethylene terephthalate (PET) produced by electrospinning [204], membranes manufactured by dry stretching of hollow fibers of polypropylene [205], fluidized bed filter [206], and all metallic stainless-steel screen mesh filters [207]. Research with fiberglass filters is also common in the literature due to the fact of its advantages, such as being low cost, catching larger debris, and not impeding airflow [208–210]. In addition to glass fibers, some authors also evaluated the collection of NaCl nanoparticles by polytetrafluoroethylene [208] and polypropylene filters [208], and cellulose [210]. Kim et al. [209] verified that, for particles smaller than 2 nm, the penetrations of these particles increased with a decrease in the particle size, in addition to a possible phenomenon of thermal rebound.

The above studies used systems that simulated the contamination of nanoparticles in an airflow. Other studies evaluated the collection of real emissions, such as emissions during 3D printing [211], waste incinerators [212], chassis dynamometers and on a road [213], heavy-duty diesel engines operating with fuels with sulfur levels relevant to marine operation [214], and hygroscopic aerosols emitted from e-cigarette and heated tobacco products [215–220]. Emissions of biological materials, such as viruses and bacteria, are also the focus of several studies that verified the efficiency of filter media used in personal protective equipment [221–224]. Numerical research was carried out in several studies, but the focus on the development of models and theoretical investigations occurred only in some studies [225–229]. Several authors have developed and suggested methodologies for filtration tests involving the collection of nanoparticles [230–233].

Table 2 summarizes several works related to the study of filters for collecting nanoparticles. Some of these studies are described with more information. Different types of filters were evaluated with low surface velocities (<1.5 m/s). Particles were collected in size ranges that include nanoparticles. It can be observed that most of the evaluated filters, within the described conditions, presented collection efficiency above 95%.

Table 2. Summary of parameters used in nanoparticle filtration studies.

Filters	Diameter Nanoparticle (nm)	Surface Velocity (m/s)	Emission Source	Main Results	Study
MERV 8; MERV 14; HEPA	300	0.25–1.50	Airflow	The most penetrating particle size was 0.3 μm	Brochot et al. [199]
HEPA + fiberglass; HEPA + micro quartz	7.4–289	0.05	Airflow	Efficiency of up to 99% and quality factors of 0.01	Bortolassi, Guerra and Aguiar [201]
HEPA + fiberglass; HEPA + micro quartz	7.4–289	0.05	Airflow	Efficiencies higher than 99.9% for up to 1 h	Bortolassi, Guerra and Aguiar [202]
PET nanofibers	7–300	0.05	Airflow	Efficiencies higher than 99.99%	Bonfim et al. [204]
Polypropylene fibers	18.1–100	0.05–0.15	Burning incense sticks	Efficiencies higher than 99% (>60 nm) and between 69 and 86% (<60 nm)	Bulejko et al. [205]
Respirator filters; Granular activated carbon	1.5–30	0.033–0.16	Airflow	Fibrous filters: 100% efficiency (>0.3 nm) Activated carbon: efficiencies of 90 to 99.5% (>0.3 nm)	Kim, Kang and Pui [203]
Fluidized bed filter with carbon nanotubes	50–300	0.016–0.017	Airflow	Efficiencies above 99.70%, and the larger the bed the greater the efficiency	Wang et al. [206]
Stainless-steel screen mesh filters	3–20	0.095	Airflow	Evaluate the behavior of the collection, thermal recovery, and thermal rebound	Shin et al. [207]
Fiberglass; Polytetrafluoroethylene; Polypropylene filters	13.6–532.8	0.03–0.21	Airflow	The efficiency was 99.07% for polytetrafluoroethylene, 98.23% for fiberglass, and 95.84–98.73% for polypropylene	Zhou et al. [208]
Fiberglass filters	2–100	0.025	Airflow	The penetrations of the particles increased with the decrease in particle size (for particles < 2 nm)	Kim et al. [209]
Cellulose and glass fibers (HEPA and ULPA)	10–100	0.053–0.096	Airflow	Best efficiency: HEPA H14, and ULPA U15 filters	Golanski et al. [210]
Activated carbon filter; Electret and antibacterial filter; Polyethylene filter; Nanomembrane filter; HEPA filter	10–420	0.042	3D printing	Efficiency: HEPA filter (99.95%), nanomembrane filter (95.66%), activated carbon filter (94.34%), polyethylene filter (92.89%), and electret filter (70%)	Kwon et al. [211]
Polytetrafluoroethylene fibers; Polyimide fibers	15	0.015–0.10	Waste incinerators in commercial needlefelt	Efficiency above 90%	Förster et al. [212]
-	>23	-	Heavy diesel vehicles, vehicles with port fuel injection engines, and gasoline direct injection passenger cars	The highest emissions were measured for heavy vehicles and vehicles with port fuel injection engines.	Giechaskiel et al. [213]
Glass fiber; Polytetrafluoroethylene membrane; Tissuquartz membrane	14–600	-	Heavy-duty diesel engines	None of the filters were more effective	Ushakov et al. [214]
Certified masks; Noncertified masks	50–300	0.37	Airflow	Certified masks efficiency above 90%, noncertified masks below 80%	Lee et al. [221]
Face masks	40 (median)	0.465	Airflow	N95 2 layers, KN95, 3M 8511, and FTR467 ULPA: efficiencies higher than 95%	Hill, Hull, and MacCuspie [222]
N95 respirators	20–800	-	Airflow	The most penetrating particle size is ~45 nm	Rengasamy and Eimer [223]

There has been progress in research, and the results show that it is possible to obtain high efficiencies for fine particles. To efficiently remove particles from the air, filters must be able to intercept particles with a wide range of possible diameters. Therefore, fine fibers, compact stacking structures, and sufficient thickness are characteristics that increase

particle capture efficiency [234]. The demand for these properties has been increasing in recent years and with it the development of filter media produced by nanofibers.

5.2.2. Coating, Precoating, and Other Surface Treatments

One of the easiest ways to add new properties and improve a filter's efficiency is by adding coatings to the surface of fibers. These coatings are added to the surface of membrane fibers, allowing them to have a greater affinity with certain substances. Therefore, it is possible to increase the filtration efficiency of filter nanoparticles that previously had low efficiency at this scale. In a study by Liu, Pui, and Wang [235], three filters (one of nonwoven nylon and two of nonwoven polyester) were coated with a polytetrafluoroethylene membrane. Chen, Ji, and Qi [236] modified the surface of glass microfiber filters using low-pressure plasma technology. Modifications were also made for the filters to acquire oleophilic or oleophobic characteristics. Innocentini et al. [237] used commercial filters of α -SiC foams coated with Si₂N₂O nanowires through an in situ process of catalyst-assisted pyrolysis. The efficiency of the nanoparticle collection was greater than 99% and similar to groups of EPA (E12) and HEPA (H13) filters. Cho et al. [238] used a cellulose substrate to electrospun polyacrylonitrile nanofibers with and without TiO₂ nanoparticles. The evaluation of coatings with catalytic capacity and focused on VOC removal was performed by Zhang et al. [239] and Dai et al. [240], using a metal–organic framework (MOFs) and MnO₂ nanocrystals, respectively.

The use of coatings for the introduction of biocides characteristics has been widely investigated in the literature, for example, by employing coatings with AgNO₃ [241], *Sophora flavescens* [242], carbon nanotubes [243], silver nanocluster/silica composite [244], Ag nanoparticles [245], imidazole nanoparticles (IMI) and Ag [246], Cu nanoparticles [247], Ag, Zn, and Fe [248]. With the global COVID-19 pandemic, several studies have focused on removing this virus from the air and the use of coating was highly evaluated, such as coatings of Ag/TiO₂ [249], CuO nanoparticles [250], and Ag nanoparticles [251]. Evaluations of other viruses, such as MS2 bacteriophage, were performed in the work of Park et al. [252], with SiO₂/Ag nanoparticles coating, and the work of Joe et al. [253], with SiO₂ nanoparticles coated with Ag nanoparticles.

A different approach was carried out in the work of Andrade, Sartim, and Aguiar [254] with polyester filters. The authors used the technique of precoating with hydrated lime and dolomite limestone to evaluate the effects on the collection of powder from the steel industry and nanoparticles. The results were compared with a polyester filter with polytetrafluoroethylene membrane (PTFE). The results showed that precoated polyester had a longer cycle duration and lower pressure drop than polyester with a PTFE membrane. The efficiency was higher with precoating with dolomitic limestone than with hydrated lime. However, the polyester filter media with PTFE membrane presented the best results when only nanoparticles were evaluated, presenting a collection efficiency greater than 90%.

5.2.3. Development of Filter Media with Nanofibers

In recent years, thanks to the emergence of nanotechnology, new devices have been developed with high performance for air purification using nanofibers. Nanofiber membranes have a large specific surface area, controllable morphology in the process, porosity, and structure with interconnected pores, characteristics of the interest in the field of filtration, as it allows for the development of filtering media with a low-pressure drop, high filtration efficiency, dust holding capacity, and high productivity. With the development of nanotechnology and the possibility of producing nanofibers at an industrial scale, several companies started to use this type of filter media in their products, such as fiberglass, PTFE, and fluororesinone [255]. Another approach was carried out by Tang et al. [256] who introduced nanofibers into fibrous filter media and developed an appropriate method for applying these nanofibers.

The above studies focused mainly on the evaluation of commercial filters in the collection of nanoparticles. However, the development of new materials is important for

improving the efficiency of collection and adding new characteristics to the filter media for applications in various areas. Furthermore, the filtration process using nanofibers can be improved by changing the fiber diameter or through new designs, such as a spider-net structure [257], inducing electrostatic force in nanofibers, multistructured electrospun nanofibers, as well as through the functionalization of nanofibers in order to improve properties, such as antiviral and antibacterial activity [2]. To exemplify, Li et al. [258], developed bead-shaped PAN nanofiber membranes with graphene oxide and evaluated their performance as an air filter. During electrospinning, the continuous jet of polymeric solution can be interrupted and, due to the instability, there is the formation of bead structures in the nanofibers [259]. The membrane developed by Li and coworkers was compared with other commercial filters and PAN fibers, and due to the fact of its high porosity, the pressure drop was 8 Pa and the collection efficiency was 99.97%. In another example, Kim et al. [260] modified the surface of PAN nanofibers using an oxygen plasma treatment. The results showed a decrease in the diameter of the nanofibers and an increase in the surface roughness, generating electrostatic attraction, which was reflected in the increase in the filtration efficiency.

The electrospinning technique is widely used in the production of nanofibers, since the fibers produced have a uniform appearance, in addition to allowing for the use of various polymeric solutions, such as polyurethane [261], cellulose acetate [262], poly(vinyl alcohol) [263], and even polymeric waste, such as PET [264], with a very wide range of applications [265–267]. This technique has also been evaluated numerically allowing to relate the electrospinning control parameters (such as the flow, electric field, concentration, and electrospinning time) with the morphology of nanofibers, permeability, and collection efficiency for particles [268,269].

Another way to functionalize the fibers and introduce new properties is by adding nanoparticles to the polymeric solution used in the electrospinning process, such as coaxial fibers of poly(m-phenylene isophthalamide) (PMIA) as the core and polyacrylonitrile (PAN)/Ag nanoparticles as the shell [270], polyvinyl alcohol solutions containing TiO₂ nanoparticles and activated carbon [271], doped with Ag nanoparticles [272], or coated with Ag, TiO₂, and Ag/TiO₂ [273], improving the mechanical properties and introducing a biocide characteristic. Fibers at a nanometric scale have diameters compatible with several molecules, as well as the size of viruses and bacteria, making them attractive for application in filters with catalyzed and biocidal action, making possible the retention of these pathogens. They also have an improved service life and great particulate material retention capacity [191].

Furthermore, the introduction of nanoparticles can also allow for the introduction of an electrostatic characteristic, producing electret filters. Some particles that can be used are SiO₂ nanoparticles [274,275], boehmite nanoparticles [276], SiO₂ nanoparticles modified by γ -glycidoxypropyltrimethoxysilane as a charge enhancer [277], and polytetrafluoroethylene nanoparticles as charge enhancers [278]. Another way is to produce fully polymeric electret fibers, as suggested by Li et al. [279]. The authors did not add charge intensifier nanoparticles and were able to prepare hybrid electret fibers by studying the complementarity of the electrical responses between electrolyte polymers. The coupling of electrical polarization behaviors of polystyrene, with a low dielectric constant, and polyvinylidene fluoride fluoride, with a high dielectric constant, allowed the hybrid fibers to present an improved electret effect and high porosity. Charges injected into the matrix of polystyrene fibers generated local electric fields showing the same direction as the external electric field; however, the orientation of the polyvinylidene fluoride fluoride dipoles generated local electric fields in the opposite direction to the external direction. An interesting point of the work was that the property of the electrode was obtained without relying on toxic nanoparticles as charge intensifiers, which was never previously reported in electrospun electret fibers and melt electret fibers.

Other studies also used the electrospinning technique and obtained nanofibers of poly(vinylidene fluoride)/polystyrene [280], soy protein isolate/polymide-6/silver ni-

trate [281], chitosan/polymide-6 [282], polyester/cyclodextrin [283], polyvinyl alcohol/co/polyethylene/TiO₂ [284], polyvinyl alcohol/co/polyethylene [285], polysulfone/polyacrylonitrile/polyamide-6 [286], polydopamine/coated halloysite nanotubes [287], polyimide/SiO₂ [288], polyacrylonitrile/SiO₂ [289], polysulfone/titania [290], polylactic acid [291], polylactic acid/chitosan [292], polyacrylonitrile/MOF [293,294], polyacrylonitrile/TiO₂/Ag [295], polyacrylonitrile-MgO [296,297], polyethersulfone/BaTiO₃ [298], poly-3-hydroxybutyrate/TiO₂ [299], curly wool-like polyvinylidene fluoride nanofibers [300], and polylactic acid/polycaprolactone/Ag/Zn [301].

Some authors suggest a modification of the electrospinning technique for application without needles [302,303], allowing to obtain fibers smaller than 100 nm, a high efficiency, and bacterial activity. Other methods employed were meltblowing [304], force-spinning [305], and a cold-pressing method, including paste extrusion, stretching, and heating [306]. The mixture of different techniques for the production of nanofibers was evaluated by Zhang et al. [307] (electrospinning techniques with physical bonding processes) and Xu et al. [308] (meltblowing with electrospinning).

A summary of these studies is shown in Table 3. It is important to mention that most of these studies used the particle size to calculate the efficiencies. The use of filter media with nanofibers allowed for increases in the collection efficiency of nanoparticles and air permeability. In addition, the various processes of making these materials also proposed significant advances in the filtration of bioaerosols and the addition of nanoparticles with different properties. It is important to note that this area has great development potential, and some processes still need to be optimized to make their use economically viable.

The use of nanofibers in the filtration process has been considered as a new generation of materials capable of efficiently removing pollutant particles due to the fact of their characteristics such as high specific surface area, high porosity, and the possibility of building new designs. Despite the great potential of using nanofibers in filtration processes, there are still many challenges to be solved: (i) the use of different supports for the deposition of nanofibers shows that there is a need to improve the mechanical properties of nanofibers, enabling their use in more severe conditions; (ii) one of the challenges that must be faced is the use of toxic solvents for the production of nanofibers, which has led some research groups to explore less toxic solvents or so-called “green solvents”; (iii) many of the nanofibers production processes are still at the laboratory scale, and this shows the need to both improve the electrospinning process as well as to develop new products and technology capable of increasing the scale of production; (iv) with the development of new structures employing nanofibers, new models could be developed that would be able to describe the filtration efficiency and the pressure drop for different nanofiber structures; (v) for nanofibers functionalized with 0D, 1D, or 2D structures, care must be taken to ensure that these nanostructures do not become detached during use, and this adhesion strength of nanoparticles reflects on the reuse of filters and also on the safety of those who use them by preventing the detachment of, for example, nanoparticles; (vi) the use of recycled polymers which, together with green solvents, would make the electrospinning process more ecofriendly; (vii) the use of nanofiber membranes under real conditions and with real samples would lead to approaches for the use of more realistic nanofibers.

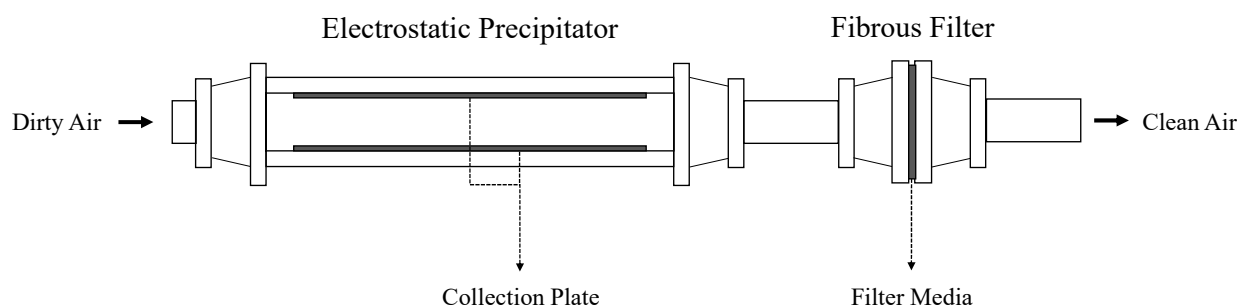
As a recommendation for new researchers and new works, it is important to ensure the production of nanofibers with a more environmentally friendly process by exploring recycled polymers and nontoxic solvents and providing conditions for nanofibers to go beyond laboratory limits.

Table 3. Summary of various nanofibers for air filtration.

Technique	Materials	Diameter (nm)	Basis Weight (g/m ²)	PMs (μm)	Air Flow Rate (L/min)	Efficiency (%)	Pressure Drop (Pa)	QF (Pa-1)	Mechanical Strength (MPa)	Study
Electrospinning	PAN/GO	90	0.35	2.5	5.3	99.97	8	1.033	-	[258]
Electro-blow spinning	Polysulfone (PSU)	105	5.5	0.3	95	63.26	55	0.18	1.18	[309]
Electrospinning	Poly(aryl sulfide sulfone)/GO@silver	403	-	2.5	32	99.63	79.17	-	2.39	[310]
Electrospinning	Poly(vinyl alcohol)	150	-	1	22	89.07	220	0.01	-	[311]
Supersonic solution blowing (electrospinning and supersonic gas blowing)	Waste cigarette butts nanofibers between two spunbond polyester membranes	92.4	1.55	2	90	99.99	50.4	0.06	-	[312]
Electrospinning	PAN/cooper chloride (CuCl ₂)	117–522	-	2.5	2–7	93–99.9	20–80	0.04–1.2	-	[313]
Electrospinning	PAN/polydopamine-coated halloysite	200–250	-	Bioaerosol (<i>S. aureus</i>)	0.5	99.97	60	0.14	-	[287]
Electrospinning	Polyvinylidene fluoride (PVDF)/TiO ₂	286	-	Bioaerosol (<i>S. aureus</i>)	27.3	99.88	68	-	-	[314]
Electrospinning	Polyamide 6 (PA6), poly(vinyl pyrrolidone) (PVP), chitosan (CS), and curcumin (Cur)	297	-	0.3	32	99.83	54	0.118	-	[315]
Electrospinning	PAN/ZnO	200–300	0.4	0.1–4	160	99.86	486	-	-	[316]
Solution blow spinning	Nylon/silver nanoparticles	173	1	0.3	32	98.63	110	0.04	1.7	[317]
Electrospinning	PAN	404	-	0.3	5.5	99.60	62	0.09	-	[318]
Electrospinning	Polyamide-imide	1000	16.3	0.1–10	20	84.24	46.35	0.04	2	[319]
Electrospinning	PAN	70	1.77	0.3	20	96.5	14.3	0.19	2.7	[320]
Electrospinning	Polyethylene terephthalate (PET) wastes	1290	-	2.5	1.5	98.3	212	-	3.5	[204]
Electrospinning	Zein	200–500	6.7	0.3	-	99	109	0.026	-	[321]

5.2.4. Hybrid Filters and Electrostatic Filtration

The use of processes that provide an electrostatic characteristic to the filtration process can strongly increase the efficiency of nanoparticle collection. As demonstrated earlier, they are particularly sensitive to the electrostatic collection mechanism. Several ways to add charges to fibers or particles have been evaluated in the literature. One of the most advantageous processes is the union of electrostatic precipitators and bag filters, called hybrid filters, as shown in Figure 9. This equipment is not commonly evaluated in the nanometric range; however, Castro et al. [51] used it in the collection of NaCl nanoparticles with a diameter between 10 and 300 nm. In place of the collecting plate, Tian, Mo, and Li [322] proposed the use of a metal foam filter placed with 16 cm pins attached to a high-voltage source with negative polarity. The authors mention that, unlike electrostatic precipitators, in this system, the charged particles pass parallel to the collecting electrodes and, therefore, are more likely to be removed from the airflow.

**Figure 9.** Schematic representation of a hybrid filter.

Similar to hybrid filters, Feng, Long, and Mo [323] proposed the use of a filter media in the middle between pins connected to a high-voltage source and a grounded conductive plate. An electric field has been created in the space between the pin, the filter media, and the conductive plate. Another way was suggested by Shi and Ekberg [324], who used air ionizers to charge the particles before their collection in polypropylene, glass fiber filters, and modacrylic/polyester fibers with high efficiency.

In line with conductive material filters, Tian et al. [325] added MnO₂, activated carbon, ZnO, CuO, and BaTiO₃ in polyurethane foams by a quick roll-to-roll gel compression method. The agglomerates of these materials in the filters allowed large electrostatic polarization after the particles previously passed through an ionized region with voltages of up to 10 kV. An efficiency of up to 90% was obtained with a pressure drop of only 3.8 Pa at a velocity of 1.1 m/s. Choi et al. [326] manufactured bifunctional polyester/Al filters where particles also passed through a previously ionized region. The authors performed an evaluation of bioaerosols of *Staphylococcus epidermidis* and *Escherichia coli* with an efficiency of up to 96.9%. Choi et al. [327] manufactured conductive filters by the direct decomposition of Al precursor ink on the surfaces of a polyester air filter through a solution immersion process. An efficiency of up to 99.99% and a pressure drop of up to 4.9 Pa were obtained.

From another aspect, Kim et al. [328] used monolithic aerogels of syndiotactic polystyrene and polyvinylidene fluoride. Polyvinylidene fluoride chains allowed for obtaining a surface potential of up to 1.40 and filtration by electrostatic force. Efficiencies higher than 99.99% with a permeability of 10⁻¹⁰ m² were obtained for these hybrid materials. Along the same line, Zhai and Jana [329] synthesized polyimide monolithic aerogels as filter media. These gels presented a high surface area and high porosity. The filtration tests were similar to the previous study, and an efficiency above 99.95% could be obtained with similar permeabilities.

Several authors have evaluated filters with electret fibers. Tien et al. [330] produced electret filters for the collection of NaCl nanoparticles. They evaluated commercial HVAC media (MERV13) and three others produced by them: a coarse fiber (CF) layer, a melt-blown (MB) layer, and a bead-on-string (BS) layer. The experimental results revealed that the charges of the electret increased the retention capacity and the collection efficiency in the order of CF > MERV13 > BS > MB. By combining different filter layers, the CF + MERV13 + BS composite electret achieved the highest efficiency with the lowest pressure drop. Ardkapan et al. [331] evaluated the relationship between the concentration of particles and electrostatic fibers, indicating that with an increase in the efficiency of electrostatic fibers, the longer the particles are exposed. They mention that this occurs for a longer time such that the particles have to have static charging action and an electrostatic collection mechanism. Wang et al. [332] used the extrusion technique to produce polytetrafluoroethylene and polyphenylene sulfide fibers with silica nanoparticles and polyphenylene sulfide fibers. The authors mentioned that these fibers have a high charging capacity, with surface charge values greater than 9 kV when 2% of the silica nanoparticles are used. An efficiency between 89.4 and 99.7% was obtained with a pressure drop ranging between 18.4 and 55.4 Pa. Zhang et al. [333] used the meltblown spinning technique to produce polypropylene electret filters charged with corona and used magnesium stearate powders as charge additives. The filters were needle-punched to reduce the resistance to the air passage. The pressure drop reached 13.93 Pa, with a high efficiency of 99.2%. In addition, the use of magnesium particles allowed the filters to have only a 0.6% loss in efficiency and a pressure drop with heat treatments. The microfibers of electret as filter media were also evaluated in other studies [334,335]. Other studies already mentioned used the electrospinning technique to produce electret filters with nanofibers [274–279].

Using glass ball filters, Givehchi, Li, and Tan [336] evaluated the impact of electrostatic forces on the collection of NaCl particles with diameters between 10 and 100 nm. The authors report that usually glass balls contain a large number of negative ions. Electrostatic forces had an impact of up to 30% on the collection efficiency, and the authors concluded that this mechanism played a large role in the filtration of nanoaerosols. Golshahi, Tan, and Abedi [337] used a 2 mm, 4 mm, and 6 mm glass ball filter. The filtration efficiencies

were greater than 90% for particles with diameters between 10 and 100 nm. The authors reported that diffusion was the main collection mechanism.

Different approaches have been used with the electrostatic mechanism in the collection of nanoparticles, and most of them presented high collection efficiencies. These particles are particularly sensitive to this mechanism, and studies in this area are very promising. Most studies are still at the laboratory scale, especially when it comes to developments in new materials and approaches. For example, in the case of electret filters, there is the question of how long it is possible to store such charges in the fibers. It is more common industrially to use hybrid filters or prechargers, but this increases the operational costs of the processes by the need for high voltage. However, there are still some gaps in some technologies, and it is important to work in this area to further optimize processes and create different ways of using electrostatic processes in an economically viable and sustainable way.

6. Final Considerations

This review covers various aspects of nanoparticle filtration and electrostatic precipitation, including recent technologies used to increase particle collection efficiency. Particles with diameters of approximately 0.3 μm or less have a low collection efficiency and this fact is limiting for some processes. Therefore, the study of new techniques and new filter media that are efficient for nanoparticles is important. Thus, this review helps other researchers to further develop these technologies that enable the efficient collection of particles in the range of 1 to 300 nm. This will allow the reduction of nanoparticle emissions into the atmosphere, also protecting against the health problems that nanoparticles cause.

When using electrostatic precipitators, it was found that the greatest difficulty is to make these extremely small particles acquire charges. The diffusion mechanism makes it difficult to collect when using this method. However, at low velocities, a high efficiency can be obtained. Studies with different arrangements and configurations were also observed, but most focus on the analysis of the operating conditions. The use of wet precipitators provides high efficiency, but the formation of a new liquid effluent and the difficulty of recovering particles with added value encourages the search for alternatives. Particle agglomeration, on the other hand, did not show significant gains, with efficiency values close to the other studies. Changes in geometry seem to have a large impact on the collection efficiency and help to avoid some phenomena such as electrostatic shielding.

For filters, even though different commercial filtering media are used, the research is focused on the development of new filters with different characteristics. A highly evaluated form was to use functionalized fibers using coating or a process such as electrospinning. These filter media have been successfully used to filter ultrafine particles and bioaerosols (such as bacteria and SARS-CoV-2). Based on new structures and designs, filtering media with nanofibers can be developed with a high collection efficiency and interesting properties, which can also contribute to pre-existing filters. Multistructures of nanofibers and microfibers have been used to achieve high filtration efficiency, lower pressure drops, and the removal of particulates and volatile compounds. Greater efforts must be devoted to the production of reusable fibers that maintain their properties even after long periods of use and to ensure an ecofriendlier production process by using recycled polymers. Electret filters have shown promise by introducing electrostatic mechanisms and highly increasing the collection efficiency. Hybrid filters are promising for the collection of particulate matter. However, most studies focused on the collection of microparticles, and still, few covered the collection of nanoparticles.

Author Contributions: Conceptualization, F.d.A.L., G.B.M., P.A.M.C., M.L.A. and V.G.G.; validation, F.d.A.L., G.B.M., P.A.M.C., M.L.A. and V.G.G.; resources, M.L.A. and V.G.G.; writing—original draft preparation, F.d.A.L., G.B.M. and P.A.M.C.; writing—review and editing, F.d.A.L., G.B.M., P.A.M.C., M.L.A. and V.G.G.; supervision, M.L.A. and V.G.G.; project administration, M.L.A. and V.G.G.; funding acquisition, M.L.A. and V.G.G. All authors have read and agreed to the published version of the manuscript.

Funding: This research was funded by Conselho Nacional de Desenvolvimento Científico e Tecnológico—Brazil (CNPq, grant 132752/2019-0) and Coordenação de Aperfeiçoamento de Pessoal de Nível Superior—Brazil (CAPES, Finance Code 001).

Institutional Review Board Statement: Not applicable.

Informed Consent Statement: Not applicable.

Data Availability Statement: Not applicable.

Conflicts of Interest: The authors declare no conflict of interest.

References

1. DeMello, A.J.; Woolley, A.T. Nanotechnology. *Curr. Opin. Chem. Biol.* **2010**, *14*, 545–547. [CrossRef] [PubMed]
2. Gyles, C. Nanotechnology. *Can. Vet. J. La Rev. Vet. Can.* **2012**, *53*, 819–822.
3. Quina, F.H. Nanotecnologia e o Meio Ambiente: Perspectivas e Riscos. *Quim. Nova* **2004**, *27*, 1028–1029. [CrossRef]
4. Vance, M.E.; Kuiken, T.; Vejerano, E.P.; McGinnis, S.P.; Hochella, M.F.; Hull, D.R. Nanotechnology in the Real World: Redeveloping the Nanomaterial Consumer Products Inventory. *Beilstein J. Nanotechnol.* **2015**, *6*, 1769–1780. [CrossRef]
5. ISO. ISO/TS 12025. Available online: <https://www.iso.org/obp/ui/#iso:std:iso:ts:12025:ed-1:v1:en:bibref:5> (accessed on 29 January 2020).
6. Hinds, W.C. *Aerosol Technology: Properties, Behaviour, and Measurement of Airborne Particles*, 2nd ed.; John Wiley & Sons: New York, NY, USA, 1999; ISBN 0-471-19410-7.
7. Alonso, M.; Alguacil, F.J. Electrostatic Precipitation of Ultrafine Particles Enhanced by Simultaneous Diffusional Deposition on Wire Screens. *J. Air Waste Manag. Assoc.* **2002**, *52*, 1342–1347. [CrossRef] [PubMed]
8. Oliveira, A.E.; Guerra, V.G. Electrostatic Precipitation of Nanoparticles and Submicron Particles: Review of Technological Strategies. *Process Saf. Environ. Prot.* **2021**, *153*, 422–438. [CrossRef]
9. Gauthier, C.; Genet, C. Nanotechnologies and Green Knowledge Creation: Paradox or Enhancer of Sustainable Solutions? *J. Bus. Ethics* **2014**, *124*, 571–583. [CrossRef]
10. Lekamge, S.; Miranda, A.F.; Ball, A.S.; Shukla, R.; Nugegoda, D. The Toxicity of Coated Silver Nanoparticles to *Daphnia Carinata* and Trophic Transfer from *Alga Raphidocelis Subcapitata*. *PLoS ONE* **2019**, *14*, e0214398. [CrossRef]
11. Jovanović, B.; Palić, D.Š. Immunotoxicology of Non-Functionalized Engineered Nanoparticles in Aquatic Organisms with Special Emphasis on Fish—Review of Current Knowledge, Gap Identification, and Call for Further Research. *Aquat. Toxicol.* **2012**, *118–119*, 141–151. [CrossRef]
12. Carbone, S.; Vittori Antisari, L.; Gaggia, F.; Baffoni, L.; Di Gioia, D.; Vianello, G.; Nannipieri, P. Bioavailability and Biological Effect of Engineered Silver Nanoparticles in a Forest Soil. *J. Hazard. Mater.* **2014**, *280*, 89–96. [CrossRef]
13. Adams, R.A.; Potter, S.; Bérubé, K.; Higgins, T.P.; Jones, T.P.; Evans, S.A. Prolonged Systemic Inflammation and Damage to the Vascular Endothelium Following Intratracheal Instillation of Air Pollution Nanoparticles in Rats. *Clin. Hemorheol. Microcirc.* **2019**, *72*, 1–10. [CrossRef]
14. Gwinn, M.R.; Vallyathan, V. Nanoparticles: Health Effects—Pros and Cons. *Environ. Health Perspect.* **2006**, *114*, 1818–1825. [CrossRef]
15. Pomatto, L.C.D.; Cline, M.; Woodward, N.; Pakbin, P.; Sioutas, C.; Morgan, T.E.; Finch, C.E.; Forman, H.J.; Davies, K.J.A. Aging Attenuates Redox Adaptive Homeostasis and Proteostasis in Female Mice Exposed to Traffic-Derived Nanoparticles (‘Vehicular Smog’). *Free Radic. Biol. Med.* **2018**, *121*, 86–97. [CrossRef]
16. Semmler-Behnke, M.; Kreyling, W.G.; Lipka, J.; Fertsch, S.; Wenk, A.; Takenaka, S.; Schmid, G.; Brandau, W. Biodistribution of 1.4- and 18-Nm Gold Particles in Rats. *Small* **2008**, *4*, 2108–2111. [CrossRef] [PubMed]
17. Brunekreef, B.; Holgate, S.T. Air Pollution and Health. *Lancet* **2002**, *360*, 1233–1242. [CrossRef] [PubMed]
18. Calderón-Garcidueñas, L.; González-Maciél, A.; Mukherjee, P.S.; Reynoso-Robles, R.; Pérez-Guillé, B.; Gayosso-Chávez, C.; Torres-Jardón, R.; Cross, J.V.; Ahmed, I.A.M.M.; Karloukovski, V.V.; et al. Combustion- and Friction-Derived Magnetic Air Pollution Nanoparticles in Human Hearts. *Environ. Res.* **2019**, *176*, 108567. [CrossRef]
19. Oberdörster, G.; Oberdörster, E.; Oberdörster, J. Nanotoxicology: An Emerging Discipline Evolving from Studies of Ultrafine Particles. *Environ. Health Perspect.* **2005**, *113*, 823–839. [CrossRef]
20. Oberdörster, G.; Sharp, Z.; Atudorei, V.; Elder, A.; Gelein, R.; Kreyling, W.; Cox, C. Translocation of Inhaled Ultrafine Particles to the Brain. *Inhal. Toxicol.* **2004**, *16*, 437–445. [CrossRef]
21. Wu, J.; Ding, T.; Sun, J. Neurotoxic Potential of Iron Oxide Nanoparticles in the Rat Brain Striatum and Hippocampus. *Neurotoxicology* **2013**, *34*, 243–253. [CrossRef]
22. Maher, B.A.; Ahmed, I.A.M.M.; Karloukovski, V.; MacLaren, D.A.; Foulds, P.G.; Allsop, D.; Mann, D.M.A.A.; Torres-Jardón, R.; Calderon-Garciduenas, L. Magnetite Pollution Nanoparticles in the Human Brain. *Proc. Natl. Acad. Sci. USA* **2016**, *113*, 10797–10801. [CrossRef] [PubMed]
23. Win-Shwe, T.T.; Fujimaki, H. Nanoparticles and Neurotoxicity. *Int. J. Mol. Sci.* **2011**, *12*, 6267–6280. [CrossRef]
24. Veronesi, B.; Makwana, O.; Pooler, M.; Chen, L.C. Effects of Subchronic Exposure to Concentrated Ambient Particles: VII. Degeneration of Dopaminergic Neurons in Apo E^{-/-} Mice. *Inhal. Toxicol.* **2005**, *17*, 235–241. [CrossRef] [PubMed]

25. Cupaioli, F.A.; Zucca, F.A.; Boraschi, D.; Zecca, L. Engineered Nanoparticles. How Brain Friendly Is This New Guest? *Prog. Neurobiol.* **2014**, *119–120*, 20–38. [[CrossRef](#)] [[PubMed](#)]
26. Mohnen, V.; Hidy, G.M. Measurements of Atmospheric Nanoparticles (1875–1980). *Bull. Am. Meteorol. Soc.* **2010**, *91*, 1525–1539. [[CrossRef](#)]
27. Calderón-Garcidueñas, L.; Ayala, A. Air Pollution, Ultrafine Particles, and Your Brain: Are Combustion Nanoparticle Emissions and Engineered Nanoparticles Causing Preventable Fatal Neurodegenerative Diseases and Common Neuropsychiatric Outcomes? *Environ. Sci. Technol.* **2022**, *56*, 6847–6856. [[CrossRef](#)]
28. Nazarenko, Y.; Zhen, H.; Han, T.; Lioy, P.J.; Mainelis, G. Potential for Inhalation Exposure to Engineered Nanoparticles from Nanotechnology-Based Cosmetic Powders. *Environ. Health Perspect.* **2012**, *120*, 885–892. [[CrossRef](#)] [[PubMed](#)]
29. Tillett, T. A Compact Exposure: Estimating Inhalation of Engineered Nanoparticles in Cosmetic Powders. *Environ. Health Perspect.* **2012**, *120*, a245. [[CrossRef](#)] [[PubMed](#)]
30. Hillman, A.L.; Abbott, M.B.; Valero-Garcés, B.L.; Morellon, M.; Barreiro-Lostres, F.; Bain, D.J. Lead Pollution Resulting from Roman Gold Extraction in Northwestern Spain. *Holocene* **2017**, *27*, 1465–1474. [[CrossRef](#)]
31. Harra, J.; Mäkitalo, J.; Siikanen, R.; Virkki, M.; Genty, G.; Kobayashi, T.; Kauranen, M.; Mäkelä, J.M. Size-Controlled Aerosol Synthesis of Silver Nanoparticles for Plasmonic Materials. *J. Nanoparticle Res.* **2012**, *14*. [[CrossRef](#)]
32. Boddu, S.R.; Gutti, V.R.; Ghosh, T.K.; Tompson, R.V.; Loyalka, S.K. Gold, Silver, and Palladium Nanoparticle/Nano-Agglomerate Generation, Collection, and Characterization. *J. Nanoparticle Res.* **2011**, *13*, 6591–6601. [[CrossRef](#)]
33. Souza, J.P.; Mansano, A.S.; Venturini, F.P.; Marangoni, V.S.; Lins, P.M.P.; Silva, B.P.C.; Dressler, B.; Zucolotto, V. Toxicity of Gold Nanorods on *Ceriodaphnia Dubia* and *Danio Rerio* after Sub-Lethal Exposure and Recovery. *Environ. Sci. Pollut. Res.* **2021**, *28*, 25316–25326. [[CrossRef](#)]
34. Bumajdad, A.; Nazeer, A.A.; Al Sagheer, F.; Nahar, S.; Zaki, M.I. Controlled Synthesis of ZrO₂ Nanoparticles with Tailored Size, Morphology and Crystal Phases via Organic/Inorganic Hybrid Films. *Sci. Rep.* **2018**, *8*, 3695. [[CrossRef](#)]
35. Sheth, P.; Sandhu, H.; Singhal, D.; Malick, W.; Shah, N.; Serpil Kislalioglu, M. Nanoparticles in the Pharmaceutical Industry and the Use of Supercritical Fluid Technologies for Nanoparticle Production. *Curr. Drug Deliv.* **2012**, *9*, 269–284. [[CrossRef](#)]
36. Abdel-Mageed, H.M.; Fouad, S.A.; Teaima, M.H.; Abdel-Aty, A.M.; Fahmy, A.S.; Shaker, D.S.; Mohamed, S.A. Optimization of Nano Spray Drying Parameters for Production of α -Amylase Nanopowder for Biotherapeutic Applications Using Factorial Design. *Dry. Technol.* **2019**, *37*, 2152–2160. [[CrossRef](#)]
37. Dobrowolski, A.; Strob, R.; Niefeld, J.; Pieloth, D.; Wiggers, H.; Thommes, M. Preparation of Spray Dried Submicron Particles: Part B—Particle Recovery by Electrostatic Precipitation. *Int. J. Pharm.* **2018**, *548*, 237–243. [[CrossRef](#)] [[PubMed](#)]
38. Aisida, S.O.; Akpa, P.A.; Ahmad, I.; Zhao, T.; Maaza, M.; Ezema, F.I. Bio-Inspired Encapsulation and Functionalization of Iron Oxide Nanoparticles for Biomedical Applications. *Eur. Polym. J.* **2020**, *122*, 109371. [[CrossRef](#)]
39. Aseri, A.; Garg, S.K.; Nayak, A.; Trivedi, S.K.; Ahsan, J. Magnetic Nanoparticles: Magnetic Nano-Technology Using Biomedical Applications and Future Prospects. *Int. J. Pharm. Sci. Rev. Res.* **2015**, *31*, 119–131.
40. Materón, E.M.; Miyazaki, C.M.; Carr, O.; Joshi, N.; Picciani, P.H.S.; Dalmaschio, C.J.; Davis, F.; Shimizu, F.M. Magnetic Nanoparticles in Biomedical Applications: A Review. *Appl. Surf. Sci. Adv.* **2021**, *6*, 100163. [[CrossRef](#)]
41. Feitosa, N.d.R. Desempenho de Meios Filtrantes Na Remoção de Partículas Nanométricas de Aerossóis. Dissertação (Mestrado), Universidade Federal de São Carlos, São Carlos, Brazil, 2009.
42. Cyrs, W.D.; Boysen, D.A.; Casuccio, G.; Lersch, T.; Peters, T.M. Nanoparticle Collection Efficiency of Capillary Pore Membrane Filters. *J. Aerosol Sci.* **2010**, *41*, 655–664. [[CrossRef](#)]
43. Wang, C.S.; Otani, Y. Removal of Nanoparticles from Gas Streams by Fibrous Filters: A Review. *Ind. Eng. Chem. Res.* **2013**, *52*, 5–17. [[CrossRef](#)]
44. Cadavid-Rodriguez, M.C.; Charvet, A.; Bemer, D.; Thomas, D. Optimization of Bubble Column Performance for Nanoparticle Collection. *J. Hazard. Mater.* **2014**, *271*, 24–32. [[CrossRef](#)] [[PubMed](#)]
45. Lin, G.Y.; Cuc, L.T.; Lu, W.; Tsai, C.J.; Chein, H.M.; Chang, F.T. High-Efficiency Wet Electrocyclone for Removing Fine and Nanosized Particles. *Sep. Purif. Technol.* **2013**, *114*, 99–107. [[CrossRef](#)]
46. de Aquino Lima, F.; Guerra, V.G. Influence of Wire Spacing and Plate Spacing on Electrostatic Precipitation of Nanoparticles: An Approach Involving Electrostatic Shielding and Diffusion Charging. *Particuology* **2023**, *80*, 127–139. [[CrossRef](#)]
47. Andrade, R.G.S.A.; Guerra, V.G. Discharge Electrode Influence on Electrostatic Precipitation of Nanoparticles. *Powder Technol.* **2021**, *379*, 417–427. [[CrossRef](#)]
48. Knutson, E.O. History of Diffusion Batteries in Aerosol Measurements. *Aerosol Sci. Technol.* **1999**, *31*, 83–128. [[CrossRef](#)]
49. Fierz, M.; Scherrer, L.; Burtscher, H. Real-Time Measurement of Aerosol Size Distributions with an Electrical Diffusion Battery. *J. Aerosol Sci.* **2002**, *33*, 1049–1060. [[CrossRef](#)]
50. Parker, K.R. *Applied Electrostatic Precipitation*; Blackie Academic & Professional: London, UK, 1997; ISBN 9789401071932.
51. Castro, B.J.C.; Lacerda, C.R.; Melo, B.R.; Sartim, R.; Aguiar, M.L. Performance Assessment of a Bench Scale Hybrid Filter in the Collection of Nanoparticles. *Process Saf. Environ. Prot.* **2021**, *154*, 32–42. [[CrossRef](#)]
52. Fann, N.; Lamson, A.D.; Anenberg, S.C.; Wesson, K.; Risley, D.; Hubbell, B.J. Estimating the National Public Health Burden Associated with Exposure to Ambient PM_{2.5} and Ozone. *Risk Anal.* **2012**, *32*, 81–95. [[CrossRef](#)]
53. Laumbach, R.J.; Kipen, H.M. Respiratory Health Effects of Air Pollution: Update on Biomass Smoke and Traffic Pollution. *J. Allergy Clin. Immunol.* **2012**, *129*, 3–11. [[CrossRef](#)]

54. Fiordelisi, A.; Piscitelli, P.; Trimarco, B.; Coscioni, E.; Iaccarino, G.; Sorriento, D. The Mechanisms of Air Pollution and Particulate Matter in Cardiovascular Diseases. *Heart Fail. Rev.* **2017**, *22*, 337–347. [[CrossRef](#)]
55. Miller, M.R.; Newby, D.E. Air Pollution and Cardiovascular Disease: Car Sick. *Cardiovasc. Res.* **2020**, *116*, 279–294. [[CrossRef](#)] [[PubMed](#)]
56. Oberdörster, G. Pulmonary Effects of Inhaled Ultrafine Particles. *Int. Arch. Occup. Environ. Health* **2000**, *74*, 1–8. [[CrossRef](#)]
57. Warheit, D.B. Nanoparticles: Health Impacts? *Mater. Today* **2004**, *7*, 32–35. [[CrossRef](#)]
58. Phairuang, W.; Piriyaakarnsakul, S.; Inerb, M.; Hongtieab, S.; Thongyen, T.; Chomane, J.; Boongla, Y.; Suriyawong, P.; Samae, H.; Chanonmuang, P.; et al. Ambient Nanoparticles (PM_{0.1}) Mapping in Thailand. *Atmosphere* **2022**, *14*, 66. [[CrossRef](#)]
59. Schraufnagel, D.E. The Health Effects of Ultrafine Particles. *Exp. Mol. Med.* **2020**, *52*, 311–317. [[CrossRef](#)] [[PubMed](#)]
60. Kwon, H.-S.; Ryu, M.H.; Carlsten, C. Ultrafine Particles: Unique Physicochemical Properties Relevant to Health and Disease. *Exp. Mol. Med.* **2020**, *52*, 318–328. [[CrossRef](#)]
61. Li, N.; Georas, S.; Alexis, N.; Fritz, P.; Xia, T.; Williams, M.A.; Horner, E.; Nel, A. A Work Group Report on Ultrafine Particles (American Academy of Allergy, Asthma & Immunology): Why Ambient Ultrafine and Engineered Nanoparticles Should Receive Special Attention for Possible Adverse Health Outcomes in Human Subjects. *J. Allergy Clin. Immunol.* **2016**, *138*, 386–396. [[CrossRef](#)]
62. Nel, A. Toxic Potential of Materials at the Nanolevel. *Science* **2006**, *311*, 622–627. [[CrossRef](#)]
63. Yang, M.; Jalava, P.; Hakkarainen, H.; Roponen, M.; Leskinen, A.; Komppula, M.; Dong, G.-P.; Lao, X.-Q.; Wu, Q.-Z.; Xu, S.-L.; et al. Fine and Ultrafine Airborne PM Influence Inflammation Response of Young Adults and Toxicological Responses in Vitro. *Sci. Total Environ.* **2022**, *836*, 155618. [[CrossRef](#)]
64. Nóbrega, S.W.; Falaguasta, M.C.R.; Coury, J.R. A Study of a Wire-Plate Electrostatic Precipitator Operating in the Removal of Polydispersed Particles. *Braz. J. Chem. Eng.* **2004**, *21*, 275–284. [[CrossRef](#)]
65. Pui, D.Y.H.; Chen, D.-R. Nanometer Particles: A New Frontier for Multidisciplinary Research. *J. Aerosol Sci.* **1997**, *28*, 539–544. [[CrossRef](#)]
66. Oliveira, A.E.; Guerra, V.G. Effect of Low Gas Velocity on the Nanoparticle Collection Performance of an Electrostatic Precipitator. *Sep. Sci. Technol.* **2019**, *54*, 1211–1220. [[CrossRef](#)]
67. Oliveira, A.E.; Guerra, V.G. Influence of Particle Concentration and Residence Time on the Efficiency of Nanoparticulate Collection by Electrostatic Precipitation. *J. Electrostat.* **2018**, *96*, 1–9. [[CrossRef](#)]
68. Joodatnia, P.; Kumar, P.; Robins, A. Fast Response Sequential Measurements and Modelling of Nanoparticles inside and Outside a Car Cabin. *Atmos. Environ.* **2013**, *71*, 364–375. [[CrossRef](#)]
69. Bencs, L.; Horemans, B.; Buczyńska, A.J.; Van Grieken, R. Uneven Distribution of Inorganic Pollutants in Marine Air Originating from Ocean-Going Ships. *Environ. Pollut.* **2017**, *222*, 226–233. [[CrossRef](#)] [[PubMed](#)]
70. The Nanodatabase Search Database. Available online: <http://nanodb.dk/en/> (accessed on 10 February 2020).
71. Project on Emerging Nanotechnologies Consumer Products Inventory. Available online: <https://www.nanotechproject.tech/cpi/products/> (accessed on 10 February 2020).
72. Weichenthal, S.; Dufresne, A.; Infante-Rivard, C.; Joseph, L. Determinants of Ultrafine Particle Exposures in Transportation Environments: Findings of an 8-Month Survey Conducted in Montréal, Canada. *J. Expo. Sci. Environ. Epidemiol.* **2008**, *18*, 551–563. [[CrossRef](#)]
73. Matson, U. Indoor and Outdoor Concentrations of Ultrafine Particles in Some Scandinavian Rural and Urban Areas. *Sci. Total Environ.* **2005**, *343*, 169–176. [[CrossRef](#)]
74. Nevshupa, R.; Jimenez-Relinque, E.; Grande, M.; Martinez, E.; Castellote, M. Assessment of Urban Air Pollution Related to Potential Nanoparticle Emission from Photocatalytic Pavements. *J. Environ. Manag.* **2020**, *272*, 111059. [[CrossRef](#)] [[PubMed](#)]
75. Heitbrink, W.A.; Evans, D.E.; Peters, T.M.; Slaviv, T.J. Characterization and Mapping of Very Fine Particles in an Engine Machining and Assembly Facility. *J. Occup. Environ. Hyg.* **2007**, *4*, 341–351. [[CrossRef](#)]
76. Pond, Z.A.; Saha, P.K.; Coleman, C.J.; Presto, A.A.; Robinson, A.L.; Arden Pope, C., III. Mortality Risk and Long-Term Exposure to Ultrafine Particles and Primary Fine Particle Components in a National U.S. Cohort. *Environ. Int.* **2022**, *167*, 107439. [[CrossRef](#)]
77. Verma, V.; Ning, Z.; Cho, A.K.; Schauer, J.J.; Shafer, M.M.; Sioutas, C. Redox Activity of Urban Quasi-Ultrafine Particles from Primary and Secondary Sources. *Atmos. Environ.* **2009**, *43*, 6360–6368. [[CrossRef](#)]
78. Moore, K.F.; Ning, Z.; Ntziachristos, L.; Schauer, J.J.; Sioutas, C. Daily Variation in the Properties of Urban Ultrafine Aerosol—Part I: Physical Characterization and Volatility. *Atmos. Environ.* **2007**, *41*, 8633–8646. [[CrossRef](#)]
79. Ning, Z.; Geller, M.D.; Moore, K.F.; Sheesley, R.; Schauer, J.J.; Sioutas, C. Daily Variation in Chemical Characteristics of Urban Ultrafine Aerosols and Inference of Their Sources. *Environ. Sci. Technol.* **2007**, *41*, 6000–6006. [[CrossRef](#)] [[PubMed](#)]
80. Saffari, A.; Hasheminassab, S.; Wang, D.; Shafer, M.M.; Schauer, J.J.; Sioutas, C. Impact of Primary and Secondary Organic Sources on the Oxidative Potential of Quasi-Ultrafine Particles (PM_{0.25}) at Three Contrasting Locations in the Los Angeles Basin. *Atmos. Environ.* **2015**, *120*, 286–296. [[CrossRef](#)]
81. Hama, S.M.L.; Cordell, R.L.; Monks, P.S. Quantifying Primary and Secondary Source Contributions to Ultrafine Particles in the UK Urban Background. *Atmos. Environ.* **2017**, *166*, 62–78. [[CrossRef](#)]
82. Robinson, A.L.; Donahue, N.M.; Shrivastava, M.K.; Weitkamp, E.A.; Sage, A.M.; Grieshop, A.P.; Lane, T.E.; Pierce, J.R.; Pandis, S.N. Rethinking Organic Aerosols: Semivolatile Emissions and Photochemical Aging. *Science* **2007**, *315*, 1259–1262. [[CrossRef](#)]

83. Li, Q.; Wyatt, A.; Kamens, R.M. Oxidant Generation and Toxicity Enhancement of Aged-Diesel Exhaust. *Atmos. Environ.* **2009**, *43*, 1037–1042. [[CrossRef](#)]
84. Goel, A.; Kumar, P. Vertical and Horizontal Variability in Airborne Nanoparticles and Their Exposure around Signalised Traffic Intersections. *Environ. Pollut.* **2016**, *214*, 54–69. [[CrossRef](#)] [[PubMed](#)]
85. Cheng, Y.H.; Huang, C.H.; Huang, H.L.; Tsai, C.J. Concentrations of Ultrafine Particles at a Highway Toll Collection Booth and Exposure Implications for Toll Collectors. *Sci. Total Environ.* **2010**, *409*, 364–369. [[CrossRef](#)]
86. Rönkkö, T.; Pirjola, L.; Ntziachristos, L.; Heikkilä, J.; Karjalainen, P.; Hillamo, R.; Keskinen, J. Vehicle Engines Produce Exhaust Nanoparticles Even When Not Fueled. *Environ. Sci. Technol.* **2014**, *48*, 2043–2050. [[CrossRef](#)]
87. Holmén, B.A.; Ayala, A. Ultrafine PM Emissions from Natural Gas, Oxidation-Catalyst Diesel, and Particle-Trap Diesel Heavy-Duty Transit Buses. *Environ. Sci. Technol.* **2002**, *36*, 5041–5050. [[CrossRef](#)] [[PubMed](#)]
88. Mayer, A.; Burtscher, H.; Loretz, S.; Kasper, M.; Czerwinski, J. High Air Pollution in Vehicle Cabins Due to Traffic Nanoparticle Emission Exposure and a Solution for In-Use Vehicles. *IOP Conf. Ser. Mater. Sci. Eng.* **2018**, *421*, 032018. [[CrossRef](#)]
89. Al-Dabbous, A.N.; Kumar, P. The Influence of Roadside Vegetation Barriers on Airborne Nanoparticles and Pedestrians Exposure under Varying Wind Conditions. *Atmos. Environ.* **2014**, *90*, 113–124. [[CrossRef](#)]
90. Cheng, Y.H.; Chao, Y.C.; Wu, C.H.; Tsai, C.J.; Uang, S.N.; Shih, T.S. Measurements of Ultrafine Particle Concentrations and Size Distribution in an Iron Foundry. *J. Hazard. Mater.* **2008**, *158*, 124–130. [[CrossRef](#)] [[PubMed](#)]
91. Wheatley, A.D.; Sadhra, S. Occupational Exposure to Diesel Exhaust Fumes. *Ann. Occup. Hyg.* **2004**, *48*, 369–376. [[CrossRef](#)]
92. Wu, J.; Tou, F.; Guo, X.; Liu, C.; Sun, Y.; Xu, M.; Liu, M.; Yang, Y. Vast Emission of Fe- and Ti-Containing Nanoparticles from Representative Coal-Fired Power Plants in China and Environmental Implications. *Sci. Total Environ.* **2022**, *838*, 156070. [[CrossRef](#)]
93. Elihn, K.; Berg, P. Ultrafine Particle Characteristics in Seven Industrial Plants. *Ann. Occup. Hyg.* **2009**, *53*, 475–484. [[CrossRef](#)] [[PubMed](#)]
94. Gonet, T.; Maher, B.A. Airborne, Vehicle-Derived Fe-Bearing Nanoparticles in the Urban Environment: A Review. *Environ. Sci. Technol.* **2019**, *53*, 9970–9991. [[CrossRef](#)] [[PubMed](#)]
95. Oliveira, M.L.S.; Pinto, D.; Tutikian, B.F.; da Boit, K.; Saikia, B.K.; Silva, L.F.O. Pollution from Uncontrolled Coal Fires: Continuous Gaseous Emissions and Nanoparticles from Coal Mines. *J. Clean. Prod.* **2019**, *215*, 1140–1148. [[CrossRef](#)]
96. Natasha; Shahid, M.; Dumat, C.; Khalid, S.; Rabbani, F.; Farooq, A.B.U.; Amjad, M.; Abbas, G.; Niazi, N.K. Foliar Uptake of Arsenic Nanoparticles by Spinach: An Assessment of Physiological and Human Health Risk Implications. *Environ. Sci. Pollut. Res.* **2019**, *26*, 20121–20131. [[CrossRef](#)]
97. Zhang, Q.; Lu, D.; Wang, D.; Yang, X.; Zuo, P.; Yang, H.; Fu, Q.; Liu, Q.; Jiang, G. Separation and Tracing of Anthropogenic Magnetite Nanoparticles in the Urban Atmosphere. *Environ. Sci. Technol.* **2020**, *54*, 9274–9284. [[CrossRef](#)]
98. Torti, S.V.; Torti, F.M. Winning the War with Iron. *Nat. Nanotechnol.* **2019**, *14*, 499–500. [[CrossRef](#)] [[PubMed](#)]
99. Yacobi, N.R.; Malmstadt, N.; Fazlollahi, F.; DeMaio, L.; Marchelletta, R.; Hamm-Alvarez, S.F.; Borok, Z.; Kim, K.-J.; Crandall, E.D. Mechanisms of Alveolar Epithelial Translocation of a Defined Population of Nanoparticles. *Am. J. Respir. Cell Mol. Biol.* **2010**, *42*, 604–614. [[CrossRef](#)]
100. Monteiller, C.; Tran, L.; MacNee, W.; Faux, S.; Jones, A.; Miller, B.; Donaldson, K. The Pro-Inflammatory Effects of Low-Toxicity Low-Solubility Particles, Nanoparticles and Fine Particles, on Epithelial Cells in Vitro: The Role of Surface Area. *Occup. Environ. Med.* **2007**, *64*, 609–615. [[CrossRef](#)]
101. Hesketh, H.E. *Air Pollution Control: Traditional and Hazardous Pollutants*; Technomic Publishing Company: Lancaster, UK, 1996; ISBN 1-56676-413-0.
102. Dullien, F.A.L. *Introduction to Industrial Gas Cleaning*; Academic Press: San Diego, CA, USA, 1989.
103. Afshari, A.; Ekberg, L.; Forejt, L.; Mo, J.; Rahimi, S.; Siegel, J.; Chen, W.; Wargocki, P.; Zurami, S.; Zhang, J. Electrostatic Precipitators as an Indoor Air Cleaner—A Literature Review. *Sustainability* **2020**, *12*, 8774. [[CrossRef](#)]
104. Sudrajad, A.; Yusof, A.F. Review of Electrostatic Precipitator Device for Reduce of Diesel Engine Particulate Matter. *Energy Procedia* **2015**, *68*, 370–380. [[CrossRef](#)]
105. Riehle, C. Electrostatic Precipitation. In *Gas Cleaning in Demanding Applications*; Springer: Dordrecht, The Netherlands, 1997; pp. 193–228.
106. Parker, K.R. *Electrical Operation of Electrostatic Precipitators*, 1st ed.; Institution of Engineering and Technology: London, UK, 2003; ISBN 9780852961377.
107. Riehle, C. Basic and Theoretical Operation of ESPs. In *Applied Electrostatic Precipitation*; Blackie Academic & Professional: London, UK, 1997; pp. 25–87.
108. Tepper, G.; Kessick, R. A Study of Ionization and Collection Efficiencies in Electrospray-Based Electrostatic Precipitators. *J. Aerosol Sci.* **2008**, *39*, 609–617. [[CrossRef](#)]
109. Bai, Y.; Han, C.B.; He, C.; Gu, G.Q.; Nie, J.H.; Shao, J.J.; Xiao, T.X.; Deng, C.R.; Wang, Z.L. Washable Multilayer Triboelectric Air Filter for Efficient Particulate Matter PM 2.5 Removal. *Adv. Funct. Mater.* **2018**, *28*, 1706680. [[CrossRef](#)]
110. Zhao, J.; Li, H.; Yang, Z.; Zhu, L.; Zhang, M.; Feng, Y.; Qu, W.; Yang, J.; Shih, K. Dual Roles of Nano-Sulfide in Efficient Removal of Elemental Mercury from Coal Combustion Flue Gas within a Wide Temperature Range. *Environ. Sci. Technol.* **2018**, *52*, 12926–12933. [[CrossRef](#)]
111. Jiang, J.; Lee, M.-H.; Biswas, P. Model for Nanoparticle Charging by Diffusion, Direct Photoionization, and Thermionization Mechanisms. *J. Electrostat.* **2007**, *65*, 209–220. [[CrossRef](#)]

112. White, H.J. *Industrial Electrostatic Precipitation*; Addison-Wesley: Reading, UK, 1963.
113. Wettervik, B.; Johnson, T.; Jakobsson, S.; Mark, A.; Edelvik, F. A Domain Decomposition Method for Three Species Modeling of Multi-Electrode Negative Corona Discharge—With Applications to Electrostatic Precipitators. *J. Electrostat.* **2015**, *77*, 139–146. [[CrossRef](#)]
114. Park, J.-H.; Chun, C.-H. An Improved Modelling for Prediction of Grade Efficiency of Electrostatic Precipitators with Negative Corona. *J. Aerosol. Sci.* **2002**, *33*, 673–694. [[CrossRef](#)]
115. Yehia, A.; Abdel-Fattah, E.; Mizuno, A. Positive Direct Current Corona Discharges in Single Wire-Duct Electrostatic Precipitators. *AIP Adv.* **2016**, *6*, 055213. [[CrossRef](#)]
116. Kawada, Y.; Kaneko, T.; Ito, T.; Chang, J.S. Simultaneous Removal of Aerosol Particles, NO_x and SO₂ from Incense Smokes by a Dc Wire-Plate Electrostatic Precipitator under Positive Coronas. *J. Aerosol. Sci.* **2001**, *32*, 945–946. [[CrossRef](#)]
117. Chen, Q.; Fang, M.; Cen, J.; Lv, M.; Shao, S.; Xia, Z. Comparison of Positive and Negative DC Discharge under Coal Pyrolysis Gas Media at High Temperatures. *Powder Technol.* **2019**, *345*, 352–362. [[CrossRef](#)]
118. Liu, C.-Y.; Tseng, C.-H.; Wang, K.-F. The Assessment of Indoor Formaldehyde and Bioaerosol Removal by Using Negative Discharge Electrostatic Air Cleaners. *Int. J. Environ. Res. Public Health* **2022**, *19*, 7209. [[CrossRef](#)] [[PubMed](#)]
119. Chen, J.; Davidson, J.H. Ozone Production in the Negative DC Corona: The Dependence of Discharge Polarity. *Plasma Chem. Plasma Process.* **2003**, *23*, 501–518. [[CrossRef](#)]
120. Long, Z.; Yao, Q. Evaluation of Various Particle Charging Models for Simulating Particle Dynamics in Electrostatic Precipitators. *J. Aerosol. Sci.* **2010**, *41*, 702–718. [[CrossRef](#)]
121. Choudhary, K.; Gentry, J. Particle Collection Efficiency of a Bench Scale Electrostatic Precipitator in the Field Charging Region as a Function of Particle Size. *J. Colloid Interf. Sci.* **1974**, *48*, 263–280. [[CrossRef](#)]
122. Dunkle, S.G. Electrostatic Precipitators. In *Industrial Air Pollution Control Systems*; McGraw-Hill: New York, NY, USA, 1997; pp. 471–510.
123. Zhang, J.-P.; Du, Y.-Y.; Wu, H.; Liu, Y.; Ren, J.-X.; Ji, D.-M. A Numerical Simulation of Diffusion Charging Effect on Collection Efficiency in Wire-Plate Electrostatic Precipitators. *IEEE Trans. Plasma Sci.* **2011**, *39*, 1823–1828. [[CrossRef](#)]
124. Lu, Q.; Yang, Z.; Zheng, C.; Li, X.; Zhao, C.; Xu, X.; Gao, X.; Luo, Z.; Ni, M.; Cen, K. Numerical Simulation on the Fine Particle Charging and Transport Behaviors in a Wire-Plate Electrostatic Precipitator. *Adv. Powder Technol.* **2016**, *27*, 1905–1911. [[CrossRef](#)]
125. Krinke, T.J.; Deppert, K.; Magnusson, M.H.; Fissan, H. Nanostructured Deposition of Nanoparticles from the Gas Phase. *Part. Part. Syst. Charact.* **2002**, *19*, 321–326. [[CrossRef](#)]
126. Dong, M.; Zhou, F.; Zhang, Y.; Shang, Y.; Li, S. Numerical Study on Fine-Particle Charging and Transport Behaviour in Electrostatic Precipitators. *Powder Technol.* **2018**, *330*, 210–218. [[CrossRef](#)]
127. Arif, S.; Branken, D.J.; Everson, R.C.; Neomagus, H.W.J.P.; Arif, A. The Influence of Design Parameters on the Occurrence of Shielding in Multi-Electrode ESPs and Its Effect on Performance. *J. Electrostat.* **2018**, *93*, 17–30. [[CrossRef](#)]
128. Chang, C.-L.; Bai, H. Effects of Some Geometric Parameters on the Electrostatic Precipitator Efficiency at Different Operation Indexes. *Aerosol Sci. Technol.* **2000**, *33*, 228–238. [[CrossRef](#)]
129. Sumorek, A. The Influence of Shape and Dimension of Dust Particle on Electrostatic Precipitator Operation. *Przegląd Elektrotech.* **2018**, *1*, 56–59. [[CrossRef](#)]
130. Dong, M.; Zhou, F.; Shang, Y.; Li, S. Numerical Study on Electrohydrodynamic Flow and Fine-Particle Collection Efficiency in a Spike Electrode-Plate Electrostatic Precipitator. *Powder Technol.* **2019**, *351*, 71–83. [[CrossRef](#)]
131. Ning, Z.; Podlinski, J.; Shen, X.; Li, S.; Wang, S.; Han, P.; Yan, K. Electrode Geometry Optimization in Wire-Plate Electrostatic Precipitator and Its Impact on Collection Efficiency. *J. Electrostat.* **2016**, *80*, 76–84. [[CrossRef](#)]
132. Gao, M.; Zhu, Y.; Yao, X.; Shi, J.; Shangguan, W. Dust Removal Performance of Two-Stage Electrostatic Precipitators and Its Influencing Factors. *Powder Technol.* **2019**, *348*, 13–23. [[CrossRef](#)]
133. Kherbouche, F.; Benmimoun, Y.; Tilmatine, A.; Zouaghi, A.; Zouzou, N. Study of a New Electrostatic Precipitator with Asymmetrical Wire-to-Cylinder Configuration for Cement Particles Collection. *J. Electrostat.* **2016**, *83*, 7–15. [[CrossRef](#)]
134. Mo, J.; Tian, E.; Pan, J. New Electrostatic Precipitator with Dielectric Coatings to Efficiently and Safely Remove Sub-Micro Particles in the Building Environment. *Sustain. Cities Soc.* **2020**, *55*, 102063. [[CrossRef](#)]
135. Yang, D.; Guo, B.; Ye, X.; Yu, A.; Guo, J. Numerical Simulation of Electrostatic Precipitator Considering the Dust Particle Space Charge. *Powder Technol.* **2019**, *354*, 552–560. [[CrossRef](#)]
136. Yoo, K.H.; Lee, J.S.; Oh, M. Do Charging and Collection of Submicron Particles in Two-Stage Parallel-Plate Electrostatic Precipitators. *Aerosol. Sci. Technol.* **1997**, *27*, 308–323. [[CrossRef](#)]
137. Schmatloch, V.; Rauch, S. Design and Characterisation of an Electrostatic Precipitator for Small Heating Appliances. *J. Electrostat.* **2005**, *63*, 85–100. [[CrossRef](#)]
138. Zhuang, Y.; Jin Kim, Y.; Gyu Lee, T.; Biswas, P. Experimental and Theoretical Studies of Ultra-Fine Particle Behavior in Electrostatic Precipitators. *J. Electrostat.* **2000**, *48*, 245–260. [[CrossRef](#)]
139. Morawska, L.; Agranovski, V.; Ristovski, Z.; Jamriska, M. Effect of Face Velocity and the Nature of Aerosol on the Collection of Submicrometer Particles by Electrostatic Precipitator. *Indoor Air* **2002**, *12*, 129–137. [[CrossRef](#)] [[PubMed](#)]
140. Mertens, J.; Lepaumier, H.; Rogiers, P.; Desagher, D.; Goossens, L.; Duterque, A.; Le Cadre, E.; Zarea, M.; Blondeau, J.; Webber, M. Fine and Ultrafine Particle Number and Size Measurements from Industrial Combustion Processes: Primary Emissions Field Data. *Atmos. Pollut. Res.* **2020**, *11*, 803–814. [[CrossRef](#)]

141. Oliveira, A.E.; Guerra, V.G. Efficiency of Electrostatic Precipitation of NiO Nanoparticles Dispersed by Atomization. *Sep. Sci. Technol.* **2020**, *55*, 2400–2409. [[CrossRef](#)]
142. Oliveira, A.E.; Guerra, V.G. Electrostatic Precipitation of Nickel (II) Oxide and Sodium Chloride Nanoparticles: Operating Conditions Promoting Sputtering with Electro-Fluid Dynamics Analysis. *Process Saf. Environ. Prot.* **2021**, *147*, 450–459. [[CrossRef](#)]
143. Miller, A.; Frey, G.; King, G.; Sunderman, C. A Handheld Electrostatic Precipitator for Sampling Airborne Particles and Nanoparticles. *Aerosol Sci. Technol.* **2010**, *44*, 417–427. [[CrossRef](#)]
144. Roux, J.M.; Sarda-Estève, R.; Delapierre, G.; Nadal, M.H.; Bossuet, C.; Olmedo, L. Development of a New Portable Air Sampler Based on Electrostatic Precipitation. *Environ. Sci. Pollut. Res.* **2016**, *23*, 8175–8183. [[CrossRef](#)]
145. Vaddi, R.S.; Guan, Y.; Novosselov, I. Behavior of Ultrafine Particles in Electro-Hydrodynamic Flow Induced by Corona Discharge. *J. Aerosol Sci.* **2020**, *148*, 105587. [[CrossRef](#)] [[PubMed](#)]
146. Nouri, H.; Zouzou, N.; Dascalescu, L.; Zebboudj, Y. Investigation of Relative Humidity Effect on the Particles Velocity and Collection Efficiency of Laboratory Scale Electrostatic Precipitator. *Process Saf. Environ. Prot.* **2016**, *104*, 225–232. [[CrossRef](#)]
147. Liu, Y.; Hu, B.; Zhou, L.; Jiang, Y.; Yang, L. Improving the Removal of Fine Particles with an Electrostatic Precipitator by Chemical Agglomeration. *Energy Fuels* **2016**, *30*, 8441–8447. [[CrossRef](#)]
148. Bin, H.; Yang, Y.; Lei, Z.; Ao, S.; Cai, L.; Linjun, Y.; Roszak, S. Experimental and DFT Studies of PM2.5 Removal by Chemical Agglomeration. *Fuel* **2018**, *212*, 27–33. [[CrossRef](#)]
149. Bin, H.; Yang, Y.; Cai, L.; Zhulin, Y.; Roszak, S.; Linjun, Y. Experimental Study on Particles Agglomeration by Chemical and Turbulent Agglomeration before Electrostatic Precipitators. *Powder Technol.* **2018**, *335*, 186–194. [[CrossRef](#)]
150. Sun, Z.; Yang, L.; Shen, A.; Zhou, L.; Wu, H. Combined Effect of Chemical and Turbulent Agglomeration on Improving the Removal of Fine Particles by Different Coupling Mode. *Powder Technol.* **2019**, *344*, 242–250. [[CrossRef](#)]
151. Sun, Z.; Yang, L.; Wu, H.; Wu, X. Agglomeration and Removal Characteristics of Fine Particles from Coal Combustion under Different Turbulent Flow Fields. *J. Environ. Sci.* **2020**, *89*, 113–124. [[CrossRef](#)] [[PubMed](#)]
152. Kim, J.H.; Lee, H.S.; Kim, H.H.; Ogata, A. Electrostatic Precipitator Enhances Fine Particles Collection Efficiency. *J. Electrostat.* **2010**, *68*, 305–310. [[CrossRef](#)]
153. Kim, W.; An, H.; Lee, D.; Lee, W.; Jung, J.H. Development of a Novel Electrostatic Precipitator System Using a Wet-Porous Electrode Array. *Aerosol Sci. Technol.* **2015**, *49*, 1100–1108. [[CrossRef](#)]
154. Son, C.; Lee, W.; Jung, D.; Lee, D.; Byon, C.; Kim, W. Use of an Electrostatic Precipitator with Wet-Porous Electrode Arrays for Removal of Air Pollution at a Precision Manufacturing Facility. *J. Aerosol Sci.* **2016**, *100*, 118–128. [[CrossRef](#)]
155. Sung, J.-H.; Kim, M.; Kim, Y.-J.; Han, B.; Hong, K.-J.; Kim, H.-J. Ultrafine Particle Cleaning Performance of an Ion Spray Electrostatic Air Cleaner Emitting Zero Ozone with Diffusion Charging by Carbon Fiber. *Build. Environ.* **2019**, *166*, 106422. [[CrossRef](#)]
156. Teng, C.; Fan, X.; Li, J. Effect of Charged Water Drop Atomization on Particle Removal Performance in Plate Type Wet Electrostatic Precipitator. *J. Electrostat.* **2020**, *104*, 103426. [[CrossRef](#)]
157. Anderlohr, C.; Schaber, K. Direct Transfer of Gas-Borne Nanoparticles into Liquid Suspensions by Means of a Wet Electrostatic Precipitator. *Aerosol Sci. Technol.* **2015**, *49*, 1281–1290. [[CrossRef](#)]
158. Chen, T.M.; Tsai, C.J.; Yan, S.Y.; Li, S.N. An Efficient Wet Electrostatic Precipitator for Removing Nanoparticles, Submicron and Micron-Sized Particles. *Sep. Purif. Technol.* **2014**, *136*, 27–35. [[CrossRef](#)]
159. Dey, L.; Venkataraman, C. A Wet Electrostatic Precipitator (WESP) for Soft Nanoparticle Collection. *Aerosol Sci. Technol.* **2012**, *46*, 750–759. [[CrossRef](#)]
160. Saiyasitpanich, P.; Keener, T.C.; Lu, M.; Khang, S.-J.; Evans, D.E. Collection of Ultrafine Diesel Particulate Matter (DPM) in Cylindrical Single-Stage Wet Electrostatic Precipitators. *Environ. Sci. Technol.* **2006**, *40*, 7890–7895. [[CrossRef](#)] [[PubMed](#)]
161. Halstead, M.; Gray, N.; Gonzalez-Jimenez, N.; Fresquez, M.; Valentin-Blasini, L.; Watson, C.; Pappas, R.S. Analysis of Toxic Metals in Electronic Cigarette Aerosols Using a Novel Trap Design. *J. Anal. Toxicol.* **2020**, *44*, 149–155. [[CrossRef](#)]
162. Borgerding, M.F.; Milhous, L.A.; Hicks, R.D.; Giles, J.A. Cigarette Smoke Composition. Part 2. Method for Determining Major Components in Smoke of Cigarettes That Heat Instead of Burn Tobacco. *J. AOAC Int.* **1990**, *73*, 610–615. [[CrossRef](#)]
163. Rhoades, C.B.; White, R.T. Mainstream Smoke Collection by Electrostatic Precipitation for Acid Dissolution in a Microwave Digestion System Prior to Trace Metal Determination. *J. AOAC Int.* **1997**, *80*, 1320–1331. [[CrossRef](#)]
164. Zukeran, A.; Sawano, H.; Yasumoto, K. Collection Characteristic of Nanoparticles Emitted from a Diesel Engine with Residual Fuel Oil and Light Fuel Oil in an Electrostatic Precipitator. *Energies* **2019**, *12*, 3321. [[CrossRef](#)]
165. Flagan, R.C.; Seinfeld, J.H. *Fundamentals of Air Pollution Engineering*. Courier Corporation: Chelmsford, MA, USA, 2012.
166. Intra, P.; Tippayawong, N. An Overview of Unipolar Charger Developments for Nanoparticle Charging. *Aerosol. Air Qual. Res.* **2011**, *11*, 187–209. [[CrossRef](#)]
167. Li, M.; Christofides, P.D. Collection Efficiency of Nanosize Particles in a Two-Stage Electrostatic Precipitator. *Ind. Eng. Chem. Res.* **2006**, *45*, 8484–8491. [[CrossRef](#)]
168. Lin, G.-Y.; Tsai, C.-J. Numerical Modeling of Nanoparticle Collection Efficiency of Single-Stage Wire-in-Plate Electrostatic Precipitators. *Aerosol Sci. Technol.* **2010**, *44*, 1122–1130. [[CrossRef](#)]
169. Pui, D.Y.H.; Fruin, S.; McMurry, P.H. Unipolar Diffusion Charging of Ultrafine Aerosols. *Aerosol Sci. Technol.* **1988**, *8*, 173–187. [[CrossRef](#)]

170. Qi, C.; Chen, D.-R.; Greenberg, P. Performance Study of a Unipolar Aerosol Mini-Charger for a Personal Nanoparticle Sizer. *J. Aerosol Sci.* **2008**, *39*, 450–459. [CrossRef]
171. Alshehhi, M.; Shooshtari, A.; Dessiatoun, S.; Ohadi, M.; Goharzadeh, A. Parametric Performance Analysis of an Electrostatic Wire-Cylinder Aerosol Separator in Laminar Flow Using a Numerical Modeling Approach. *Sep. Sci. Technol.* **2010**, *45*, 299–309. [CrossRef]
172. Pirhadi, M.; Mousavi, A.; Sioutas, C. Evaluation of a High Flow Rate Electrostatic Precipitator (ESP) as a Particulate Matter (PM) Collector for Toxicity Studies. *Sci. Total Environ.* **2020**, *739*, 140060. [CrossRef]
173. Kim, H.J.; Han, B.; Kim, Y.J.; Yoa, S.J. Characteristics of an Electrostatic Precipitator for Submicron Particles Using Non-Metallic Electrodes and Collection Plates. *J. Aerosol Sci.* **2010**, *41*, 987–997. [CrossRef]
174. Yang, Z.; Zheng, C.; Liu, S.; Guo, Y.; Liang, C.; Wang, Y.; Hu, D.; Gao, X. A Combined Wet Electrostatic Precipitator for Efficiently Eliminating Fine Particle Penetration. *Fuel Process. Technol.* **2018**, *180*, 122–129. [CrossRef]
175. Li, Z.; Liu, Y.; Xing, Y.; Tran, T.M.P.; Le, T.C.; Tsai, C.J. Novel Wire-on-Plate Electrostatic Precipitator (WOP-EP) for Controlling Fine Particle and Nanoparticle Pollution. *Environ. Sci. Technol.* **2015**, *49*, 8683–8690. [CrossRef]
176. Chen, L.; Gonze, E.; Ondarts, M.; Outin, J.; Gonthier, Y. Electrostatic Precipitator for Fine and Ultrafine Particle Removal from Indoor Air Environments. *Sep. Purif. Technol.* **2020**, *247*, 116964. [CrossRef]
177. Huang, S.H.; Chen, C.C. Ultrafine Aerosol Penetration through Electrostatic Precipitators. *Environ. Sci. Technol.* **2002**, *36*, 4625–4632. [CrossRef] [PubMed]
178. Knuttsen, F.; Parker, K.R. Mechanical Design Considerations for Dry Precipitators. In *Applied Electrostatic Precipitation*; Blackie Academic & Professional: London, UK, 1997; pp. 89–112.
179. NEUNDORFER Electrostatic Precipitator. Available online: <http://www.neundorfer.com/knowledgebase/> (accessed on 14 May 2020).
180. Davidson, J.H.; Mckinney, P.J. EHD Flow Visualization in the Wire-Plate and Barbed Plate Electrostatic Precipitator. *IEEE Trans. Ind. Appl.* **1991**, *27*, 154–160. [CrossRef]
181. El Dein, A.Z.; Usama, K. Experimental and Simulation Study of V-I Characteristics of Wire-Plate Electrostatic Precipitators Under Clean Air Conditions. *Arab. J. Sci. Eng.* **2014**, *39*, 4037–4045. [CrossRef]
182. Andrade, R.G.S.A.; Oliveira, A.E.; Guerra, V.G. Graphical Methodology to Study the Corona Onset Voltage for Electrostatic Precipitation of Nanoparticles. *Theor. Found. Chem. Eng.* **2022**, *56*, 504–512. [CrossRef]
183. Kasdi, A. Computation and Measurement of Corona Current Density and V-I Characteristics in Wires-to-Plates Electrostatic Precipitator. *J. Electrostat.* **2016**, *81*, 1–8. [CrossRef]
184. Bonfim, D.P.F.; Medeiros, G.B.; de Oliveira, A.E.; Guerra, V.G.; Aguiar, M.L. Nanomaterials in the Environment: Definitions, Characterizations, Effects, and Applications. In *Environmental, Ethical, and Economical Issues of Nanotechnology*; Hussain, C.M., da Costa, G.M., Eds.; Jenny Stanford Publishing Pte. Ltd.: New York, NY, USA, 2022; pp. 1–30. ISBN 978-981-4877-76-3.
185. Li, P.; Wang, C.; Zhang, Y.; Wei, F. Air Filtration in the Free Molecular Flow Regime: A Review of High-Efficiency Particulate Air Filters Based on Carbon Nanotubes. *Small* **2014**, *10*, 4543–4561. [CrossRef]
186. Bai, H.; Qian, X.; Fan, J.; Shi, Y.; Duo, Y.; Guo, C.; Wang, X. Theoretical Model of Single Fiber Efficiency and the Effect of Microstructure on Fibrous Filtration Performance: A Review. *Ind. Eng. Chem. Res.* **2021**, *60*, 3–36. [CrossRef]
187. Givehchi, R.; Tan, Z. An Overview of Airborne Nanoparticle Filtration and Thermal Rebound Theory. *Aerosol. Air Qual. Res.* **2014**, *14*, 46–63. [CrossRef]
188. Abdolghader, P.; Brochot, C.; Haghighat, F.; Bahloul, A. Airborne Nanoparticles Filtration Performance of Fibrous Media: A Review. *Sci. Technol. Built Environ.* **2018**, *24*, 648–672. [CrossRef]
189. Kanaoka, C. Fine Particle Filtration Technology Using Fiber as Dust Collection Medium. *KONA Powder Part. J.* **2019**, *36*, 88–113. [CrossRef]
190. Yang, C. Aerosol Filtration Application Using Fibrous Media—An Industrial Perspective. *Chin. J. Chem. Eng.* **2012**, *20*, 1–9. [CrossRef]
191. Zhang, S.; Rind, N.A.; Tang, N.; Liu, H.; Yin, X.; Yu, J.; Ding, B. Electrospun Nanofibers for Air Filtration. In *Electrospinning: Nanofabrication and Applications*; Elsevier Inc.: Amsterdam, The Netherlands, 2019; pp. 365–389. ISBN 9780323512701.
192. Wang, C.-S. Electrostatic Forces in Fibrous Filters—a Review. *Powder Technol.* **2001**, *118*, 166–170. [CrossRef]
193. Chow, J.C.; Watson, J.G.; Wang, X.; Abbasi, B.; Reed, W.R.; Parks, D. Review of Filters for Air Sampling and Chemical Analysis in Mining Workplaces. *Minerals* **2022**, *12*, 1314. [CrossRef]
194. Mouret, G.; Chazelet, S.; Thomas, D.; Bemer, D. Discussion about the Thermal Rebound of Nanoparticles. *Sep. Purif. Technol.* **2011**, *78*, 125–131. [CrossRef]
195. Brummer, V.; Jecha, D.; Lestinsky, P.; Skryja, P.; Gregor, J.; Stehlik, P. The Treatment of Waste Gas from Fertilizer Production - An Industrial Case Study of Long Term Removing Particulate Matter with a Pilot Unit. *Powder Technol.* **2016**, *297*, 374–383. [CrossRef]
196. Findanis, N.; Southam, M. Control and Management of Particulate Emissions Using Improved Reverse Pulse-Jet Cleaning Systems. *Procedia Eng.* **2012**, *49*, 228–238. [CrossRef]
197. Liu, X.; Shen, H.; Nie, X. Study on the Filtration Performance of the Baghouse Filters for Ultra-Low Emission as a Function of Filter Pore Size and Fiber Diameter. *Int. J. Environ. Res. Public Health* **2019**, *16*, 247. [CrossRef] [PubMed]
198. Tcharkhtchi, A.; Abbasnezhad, N.; Zarbini Seydani, M.; Zirak, N.; Farzaneh, S.; Shirinbayan, M. An Overview of Filtration Efficiency through the Masks: Mechanisms of the Aerosols Penetration. *Bioact. Mater.* **2021**, *6*, 106–122. [CrossRef]

199. Brochot, C.; Abdolghader, P.; Haghghat, F.; Bahloul, A. Performance of Mechanical Filters Used in General Ventilation against Nanoparticles. *Sci. Technol. Built Environ.* **2020**, *26*, 1387–1396. [[CrossRef](#)]
200. Brochot, C.; Bahloul, A.; Abdolghader, P.; Haghghat, F. Performance of Mechanical Filters Used in General Ventilation against Nanoparticles. *IOP Conf. Ser. Mater. Sci. Eng.* **2019**, *609*, 032044. [[CrossRef](#)]
201. Bortolassi, A.C.C.; Guerra, V.G.; Aguiar, M.L. Evaluation of Different HEPA Filter Media for Removing Nickel Oxide Nanoparticles from Air Filtration. *Tecnol. em Metal. Mater. e Mineração* **2019**, *16*, 426–431. [[CrossRef](#)]
202. Bortolassi, A.C.C.; Guerra, V.G.; Aguiar, M.L. Characterization and Evaluate the Efficiency of Different Filter Media in Removing Nanoparticles. *Sep. Purif. Technol.* **2017**, *175*, 79–86. [[CrossRef](#)]
203. Kim, C.; Kang, S.; Pui, D.Y.H. Removal of Airborne Sub-3 Nm Particles Using Fibrous Filters and Granular Activated Carbons. *Carbon N. Y.* **2016**, *104*, 125–132. [[CrossRef](#)]
204. Bonfim, D.P.F.; Cruz, F.G.S.; Bretas, R.E.S.; Guerra, V.G.; Aguiar, M.L. A Sustainable Recycling Alternative: Electrospun Pet-Membranes for Air Nanofiltration. *Polymers* **2021**, *13*, 1166. [[CrossRef](#)]
205. Bulejko, P.; Dohnal, M.; Pospíšil, J.; Svěrák, T. Air Filtration Performance of Symmetric Polypropylene Hollow-Fibre Membranes for Nanoparticle Removal. *Sep. Purif. Technol.* **2018**, *197*, 122–128. [[CrossRef](#)]
206. Wang, C.; Li, P.; Zong, Y.; Zhang, Y.; Li, S.; Wei, F. A High Efficiency Particulate Air Filter Based on Agglomerated Carbon Nanotube Fluidized Bed. *Carbon N. Y.* **2014**, *79*, 424–431. [[CrossRef](#)]
207. Shin, W.G.; Mulholland, G.W.; Kim, S.C.; Pui, D.Y.H. Experimental Study of Filtration Efficiency of Nanoparticles below 20 nm at Elevated Temperatures. *J. Aerosol Sci.* **2008**, *39*, 488–499. [[CrossRef](#)]
208. Zhou, Z.-J.; Zhou, B.; Tseng, C.-H.; Hu, S.-C.; Shiue, A.; Leggett, G. Evaluation of Characterization and Filtration Performance of Air Cleaner Materials. *Int. J. Environ. Sci. Technol.* **2021**, *18*, 2209–2220. [[CrossRef](#)]
209. Kim, C.S.; Bao, L.; Okuyama, K.; Shimada, M.; Niinuma, H. Filtration Efficiency of a Fibrous Filter for Nanoparticles. *J. Nanoparticle Res.* **2006**, *8*, 215–221. [[CrossRef](#)]
210. Golanski, L.; Guiot, A.; Rouillon, F.; Pocachard, J.; Tardif, F. Experimental Evaluation of Personal Protection Devices against Graphite Nanoaerosols: Fibrous Filter Media, Masks, Protective Clothing, and Gloves. *Hum. Exp. Toxicol.* **2009**, *28*, 353–359. [[CrossRef](#)]
211. Kwon, O.; Yoon, C.; Ham, S.; Park, J.; Lee, J.; Yoo, D.; Kim, Y. Characterization and Control of Nanoparticle Emission during 3D Printing. *Environ. Sci. Technol.* **2017**, *51*, 10357–10368. [[CrossRef](#)]
212. Förster, H.; Thajudeen, T.; Funk, C.; Peukert, W. Separation of Nanoparticles: Filtration and Scavenging from Waste Incineration Plants. *Waste Manag.* **2016**, *52*, 346–352. [[CrossRef](#)]
213. Giechaskiel, B.; Riccobono, F.; Vlachos, T.; Mendoza-Villafuerte, P.; Suarez-Bertoa, R.; Fontaras, G.; Bonnel, P.; Weiss, M. Vehicle Emission Factors of Solid Nanoparticles in the Laboratory and on the Road Using Portable Emission Measurement Systems (PEMS). *Front. Environ. Sci.* **2015**, *3*, 82. [[CrossRef](#)]
214. Ushakov, S.; Valland, H.; Nielsen, J.B.; Hennie, E. Effects of Dilution Conditions on Diesel Particle Size Distribution and Filter Mass Measurements in Case of Marine Fuels. *Fuel Process. Technol.* **2014**, *118*, 244–253. [[CrossRef](#)]
215. Larcombe, A.N.; Janka, M.A.; Mullins, B.J.; Berry, L.J.; Bredin, A.; Franklin, P.J. The Effects of Electronic Cigarette Aerosol Exposure on Inflammation and Lung Function in Mice. *Am. J. Physiol. Cell. Mol. Physiol.* **2017**, *313*, L67–L79. [[CrossRef](#)]
216. Aszyk, J.; Kubica, P.; Namieśnik, J.; Kot-Wasik, A.; Wasik, A. New Approach for E-Cigarette Aerosol Collection by an Original Automatic Aerosol Generator Utilizing Melt-Blown Non-Woven Fabric. *Anal. Chim. Acta* **2018**, *1038*, 67–78. [[CrossRef](#)] [[PubMed](#)]
217. Zhang, L.; Lin, Y.; Zhu, Y. Transport and Mitigation of Exhaled Electronic Cigarette Aerosols in a Multizone Indoor Environment. *Aerosol Air Qual. Res.* **2020**, *20*, 2536–2547. [[CrossRef](#)]
218. Werley, M.S.; Miller, J.H.; Kane, D.B.; Tucker, C.S.; McKinney, W.J.; Oldham, M.J. Prototype E-Cigarette and the Capillary Aerosol Generator (CAG) Comparison and Qualification for Use in Subchronic Inhalation Exposure Testing. *Aerosol Sci. Technol.* **2016**, *50*, 1284–1293. [[CrossRef](#)]
219. Martuzevicius, D.; Prasauskas, T.; Setyan, A.; O’Connell, G.; Cahours, X.; Julien, R.; Colard, S. Characterization of the Spatial and Temporal Dispersion Differences between Exhaled E-Cigarette Mist and Cigarette Smoke. *Nicotine Tob. Res.* **2019**, *21*, 1371–1377. [[CrossRef](#)] [[PubMed](#)]
220. Kärkelä, T.; Ebinger, J.-C.; Tapper, U.; Robyr, O.; Jalanti, T. Investigation into the Presence or Absence of Solid Particles Generated from Thermal Processes in the Aerosol from an Electrically Heated Tobacco Product with and without Filter Elements. *Aerosol Air Qual. Res.* **2021**, *21*, 200667. [[CrossRef](#)]
221. Lee, H.; Kim, S.; Joo, H.; Cho, H.; Park, K. A Study on Performance and Reusability of Certified and Uncertified Face Masks. *Aerosol Air Qual. Res.* **2022**, *22*, 210370. [[CrossRef](#)]
222. Hill, W.C.; Hull, M.S.; MacCuspie, R.I. Testing of Commercial Masks and Respirators and Cotton Mask Insert Materials Using SARS-CoV-2 Virion-Sized Particulates: Comparison of Ideal Aerosol Filtration Efficiency versus Fitted Filtration Efficiency. *Nano Lett.* **2020**, *20*, 7642–7647. [[CrossRef](#)]
223. Rengasamy, S.; Eimer, B.C. Nanoparticle Penetration through Filter Media and Leakage through Face Seal Interface of N95 Filtering Facepiece Respirators. *Ann. Occup. Hyg.* **2012**, *56*, 568–580. [[CrossRef](#)] [[PubMed](#)]
224. Majchrzycka, K.; Okrasa, M.; Jachowicz, A.; Szulc, J.; Gutarowska, B. Microbial Growth on Dust-Loaded Filtering Materials Used for the Protection of Respiratory Tract as a Factor Affecting Filtration Efficiency. *Int. J. Environ. Res. Public Health* **2018**, *15*, 1902. [[CrossRef](#)]

225. Zhou, B.; Xu, Y.; Fan, J.-Q.; Chen, L.-P.; Li, F.; Xue, K. Numerical Simulation and Experimental Validation for the Filtration Performance of Fibrous Air Filter Media with LB Method. *Aerosol Air Qual. Res.* **2017**, *17*, 2645–2658. [[CrossRef](#)]
226. Tronville, P.; Rivers, R. Properties of Nanoparticles Affecting Simulation of Fibrous Gas Filter Performance. *J. Phys. Conf. Ser.* **2015**, *617*, 012010. [[CrossRef](#)]
227. Fotovati, S.; Tafreshi, H.V.; Pourdeyhimi, B. Analytical Expressions for Predicting Performance of Aerosol Filtration Media Made up of Trilobal Fibers. *J. Hazard. Mater.* **2011**, *186*, 1503–1512. [[CrossRef](#)]
228. Mouret, G.; Calle-Chazelet, S.; Thomas, D.; Bemer, D.; Appert-Collin, J.-C. Nanoparticles Filtration by Leaked Fibrous Filters. *J. Phys. Conf. Ser.* **2009**, *170*, 012028. [[CrossRef](#)]
229. Givehchi, R.; Tan, Z. The Effect of Capillary Force on Airborne Nanoparticle Filtration. *J. Aerosol Sci.* **2015**, *83*, 12–24. [[CrossRef](#)]
230. Todea, A.M.; Schmidt, F.; Schuldt, T.; Asbach, C. Development of a Method to Determine the Fractional Deposition Efficiency of Full-Scale HVAC and HEPA Filter Cassettes for Nanoparticles ≥ 3.5 Nm. *Atmosphere* **2020**, *11*, 1191. [[CrossRef](#)]
231. Ghoshdastidar, A.J.; Ramamurthy, J.; Morissette, M.; Ariya, P.A. Development of Methodology to Generate, Measure, and Characterize the Chemical Composition of Oxidized Mercury Nanoparticles. *Anal. Bioanal. Chem.* **2020**, *412*, 691–702. [[CrossRef](#)]
232. Park, D.H.; Joe, Y.H.; Piri, A.; An, S.; Hwang, J. Determination of Air Filter Anti-Viral Efficiency against an Airborne Infectious Virus. *J. Hazard. Mater.* **2020**, *396*, 122640. [[CrossRef](#)]
233. Sachinidou, P.; Bahk, Y.K.; Tang, M.; Zhang, N.; Chen, S.S.C.; Pui, D.Y.H.; Lima, B.A.; Bosco, G.; Tronville, P.; Mosimann, T.; et al. Inter-Laboratory Validation of the Method to Determine the Filtration Efficiency for Airborne Particles in the 3–500 Nm Range and Results Sensitivity Analysis. *Aerosol Air Qual. Res.* **2017**, *17*, 2669–2680. [[CrossRef](#)]
234. Yin, N.; Liu, F. Nanofibrous Filters for PM_{2.5} Filtration: Conception, Mechanism and Progress. *Nano* **2021**, *16*, 2130004. [[CrossRef](#)]
235. Liu, J.; Pui, D.Y.H.; Wang, J. Removal of Airborne Nanoparticles by Membrane Coated Filters. *Sci. Total Environ.* **2011**, *409*, 4868–4874. [[CrossRef](#)]
236. Chen, F.; Ji, Z.; Qi, Q. Effect of Surface Wettability on Filtration Performance of Gas-Liquid Coalescing Filters. *Powder Technol.* **2019**, *357*, 377–386. [[CrossRef](#)]
237. Innocentini, M.D.d.M.; Coury, J.R.; Fukushima, M.; Colombo, P. High-Efficiency Aerosol Filters Based on Silicon Carbide Foams Coated with Ceramic Nanowires. *Sep. Purif. Technol.* **2015**, *152*, 180–191. [[CrossRef](#)]
238. Cho, D.; Naydich, A.; Frey, M.W.; Joo, Y.L. Further Improvement of Air Filtration Efficiency of Cellulose Filters Coated with Nanofibers via Inclusion of Electrostatically Active Nanoparticles. *Polymer* **2013**, *54*, 2364–2372. [[CrossRef](#)]
239. Zhang, Y.; He, X.; Zhu, Z.; Wang, W.-N.; Chen, S.-C. Simultaneous Removal of VOCs and PM_{2.5} by Metal-Organic Framework Coated Electret Filter Media. *J. Memb. Sci.* **2021**, *618*, 118629. [[CrossRef](#)]
240. Dai, Z.; Zhu, J.; Yan, J.; Su, J.; Gao, Y.; Zhang, X.; Ke, Q.; Parsons, G.N. An Advanced Dual-Function MnO₂-Fabric Air Filter Combining Catalytic Oxidation of Formaldehyde and High-Efficiency Fine Particulate Matter Removal. *Adv. Funct. Mater.* **2020**, *30*, 2001488. [[CrossRef](#)]
241. Juuti, P.; Nikka, M.; Gunell, M.; Eerola, E.; Saarinen, J.J.; Omori, Y.; Seto, T.; Mäkelä, J.M. Fabrication of Fiber Filters with Antibacterial Properties for VOC and Particle Removal. *Aerosol Air Qual. Res.* **2019**, *19*, 1892–1899. [[CrossRef](#)]
242. Chong, E.; Hwang, G.B.; Nho, C.W.; Kwon, B.M.; Lee, J.E.; Seo, S.; Bae, G.-N.; Jung, J.H. Antimicrobial Durability of Air Filters Coated with Airborne *Sophora Flavescens* Nanoparticles. *Sci. Total Environ.* **2013**, *444*, 110–114. [[CrossRef](#)]
243. Zhao, Y.; Zhong, Z.; Low, Z.-X.; Yao, Z. A Multifunctional Multi-Walled Carbon Nanotubes/Ceramic Membrane Composite Filter for Air Purification. *RSC Adv.* **2015**, *5*, 91951–91959. [[CrossRef](#)]
244. Balagna, C.; Perero, S.; Bosco, F.; Mollea, C.; Irfan, M.; Ferraris, M. Antipathogen Nanostructured Coating for Air Filters. *Appl. Surf. Sci.* **2020**, *508*, 145283. [[CrossRef](#)]
245. Joe, Y.H.; Ju, W.; Park, J.H.; Yoon, Y.H.; Hwang, J. Correlation between the Antibacterial Ability of Silver Nanoparticle Coated Air Filters and the Dust Loading. *Aerosol Air Qual. Res.* **2013**, *13*, 1009–1018. [[CrossRef](#)]
246. Zendejdel, R.; Amini, M.M.; Hajibabaei, M.; Nasiri, M.J.; Jafari, M.J.; Alavijeh, M.K. Doping Metal-Organic Framework Composites to Antibacterial Air Filter Development for Quality Control of Indoor Air. *Environ. Prog. Sustain. Energy* **2022**, *41*. [[CrossRef](#)]
247. Machry, K.; Souza, C.W.O.; Aguiar, M.L.; Bernardo, A. Prevention of Pathogen Microorganisms at Indoor Air Ventilation System Using Synthesized Copper Nanoparticles. *Can. J. Chem. Eng.* **2022**, *100*, 1739–1746. [[CrossRef](#)]
248. Ali, A.; Pan, M.; Tilly, T.B.; Zia, M.; Wu, C.Y. Performance of Silver, Zinc, and Iron Nanoparticles-Doped Cotton Filters against Airborne *E. Coli* to Minimize Bioaerosol Exposure. *Air Qual. Atmos. Heal.* **2018**, *11*, 1233–1242. [[CrossRef](#)]
249. Salama, K.F.; Alnimr, A.; Alamri, A.; Radi, M.; Alshehri, B.; Rabaan, A.A.; Alshahrani, M. Nano-Treatment of HEPA Filters in COVID-19 Isolation Rooms in an Academic Medical Center in Saudi Arabia. *J. Infect. Public Health* **2022**, *15*, 937–941. [[CrossRef](#)]
250. Perelshtein, I.; Levi, I.; Perkas, N.; Pollak, A.; Gedanken, A. CuO-Coated Antibacterial and Antiviral Car Air-Conditioning Filters. *ACS Appl. Mater. Interf.* **2022**, *14*, 24850–24855. [[CrossRef](#)]
251. Baselga, M.; Uranga-Murillo, I.; de Miguel, D.; Arias, M.; Sebastián, V.; Pardo, J.; Arruebo, M. Silver Nanoparticles-Polyethyleneimine-Based Coatings with Antiviral Activity against SARS-CoV-2: A New Method to Functionalize Filtration Media. *Materials* **2022**, *15*, 4742. [[CrossRef](#)]
252. Park, D.H.; Joe, Y.H.; Hwang, J. Dry Aerosol Coating of Anti-Viral Particles on Commercial Air Filters Using a High-Volume Flow Atomizer. *Aerosol Air Qual. Res.* **2019**, *19*, 1636–1644. [[CrossRef](#)]

253. Joe, Y.H.; Woo, K.; Hwang, J. Fabrication of an Anti-Viral Air Filter with SiO₂-Ag Nanoparticles and Performance Evaluation in a Continuous Airflow Condition. *J. Hazard. Mater.* **2014**, *280*, 356–363. [[CrossRef](#)]
254. Andrade, B.K.S.A.; Sartim, R.; Aguiar, M.L. Precoating Effects in Fine Steelmaking Dust Filtration. *Atmosphere* **2022**, *13*, 1669. [[CrossRef](#)]
255. Bao, L.; Seki, K.; Niinuma, H.; Otani, Y.; Balgis, R.; Ogi, T.; Gradon, L.; Okuyama, K. Verification of Slip Flow in Nanofiber Filter Media through Pressure Drop Measurement at Low-Pressure Conditions. *Sep. Purif. Technol.* **2016**, *159*, 100–107. [[CrossRef](#)]
256. Tang, M.; Hu, J.; Liang, Y.; Pui, D.Y. Pressure Drop, Penetration and Quality Factor of Filter Paper Containing Nanofibers. *Text. Res. J.* **2017**, *87*, 498–508. [[CrossRef](#)]
257. da Mata, G.C.; Morais, M.S.; de Oliveira, W.P.; Aguiar, M.L. Composition Effects on the Morphology of PVA/Chitosan Electrospun Nanofibers. *Polymers* **2022**, *14*, 4856. [[CrossRef](#)]
258. Li, J.; Zhang, D.; Yang, T.; Yang, S.; Yang, X.; Zhu, H. Nanofibrous Membrane of Graphene Oxide-in-Polyacrylonitrile Composite with Low Filtration Resistance for the Effective Capture of PM_{2.5}. *J. Memb. Sci.* **2018**, *551*, 85–92. [[CrossRef](#)]
259. Deshawar, D.; Gupta, K.; Chokshi, P. Electrospinning of Polymer Solutions: An Analysis of Instability in a Thinning Jet with Solvent Evaporation. *Polymer* **2020**, *202*, 122656. [[CrossRef](#)]
260. Kim, H.-J.; Park, S.J.; Park, C.S.; Le, T.-H.; Hun Lee, S.; Ha, T.H.; Kim, H.; Kim, J.; Lee, C.-S.; Yoon, H.; et al. Surface-Modified Polymer Nanofiber Membrane for High-Efficiency Microdust Capturing. *Chem. Eng. J.* **2018**, *339*, 204–213. [[CrossRef](#)]
261. Choi, H.-J.; Kim, S.B.; Kim, S.H.; Lee, M.-H. Preparation of Electrospun Polyurethane Filter Media and Their Collection Mechanisms for Ultrafine Particles. *J. Air Waste Manag. Assoc.* **2014**, *64*, 322–329. [[CrossRef](#)]
262. Almeida, D.S.; Martins, L.D.; Muniz, E.C.; Rudke, A.P.; Squizzato, R.; Beal, A.; de Souza, P.R.; Bonfim, D.P.F.; Aguiar, M.L.; Gimenes, M.L. Biodegradable CA/CPB Electrospun Nanofibers for Efficient Retention of Airborne Nanoparticles. *Process Saf. Environ. Prot.* **2020**, *144*, 177–185. [[CrossRef](#)] [[PubMed](#)]
263. Oliveira, A.E.; Aguiar, M.L.; Guerra, V.G. Improved Filter Media with PVA/Citric Acid/Triton X-100 Nanofibers for Filtration of Nanoparticles from Air. *Polym. Bull.* **2021**, *78*, 6387–6408. [[CrossRef](#)]
264. Bonfim, D.P.F.; Cruz, F.G.S.; Guerra, V.G.; Aguiar, M.L. Development of Filter Media by Electrospinning for Air Filtration of Nanoparticles from PET Bottles. *Membranes* **2021**, *11*, 293. [[CrossRef](#)] [[PubMed](#)]
265. Greiner, A.; Wendorff, J.H. Electrospinning: A Fascinating Method for the Preparation of Ultrathin Fibers. *Angew. Chem. Int. Ed.* **2007**, *46*, 5670–5703. [[CrossRef](#)]
266. Huang, Z.M.; Zhang, Y.Z.; Kotaki, M.; Ramakrishna, S. A Review on Polymer Nanofibers by Electrospinning and Their Applications in Nanocomposites. *Compos. Sci. Technol.* **2003**, *63*, 2223–2253. [[CrossRef](#)]
267. Anitha, S.; Brabu, B.; Thiruvadigal, D.J.; Gopalakrishnan, C.; Natarajan, T.S. Optical, Bactericidal and Water Repellent Properties of Electrospun Nano-Composite Membranes of Cellulose Acetate and ZnO. *Carbohydr. Polym.* **2012**, *87*, 1065–1072. [[CrossRef](#)]
268. Ismail, N.; Junior Maksoud, F.; Ghaddar, N.; Ghali, K.; Tehrani-Bagha, A. A Mathematical Model to Predict the Effect of Electrospinning Processing Parameters on the Morphological Characteristic of Nano-Fibrous Web and Associated Filtration Efficiency. *J. Aerosol Sci.* **2017**, *113*, 227–241. [[CrossRef](#)]
269. Maze, B.; Vahedi Tafreshi, H.; Wang, Q.; Pourdeyhimi, B. A Simulation of Unsteady-State Filtration via Nanofiber Media at Reduced Operating Pressures. *J. Aerosol. Sci.* **2007**, *38*, 550–571. [[CrossRef](#)]
270. Robert, B.; Nallathambi, G. Highly Oriented Poly (m-Phenylene Isophthalamide)/Polyacrylonitrile Based Coaxial Nanofibers Integrated with Electrospun Polyacrylonitrile-Silver Nanoparticle: Application in Air Filtration of Particulate and Microbial Contaminants. *J. Appl. Polym. Sci.* **2022**, *139*, 52294. [[CrossRef](#)]
271. Orlando, R.; Polat, M.; Afshari, A.; Johnson, M.S.; Fojan, P. Electrospun Nanofibre Air Filters for Particles and Gaseous Pollutants. *Sustainability* **2021**, *13*, 6553. [[CrossRef](#)]
272. Blosi, M.; Costa, A.L.; Ortelli, S.; Belosi, F.; Ravegnani, F.; Varesano, A.; Tonetti, C.; Zanoni, I.; Vineis, C. Polyvinyl Alcohol/Silver Electrospun Nanofibers: Biocidal Filter Media Capturing Virus-size Particles. *J. Appl. Polym. Sci.* **2021**, *138*, 51380. [[CrossRef](#)] [[PubMed](#)]
273. Remiro, P.d.F.R.; Sousa, C.P.; Alves, H.C.; Bernardo, A.; Aguiar, M.L. In Situ Evaluation of Filter Media Modified by Biocidal Nanomaterials to Control Bioaerosols in Internal Environments. *Water Air Soil Pollut.* **2021**, *232*, 176. [[CrossRef](#)]
274. Li, X.; Wang, N.; Fan, G.; Yu, J.; Gao, J.; Sun, G.; Ding, B. Electretted Polyetherimide-Silica Fibrous Membranes for Enhanced Filtration of Fine Particles. *J. Colloid Interf. Sci.* **2015**, *439*, 12–20. [[CrossRef](#)] [[PubMed](#)]
275. Gobi, N.; Vijayalakshmi, E.; Robert, B.; Srinivasan, N.R. Development of PAN Nano Fibrous Filter Hybridized by SiO₂ Nanoparticles Electret for High Efficiency Air Filtration. *J. Polym. Mater.* **2019**, *35*, 317–328. [[CrossRef](#)]
276. Yeom, B.Y.; Shim, E.; Pourdeyhimi, B. Boehmite Nanoparticles Incorporated Electrospun Nylon-6 Nanofiber Web for New Electret Filter Media. *Macromol. Res.* **2010**, *18*, 884–890. [[CrossRef](#)]
277. Ding, X.; Li, Y.; Si, Y.; Yin, X.; Yu, J.; Ding, B. Electrospun Polyvinylidene Fluoride/SiO₂ Nanofibrous Membranes with Enhanced Electret Property for Efficient Air Filtration. *Compos. Commun.* **2019**, *13*, 57–62. [[CrossRef](#)]
278. Wang, S.; Zhao, X.; Yin, X.; Yu, J.; Ding, B. Electret Polyvinylidene Fluoride Nanofibers Hybridized by Polytetrafluoroethylene Nanoparticles for High-Efficiency Air Filtration. *ACS Appl. Mater. Interf.* **2016**, *8*, 23985–23994. [[CrossRef](#)]
279. Li, Y.; Yin, X.; Si, Y.; Yu, J.; Ding, B. All-Polymer Hybrid Electret Fibers for High-Efficiency and Low-Resistance Filter Media. *Chem. Eng. J.* **2020**, *398*, 125626. [[CrossRef](#)]

280. He, R.; Li, J.; Chen, M.; Zhang, S.; Cheng, Y.; Ning, X.; Wang, N. Tailoring Moisture Electroactive Ag/Zn@cotton Coupled with Electrospun PVDF/PS Nanofibers for Antimicrobial Face Masks. *J. Hazard. Mater.* **2022**, *428*, 128239. [[CrossRef](#)]
281. Jiang, Z.; Zhang, H.; Zhu, M.; Lv, D.; Yao, J.; Xiong, R.; Huang, C. Electrospun Soy-Protein-Based Nanofibrous Membranes for Effective Antimicrobial Air Filtration. *J. Appl. Polym. Sci.* **2018**, *135*, 45766. [[CrossRef](#)]
282. Sun, Z.; Yue, Y.; He, W.; Jiang, F.; Lin, C.-H.; Pui, D.Y.H.; Liang, Y.; Wang, J. The Antibacterial Performance of Positively Charged and Chitosan Dipped Air Filter Media. *Buill. Environ.* **2020**, *180*, 107020. [[CrossRef](#)]
283. Kayaci, F.; Uyar, T. Electrospun Polyester/Cyclodextrin Nanofibers for Entrapment of Volatile Organic Compounds. *Polym. Eng. Sci.* **2014**, *54*, 2970–2978. [[CrossRef](#)]
284. Liu, K.; Xiao, Z.; Ma, P.; Chen, J.; Li, M.; Liu, Q.; Wang, Y.; Wang, D. Large Scale Poly(Vinyl Alcohol-Co-Ethylene)/TiO₂ Hybrid Nanofibrous Filters with Efficient Fine Particle Filtration and Repetitive-Use Performance. *RSC Adv.* **2015**, *5*, 87924–87931. [[CrossRef](#)]
285. Yi, Z.; Cheng, P.; Chen, J.; Liu, K.; Liu, Q.; Li, M.; Zhong, W.; Wang, W.; Lu, Z.; Wang, D. PVA-Co-PE Nanofibrous Filter Media with Tailored Three-Dimensional Structure for High Performance and Safe Aerosol Filtration via Suspension-Drying Procedure. *Ind. Eng. Chem. Res.* **2018**, *57*, 9269–9280. [[CrossRef](#)]
286. Zhang, S.; Tang, N.; Cao, L.; Yin, X.; Yu, J.; Ding, B. Highly Integrated Polysulfone/Polyacrylonitrile/Polyamide-6 Air Filter for Multilevel Physical Sieving Airborne Particles. *ACS Appl. Mater. Interf.* **2016**, *8*, 29062–29072. [[CrossRef](#)]
287. Demirel, O.; Kolgesiz, S.; Yuce, S.; Hayat Soytaş, S.; Koseoglu-Imer, D.Y.; Unal, H. Photothermal Electrospun Nanofibers Containing Polydopamine-Coated Halloysite Nanotubes as Antibacterial Air Filters. *ACS Appl. Nano Mater.* **2022**, *5*, 18127–18137. [[CrossRef](#)]
288. Li, D.; Shen, Y.; Wang, L.; Liu, F.; Deng, B.; Liu, Q. Hierarchical Structured Polyimide–Silica Hybrid Nano/Microfiber Filters Welded by Solvent Vapor for Air Filtration. *Polymers* **2020**, *12*, 2494. [[CrossRef](#)]
289. Wang, N.; Si, Y.; Wang, N.; Sun, G.; El-Newehy, M.; Al-Deyab, S.S.; Ding, B. Multilevel Structured Polyacrylonitrile/Silica Nanofibrous Membranes for High-Performance Air Filtration. *Sep. Purif. Technol.* **2014**, *126*, 44–51. [[CrossRef](#)]
290. Wan, H.; Wang, N.; Yang, J.; Si, Y.; Chen, K.; Ding, B.; Sun, G.; El-Newehy, M.; Al-Deyab, S.S.; Yu, J. Hierarchically Structured Polysulfone/Titania Fibrous Membranes with Enhanced Air Filtration Performance. *J. Colloid Interf. Sci.* **2014**, *417*, 18–26. [[CrossRef](#)] [[PubMed](#)]
291. Karabulut, F.N.H.; Fomra, D.; Höfler, G.; Chand, N.A.; Beckermann, G.W. Virucidal and Bactericidal Filtration Media from Electrospun Polylactic Acid Nanofibres Capable of Protecting against COVID-19. *Membranes* **2022**, *12*, 571. [[CrossRef](#)] [[PubMed](#)]
292. Li, H.; Wang, Z.; Zhang, H.; Pan, Z. Nanoporous PLA/(Chitosan Nanoparticle) Composite Fibrous Membranes with Excellent Air Filtration and Antibacterial Performance. *Polymers* **2018**, *10*, 1085. [[CrossRef](#)]
293. Lee, H.; Jeon, S. Polyacrylonitrile Nanofiber Membranes Modified with Ni-Based Conductive Metal Organic Frameworks for Air Filtration and Respiration Monitoring. *ACS Appl. Nano Mater.* **2020**, *3*, 8192–8198. [[CrossRef](#)]
294. Mirzaei, F.; Abbasi, A.; Dehghan, S.F.; Pourmand, M.R.; Mortazavi, S.-S.; Masoorian, E.; Mousavi, T.; Golbabaee, F. Removal of Bioaerosols Using Metal-Organic Frameworks Incorporated into Electrospun Nanofibers. *Fibers Polym.* **2021**, *22*, 2424–2432. [[CrossRef](#)]
295. Hartati, S.; Zulf, A.; Maulida, P.Y.D.; Yudhowijoyo, A.; Dioktyanto, M.; Saputro, K.E.; Noviyanto, A.; Rochman, N.T. Synthesis of Electrospun PAN/TiO₂/Ag Nanofibers Membrane As Potential Air Filtration Media with Photocatalytic Activity. *ACS Omega* **2022**, *7*, 10516–10525. [[CrossRef](#)]
296. Dehghan, S.F.; Golbabaee, F.; Maddah, B.; Latifi, M.; Pezeshk, H.; Hasanzadeh, M.; Akbar-Khanzadeh, F. Optimization of Electrospinning Parameters for Polyacrylonitrile-MgO Nanofibers Applied in Air Filtration. *J. Air Waste Manag. Assoc.* **2016**, *66*, 912–921. [[CrossRef](#)]
297. Habibi Mohraz, M.; Je Yu, I.; Beitollahi, A.; Farhang Dehghan, S.; Hoon Shin, J.; Golbabaee, F. Assessment of the Potential Release of Nanomaterials from Electrospun Nanofiber Filter Media. *NanoImpact* **2020**, *19*, 100223. [[CrossRef](#)]
298. Wang, N.; Cai, M.; Yang, X.; Yang, Y. Electret Nanofibrous Membrane with Enhanced Filtration Performance and Wearing Comfortability for Face Mask. *J. Colloid Interf. Sci.* **2018**, *530*, 695–703. [[CrossRef](#)]
299. Olkhov, A.; Staroverova, O.; Iordanskiy, A.; Zaikov, G. Structure and Parameters of Polyhydroxybutyrate Nanofibres. *NBI Technol.* **2016**, *4*, 22–29. [[CrossRef](#)]
300. Li, Y.; Cao, L.; Yin, X.; Si, Y.; Yu, J.; Ding, B. Ultrafine, Self-Crimp, and Electret Nano-Wool for Low-Resistance and High-Efficiency Protective Filter Media against PM0.3. *J. Colloid Interf. Sci.* **2020**, *578*, 565–573. [[CrossRef](#)] [[PubMed](#)]
301. Cheng, Y.; Li, J.; Chen, M.; Zhang, S.; He, R.; Wang, N. Environmentally Friendly and Antimicrobial Bilayer Structured Fabrics with Integrated Interception and Sterilization for Personal Protective Mask. *Sep. Purif. Technol.* **2022**, *294*, 121165. [[CrossRef](#)]
302. Wang, L.; Zhang, C.; Gao, F.; Pan, G. Needleless Electrospinning for Scaled-up Production of Ultrafine Chitosan Hybrid Nanofibers Used for Air Filtration. *RSC Adv.* **2016**, *6*, 105988–105995. [[CrossRef](#)]
303. Li, J.; Gao, F.; Liu, L.Q.; Zhang, Z. Needleless Electro-Spun Nanofibers Used for Filtration of Small Particles. *Express Polym. Lett.* **2013**, *7*, 683–689. [[CrossRef](#)]
304. Jackiewicz, A.; Werner, L. Separation of Nanoparticles from Air Using Melt-Blown Filtering Media. *Aerosol Air Qual. Res.* **2015**, *15*, 2422–2435. [[CrossRef](#)]
305. Salussoglia, A.I.P.; Tanabe, E.H.; Aguiar, M.L. Evaluation of a Vacuum Collection System in the Preparation of PAN Fibers by Forc spinning for Application in Ultrafine Particle Filtration. *J. Appl. Polym. Sci.* **2020**, *137*, 49334. [[CrossRef](#)]

306. Xu, H.; Chen, X.; Chen, M.; Luo, J.; Jin, W.; Zhu, H.; Guo, Y. Development of Antibacterial PTFE Hollow Fiber Membranes Containing Silver-Carried Zirconium Phosphate as Air Filtration Units for the Removal of Ultrafine Particles. *Fibers Polym.* **2022**, *23*, 423–435. [[CrossRef](#)]
307. Zhang, S.; Liu, H.; Yin, X.; Yu, J.; Ding, B. Anti-Deformed Polyacrylonitrile/Polysulfone Composite Membrane with Binary Structures for Effective Air Filtration. *ACS Appl. Mater. Interf.* **2016**, *8*, 8086–8095. [[CrossRef](#)]
308. Xu, Y.; Zhang, X.; Teng, D.; Zhao, T.; Li, Y.; Zeng, Y. Multi-Layered Micro/Nanofibrous Nonwovens for Functional Face Mask Filter. *Nano Res.* **2022**, *15*, 7549–7558. [[CrossRef](#)]
309. Sarac, Z.; Kilic, A.; Tasdelen-Yucedag, C. Optimization of Electro-blown Polysulfone Nanofiber Mats for Air Filtration Applications. *Polym. Eng. Sci.* **2023**. [[CrossRef](#)]
310. Su, Q.; Huang, Y.; Wei, Z.; Zhu, C.; Zeng, W.; Wang, S.; Long, S.; Zhang, G.; Yang, J.; Wang, X. A Novel Multi-Gradient PASS Nanofibrous Membranes with Outstanding Particulate Matter Removal Efficiency and Excellent Antimicrobial Property. *Sep. Purif. Technol.* **2023**, *307*, 122652. [[CrossRef](#)]
311. Kim, H.-J.; Choi, D.-I.; Sung, S.-K.; Lee, S.-H.; Kim, S.-J.; Kim, J.; Han, B.-S.; Kim, D.-I.; Kim, Y. Eco-Friendly Poly(Vinyl Alcohol) Nanofiber-Based Air Filter for Effectively Capturing Particulate Matter. *Appl. Sci.* **2021**, *11*, 3831. [[CrossRef](#)]
312. Kakoria, A.; Sinha-Ray, S. Ultrafine Nanofiber-Based High Efficiency Air Filter from Waste Cigarette Butts. *Polymer* **2022**, *255*, 125121. [[CrossRef](#)]
313. Hu, S.; Zheng, Z.; Tian, Y.; Zhang, H.; Wang, M.; Yu, Z.; Zhang, X. Preparation and Characterization of Electrospun PAN-CuCl₂ Composite Nanofiber Membranes with a Special Net Structure for High-Performance Air Filters. *Polymers* **2022**, *14*, 4387. [[CrossRef](#)] [[PubMed](#)]
314. Victor, F.S.; Kugarajah, V.; Bangaru, M.; Ranjan, S.; Dharmalingam, S. Electrospun Nanofibers of Polyvinylidene Fluoride Incorporated with Titanium Nanotubes for Purifying Air with Bacterial Contamination. *Environ. Sci. Pollut. Res.* **2021**, *28*, 37520–37533. [[CrossRef](#)]
315. Shao, Z.; Chen, Y.; Jiang, J.; Xiao, Y.; Kang, G.; Wang, X.; Li, W.; Zheng, G. Multistage-Split Ultrafine Fluffy Nanofibrous Membrane for High-Efficiency Antibacterial Air Filtration. *ACS Appl. Mater. Interf.* **2022**, *14*, 18989–19001. [[CrossRef](#)]
316. Pardo-Figueroa, M.; Chiva-Flor, A.; Figueroa-Lopez, K.; Prieto, C.; Lagaron, J.M. Antimicrobial Nanofiber Based Filters for High Filtration Efficiency Respirators. *Nanomaterials* **2021**, *11*, 900. [[CrossRef](#)]
317. Zhang, H.; Jia, L.; Li, P.; Yu, L.; Liu, Y.; Zhao, W.; Wang, H.; Li, B. Large-Scale Blow Spinning of Nanofiber Membranes for Highly Efficient Air Mechanical Filtration with Antibacterial Activity. *ACS Appl. Polym. Mater.* **2022**, *4*, 2081–2090. [[CrossRef](#)]
318. Cheng, X.; Zhao, L.; Zhang, Z.; Deng, C.; Li, C.; Du, Y.; Shi, J.; Zhu, M. Highly Efficient, Low-Resistant, Well-Ordered PAN Nanofiber Membranes for Air Filtration. *Colloids Surfaces Physicochem. Eng. Asp.* **2022**, *655*, 130302. [[CrossRef](#)]
319. Hua, Y.; Li, Y.; Ji, Z.; Cui, W.; Wu, Z.; Fan, J.; Liu, Y. Dual-Bionic, Fluffy, and Flame Resistant Polyamide-Imide Ultrafine Fibers for High-Temperature Air Filtration. *Chem. Eng. J.* **2023**, *452*, 139168. [[CrossRef](#)]
320. Huang, J.J.; Tian, Y.; Wang, R.; Tian, M.; Liao, Y. Fabrication of Bead-on-String Polyacrylonitrile Nanofibrous Air Filters with Superior Filtration Efficiency and Ultralow Pressure Drop. *Sep. Purif. Technol.* **2020**, *237*, 116377. [[CrossRef](#)]
321. Hu, J.; Xiong, Z.; Liu, Y.; Lin, J. A Biodegradable Composite Filter Made from Electrospun Zein Fibers Underlaid on the Cellulose Paper Towel. *Int. J. Biol. Macromol.* **2022**, *204*, 419–428. [[CrossRef](#)]
322. Tian, E.; Mo, J.; Li, X. Electrostatically Assisted Metal Foam Coarse Filter with Small Pressure Drop for Efficient Removal of Fine Particles: Effect of Filter Medium. *Build. Environ.* **2018**, *144*, 419–426. [[CrossRef](#)]
323. Feng, Z.; Long, Z.; Mo, J. Experimental and Theoretical Study of a Novel Electrostatic Enhanced Air Filter (EEAF) for Fine Particles. *J. Aerosol. Sci.* **2016**, *102*, 41–54. [[CrossRef](#)]
324. Shi, B.; Ekberg, L. Ionizer Assisted Air Filtration for Collection of Submicron and Ultrafine Particles—Evaluation of Long-Term Performance and Influencing Factors. *Environ. Sci. Technol.* **2015**, *49*, 6891–6898. [[CrossRef](#)]
325. Tian, E.; Xia, F.; Wu, J.; Zhang, Y.; Li, J.; Wang, H.; Mo, J. Electrostatic Air Filtration by Multifunctional Dielectric Heterocaking Filters with Ultralow Pressure Drop. *ACS Appl. Mater. Interf.* **2020**, *12*, 29383–29392. [[CrossRef](#)]
326. Choi, D.Y.; Heo, K.J.; Kang, J.; An, E.J.; Jung, S.-H.; Lee, B.U.; Lee, H.M.; Jung, J.H. Washable Antimicrobial Polyester/Aluminum Air Filter with a High Capture Efficiency and Low Pressure Drop. *J. Hazard. Mater.* **2018**, *351*, 29–37. [[CrossRef](#)]
327. Choi, D.Y.; Jung, S.-H.; Song, D.K.; An, E.J.; Park, D.; Kim, T.-O.; Jung, J.H.; Lee, H.M. Al-Coated Conductive Fibrous Filter with Low Pressure Drop for Efficient Electrostatic Capture of Ultrafine Particulate Pollutants. *ACS Appl. Mater. Interf.* **2017**, *9*, 16495–16504. [[CrossRef](#)]
328. Kim, S.J.; Raut, P.; Jana, S.C.; Chase, G. Electrostatically Active Polymer Hybrid Aerogels for Airborne Nanoparticle Filtration. *ACS Appl. Mater. Interf.* **2017**, *9*, 6401–6410. [[CrossRef](#)]
329. Zhai, C.; Jana, S.C. Tuning Porous Networks in Polyimide Aerogels for Airborne Nanoparticle Filtration. *ACS Appl. Mater. Interfaces* **2017**, *9*, 30074–30082. [[CrossRef](#)]
330. Tien, C.-Y.; Chen, J.-P.; Li, S.; Li, Z.; Zheng, Y.-M.; Peng, A.S.; Zhou, F.; Tsai, C.-J.; Chen, S.-C. Experimental and Theoretical Analysis of Loading Characteristics of Different Electret Media with Various Properties toward the Design of Ideal Depth Filtration for Nanoparticles and Fine Particles. *Sep. Purif. Technol.* **2020**, *233*, 116002. [[CrossRef](#)]
331. Ardkapan, S.R.; Johnson, M.S.; Yazdi, S.; Afshari, A.; Bergsøe, N.C. Filtration Efficiency of an Electrostatic Fibrous Filter: Studying Filtration Dependency on Ultrafine Particle Exposure and Composition. *J. Aerosol. Sci.* **2014**, *72*, 14–20. [[CrossRef](#)]

332. Wang, Y.; Xu, Y.; Wang, D.; Zhang, Y.; Zhang, X.; Liu, J.; Zhao, Y.; Huang, C.; Jin, X. Polytetrafluoroethylene/Polyphenylene Sulfide Needle-Punched Triboelectric Air Filter for Efficient Particulate Matter Removal. *ACS Appl. Mater. Interf.* **2019**, *11*, 48437–48449. [[CrossRef](#)]
333. Zhang, X.; Wang, Y.; Liu, W.; Jin, X. Needle-Punched Electret Air Filters (NEAFs) with High Filtration Efficiency, Low Filtration Resistance, and Superior Dust Holding Capacity. *Sep. Purif. Technol.* **2022**, *282*, 120146. [[CrossRef](#)]
334. Kerner, M.; Schmidt, K.; Schumacher, S.; Asbach, C.; Antonyuk, S. Ageing of Electret Filter Media Due to Deposition of Submicron Particles – Experimental and Numerical Investigations. *Sep. Purif. Technol.* **2020**, *251*, 117299. [[CrossRef](#)]
335. Kerner, M.; Schmidt, K.; Hellmann, A.; Schumacher, S.; Pitz, M.; Asbach, C.; Ripperger, S.; Antonyuk, S. Numerical and Experimental Study of Submicron Aerosol Deposition in Electret Microfiber Nonwovens. *J. Aerosol. Sci.* **2018**, *122*, 32–44. [[CrossRef](#)]
336. Givehchi, R.; Li, Q.; Tan, Z. The Effect of Electrostatic Forces on Filtration Efficiency of Granular Filters. *Powder Technol.* **2015**, *277*, 135–140. [[CrossRef](#)]
337. Golshahi, L.; Tan, Z.; Abedi, J. Granular Filtration for Airborne Nanoparticles. *ASHRAE Trans.* **2008**, *114*, 533–541.

Disclaimer/Publisher’s Note: The statements, opinions and data contained in all publications are solely those of the individual author(s) and contributor(s) and not of MDPI and/or the editor(s). MDPI and/or the editor(s) disclaim responsibility for any injury to people or property resulting from any ideas, methods, instructions or products referred to in the content.